State of California
California Natural Resources Agency
DEPARTMENT OF WATER RESOURCES

Methodology for Flow and Salinity Estimates in the Sacramento-San Joaquin Delta and Suisun Marsh

40th Annual Progress Report to the
State Water Resources Control Board in
Accordance with Water Right Decisions 1485 and 1641

December 2019

Gavin Newsom
Governor
State of California

Wade Crowfoot
Secretary for Natural Resources
California Natural Resources Agency

Karla Nemeth
Director
Department of Water Resources


DEPARTMENT OF WATER RESOURCES
STATE OF CALIFORNIA

State of California
Gavin Newsom, Governor

California Natural Resources Agency
Wade Crowfoot, Secretary for Natural Resources

Department of Water Resources
Karla Nemeth, Director

Cindy Messer, Chief Deputy Director

Chief Counsel	Public Affairs	Legislative Affairs
Spencer Kenner	Erin Mellon, Assistant Director	Kasey Schimke, Assistant Director

Assistant Chief Deputy Director	California Water Commission
Michelle Banonis	Joseph Yun, Executive Officer

Deputy Directors

Christy Jones	Statewide Emergency Preparedness & Security
Katherine S. Kishaba	Business Operations
Eric Koch	Flood Management and Dam Safety
Ted Craddock (acting)	State Water Project
Vacant	Delta Conveyance
Taryn Ravazzini	Special Initiatives
Kristopher A. Tjernell	Integrated Watershed Management

Bay-Delta Office
Tara Smith, Acting Chief

Modeling Support Branch
Tara Smith, Chief

Delta Modeling Section
Nicky Sandhu, Chief

Edited by
Min Yu, Bay-Delta Office
Robert Suits, Bay-Delta Office
Jamie Anderson, Bay-Delta Office
(See individual chapters for authors.)

Editorial review
William O'Daly, Supervisor of Technical Publications
Frank Keeley, Research Writer


DEPARTMENT OF WATER RESOURCES
STATE OF CALIFORNIA

Foreword

Presented here is the 40th annual progress report of the California Department of Water Resources' San Francisco Bay-Delta Evaluation Program, which is carried out by the Delta Modeling Section. This report is submitted annually to the State Water Resources Control Board pursuant to Water Right Decision D-1485, Term 9, which is still active pursuant to Water Right Decision D-1641, Term 8.

The report documents progress in the development and enhancement of computer models for the Delta Modeling Section of the Bay-Delta Office. It also details the latest findings of studies conducted as part of the program. This report was compiled under the direction of Nicky Sandhu, Program Manager for the Bay-Delta Evaluation Program.

Online versions of previous annual progress reports are available at: https://www.water.ca.gov/Library/Modeling-and-Analysis

For more information, contact:

Nicky Sandhu, Chief
Delta Modeling Section
Bay-Delta Office
California Department of Water Resources

Prabhjot.Sandhu@water.ca.gov
(916) 657-5071


DEPARTMENT OF WATER RESOURCES
STATE OF CALIFORNIA

Contents

Preface

Chapter 1. ECO-PTM Model Development

Various water resource management actions have been planned to protect and restore salmon populations for a healthy Sacramento-San Joaquin Delta (Delta) ecosystem. Currently, evaluating the effectiveness of these actions relies on field studies and/or expert opinion. Field studies can be costly and may not provide a comprehensive assessment for a range of applications because of limited study areas, durations, and river conditions. Expert opinion, although valuable, may under- or over-emphasize the importance of certain project components.

To supplement field studies and provide a quantitative assessment tool, the California Department of Water Resources (DWR), in collaboration with the United States Geological Survey (USGS), developed an ecological modeling tool, ECO-PTM. ECO-PTM is an individual-based juvenile salmon migration model that is based on a random-walk particle-tracking method with fish-like behaviors attached to the particles. The behavioral parameters are estimated from acoustic telemetry tag data of juvenile late-fall Chinook salmon (Tag Data) from various field studies (Perry et al. 2018). A stochastic optimization tool, Particle Swarm Optimization, is used to calibrate the swimming behavior parameters. ECO-PTM can simulate juvenile salmonid migration timing, routing, and survival.

This chapter describes ECO-PTM and its behavioral modules, and the model performance and applications to assist water resource management planning, assessment, and decision-making related to juvenile salmonid survival outcomes.

Chapter 2. DSM2-simulated 2015 Historical Flows using DCD-based Channel Depletions

In 2018, the Delta Modeling Section released the beta version of its Delta Channel Depletion (DCD) model. This model is based on the Delta Evapotranspiration of Applied Water Model (DETAW) and differs from the Delta Island Consumptive Use Model (DICU) in several significant ways, as explained in a 2017 report (Liang and Suits 2017). While DSM2-simulated EC under DICU and DCD estimated channel depletions were presented in this report, simulated in-Delta flows were not. This chapter compares DSM2-simulated flows using DICU- and DCD-generated channel depletions to

measurement-based flows in 2015 — a recent year when channel depletions could be expected to have had a greater than normal influence on in-Delta flows. Also presented is a brief analysis of using measurement-based and DSM2-simulated flows to estimate total channel depletions in several south Delta regions.

Chapter 3. 2018 Suisun Marsh Salinity Control Gates Pilot Study: Water Cost Analysis

The Delta Smelt Resiliency Strategy (California Natural Resources Agency 2016) calls for summer operation of the Suisun Marsh Salinity Control Gates (SMSCG) to reduce salinity and improve habitat in the Suisun Marsh during summer months in above normal (AN) and below normal (BN) water years. To better understand the benefits and impacts of this operation, the California Department of Water Resources (DWR) conducted a pilot project to operate the SMSCG during August 2018. To support the pilot project, the Delta Modeling Section (DMS) of DWR Bay-Delta Office was tasked with: (1) assessing potential influence of the operation on salinity at key Delta water quality compliance locations via Delta Simulation Model II (DSM2); and (2) estimating water cost to maintain salinity within the compliance standards. This chapter summarizes the results and findings of DMS' analysis.

Chapter 4. DSM2 Sediment Transport Model (GTM-SED)

The ability to model sediment and turbidity transport in the Sacramento-San Joaquin Delta (Delta) is vital, in several ways, for effective management of Delta natural resources. First, the understanding of sediment erosion and deposition in the channel network system provides information for adaptive environmental and operational management. Second, turbidity can influence Delta smelt survival in that it affects feeding success in the larval stage, ability to avoid predation, and is a migratory cue. Sediment resuspension elevates turbidity and enhances Delta smelt habitat quality. Third, the ability to model turbidity and suspended sediment transport is essential for the development of a mercury model needed to fulfill the California Department of Water Resources' (DWR) open-water compliance with the Delta Mercury Control Program (2011). For these reasons, the California Department of Water Resources' Delta Modeling Section extended its DSM2 General Transport Model (DSM2-GTM) (Hsu et al. 2016) to include sediment transport.

Chapter 5. GTM-SED Sediment Bed Integration

The California Department of Water Resources' (DWR's) Delta Modeling Section has been developing a new General Transport Model (GTM) as a part of the Delta Simulation Model 2 (DSM2) modeling suite (California Department of Water Resources 2014), and it is now being used to simulate the salinity of the Sacramento-San Joaquin River Delta (Delta) (California Department of Water Resources 2016). GTM was specifically designed so that other water quality modules could be added to it. In fact, a suspended sediment module is currently being developed and has been preliminarily calibrated for the Delta (California Department of Water Resources 2019). This suspended sediment module is referred to as the GTM-SED. In parallel, a group of mercury experts has been developing GTM modules for mercury and bed sediments, since sediment in the riverbed is closely tied to the fate of mercury. This chapter describes the recent integration of this sediment bed module into the GTM-SED to better represent the interaction of bed sediments with the suspended sediment in the water column. The revised GTM-SED module was then preliminarily recalibrated to reflect the effect of the updates. This chapter describes the integration of bed sediment into GTM-SED, related code updates, and re-calibration results.

Methodology for Flow and Salinity Estimates in the Sacramento-San Joaquin Delta and Suisun Marsh

40th Annual Progress Report
June 2019

Chapter 1
ECO-PTM Model Development

Authors: Xiaochun Wang
Delta Modeling Section
Bay-Delta Office
California Department of Water Resources


DEPARTMENT OF WATER RESOURCES
STATE OF CALIFORNIA

Contents

Figures

Tables


DEPARTMENT OF WATER RESOURCES
STATE OF CALIFORNIA

1 ECO-PTM Model Development

1.1 Introduction

A variety of water resource management actions have been implemented and are planned to protect and restore salmon populations for a healthier Sacramento-San Joaquin Delta (Delta) ecosystem. Currently, evaluating the effectiveness of these actions relies on field studies and/or expert opinion. Field studies can be costly and may not provide a complete assessment over a range of applications because of limited study areas, durations, and river conditions. Expert opinion, although valuable, may under- or over-emphasize the importance of certain project components.

To supplement field studies and provide water resource professionals a quantitative assessment tool, the California Department of Water Resources (DWR), in collaboration with the United States Geological Survey (USGS), has been developing an ecological modeling tool, ECO-PTM. ECO-PTM is an individual-based juvenile salmon migration model based on a random-walk particle-tracking method with fish-like behaviors attached to the particles. The behavioral parameters are estimated from acoustic telemetry tag data of juvenile late-fall Chinook salmon (Tag Data) from various field studies (Perry et al. 2018). A stochastic optimization tool, Particle Swarm Optimization, is used to calibrate the swimming behavior parameters. ECO-PTM can simulate juvenile salmonid migration timing, routing, and survival.

This chapter describes ECO-PTM and its behavioral modules, and the model performance and applications to assist water resource management planning, assessment, and decision making related to juvenile salmonid survival outcomes.

1.2 ECO-PTM Model

ECO-PTM is based on Delta Simulation Model II (DSM2) Particle Tracking Model (PTM). DSM2 PTM simulates the transport and fate of individual neutrally buoyant particles through the Delta. DSM2 PTM can simulate neutrally buoyant particles' responses to the changes in the Delta hydrodynamic system, but the simulation does not represent the response of juvenile salmonids without modifications to account for fish behaviors. The goal of ECO-PTM is to improve the model accuracy in simulating juvenile salmonid migration and survival in the Delta by attaching fish behaviors to the neutrally buoyant particles.

ECO-PTM implements three types of behaviors: swimming, routing, and survival. These behaviors are mathematically described by a set of statistical models (behavior modules) that were developed by fitting the models to Tag Data.

The swimming behavior module describes behaviors such as tidal confusion (swimming in the opposite direction toward the ocean), diel holding (holding during day time), selective tidal stream transport (holding during flood tides), and differential swimming velocities at different times for different juvenile salmonids. A set of equations with stochastic variables were formulated to represent these behaviors. The behavioral parameters for the equations were calibrated using a simulated maximum likelihood approach within the context of a particle swarm optimization routine to fit ECO-PTM simulated travel times to the travel times of acoustically tagged juvenile salmonids. The goal of the calibration is to select an optimized set of parameters that ECO-PTM can utilize to simulate juvenile salmonid travel times under a wide variety of hydrodynamic conditions and salmonid behavioral responses.

Simulating accurate fish travel time is important because the routing and survival modules rely on the travel time to calculate routing and survival probabilities. An accurate travel time offers correct timing for fish particles to arrive a junction, and also provides reasonable duration estimates for the fish particles to migrate through the Delta channel. Both the timing and duration are crucial to correctly calculate routing and survival probabilities.

The routing behavior module is a set of statistical models that use hydrodynamic and other junction conditions as covariates to calculate routing probabilities at junctions. Utilizing the available Tag Data, three general fitted models from the statistical analyses of the data were implemented for the four junctions: Sutter Slough (Sut. Sl.), Steamboat Slough (Stm. Sl.), Delta Cross Channel (DCC), and Georgiana Slough (Geo. Sl.). The first statistical model is for the Geo. Sl. junction and can only be applied to high-flow periods when Sacramento River (Sac. R.) flows entering the junction are greater than 14,000 cubic feet per second (cfs) and the direction of the flows are always toward the ocean (no reverse flows). The model was developed from two-dimensional (2D) tracks of acoustic tagged juvenile salmon. The 2D data allowed the development of a statistical model based on the critical streakline entrainment zone hypothesis (see Box 3 in

Perry et al. 2016) to explore the effects of such factors as fish distribution across the channel, streakline location, and fish positions relative to the streakline. The statistical model consists of two parts: (1) a beta regression model to characterize the cross-stream distribution of fish, and (2) a logistic regression model to determine the routing probability based on the relative position of fish to streakline. The covariates of the statistical model include the probability of a fish particle's relative position to the streakline, hydrodynamic variables (junction inflow, flow split, etc.), time of day, and operation of a non-physical barrier. The second model is the generalized linear model (GLM) developed by Perry, et al. (2015). Perry et al. fitted multinomial regression models to the tag data that identified when the tagged fish in Sac. R. entered the branches. The probability of an individual fish entering a given branch or remaining in Sac. R. was modeled as a multivariate Bernoulli random variable. Then, a logit link function was used to model routing probabilities as a linear function of the covariates. The covariates include: (1) discharge in Sac. R.; (2) discharge entering Georgiana Slough or DCC; (3) the flow rate of change in Sac R.; and (4) flow direction in Sac R. Time of day was considered at the beginning of the analysis but was eliminated from the model because likelihood ratio tests showed no significant improvement of model fitness. The GLM is applied to the DCC and Geo. Sl. junctions. For the Geo. Sl. junction, because the higher flow conditions (greater than 14,000 cfs) are covered by the first model, the second model is only applied to the inflows less than or equal to 14,000 cfs. The third statistical model is a similarly structured GLM (Romine et al. 2017) but applied for the junctions of Sac. R. with Sut. Sl. and Stm. Sl. For all other junctions where the tag data for routing analysis were not available, routing probabilities were calculated using the default routing probability calculation sub-model in DSM2 PTM, which routes particles proportional to flow split ratios at channel junctions.

The survival behavior module is based on the recently published model by Perry et al. (2018). For the ECO-PTM, the logit link function used by Perry et al. (2018) was replaced with an XT model to calculate fish survival probability through the Delta channels. The XT model is a predator-prey model that expresses survival of migrating juvenile salmon as a function of both distance traveled (X) and travel time (T). The model was fitted to the Tag Data from juvenile late-fall Chinook salmon migrating through the Delta during the winters of 2007–2011. To estimate model parameters, the XT model is incorporated into a Bayesian mark-recapture model that estimated

both travel times and survival probabilities of tagged fish. The XT model parameters were reach specific. The Delta was divided into nine reaches according to the locations of acoustic telemetry receiving stations for the tag studies (Perry et al. 2018). The nine reaches represent different migration routes and Delta conditions (riverine, transitional, and tidal). The parameters were estimated for each reach. Using the XT model, survival probabilities of individual fish were calculated at the end of each reach. The population survival rate for each reach was calculated according to the percentage of fish survived among the detected fish at the end of the reach. The end reach survival rates were then used to calculate survival rate for each route. There are five routes for fish to migrate from Freeport to Chipps Island (Figure 1-1). The total survival rates were calculated by combining survival rates from all routes.

Figure 1-1 Juvenile Salmonid Migration Routes from Freeport to Chipps Island

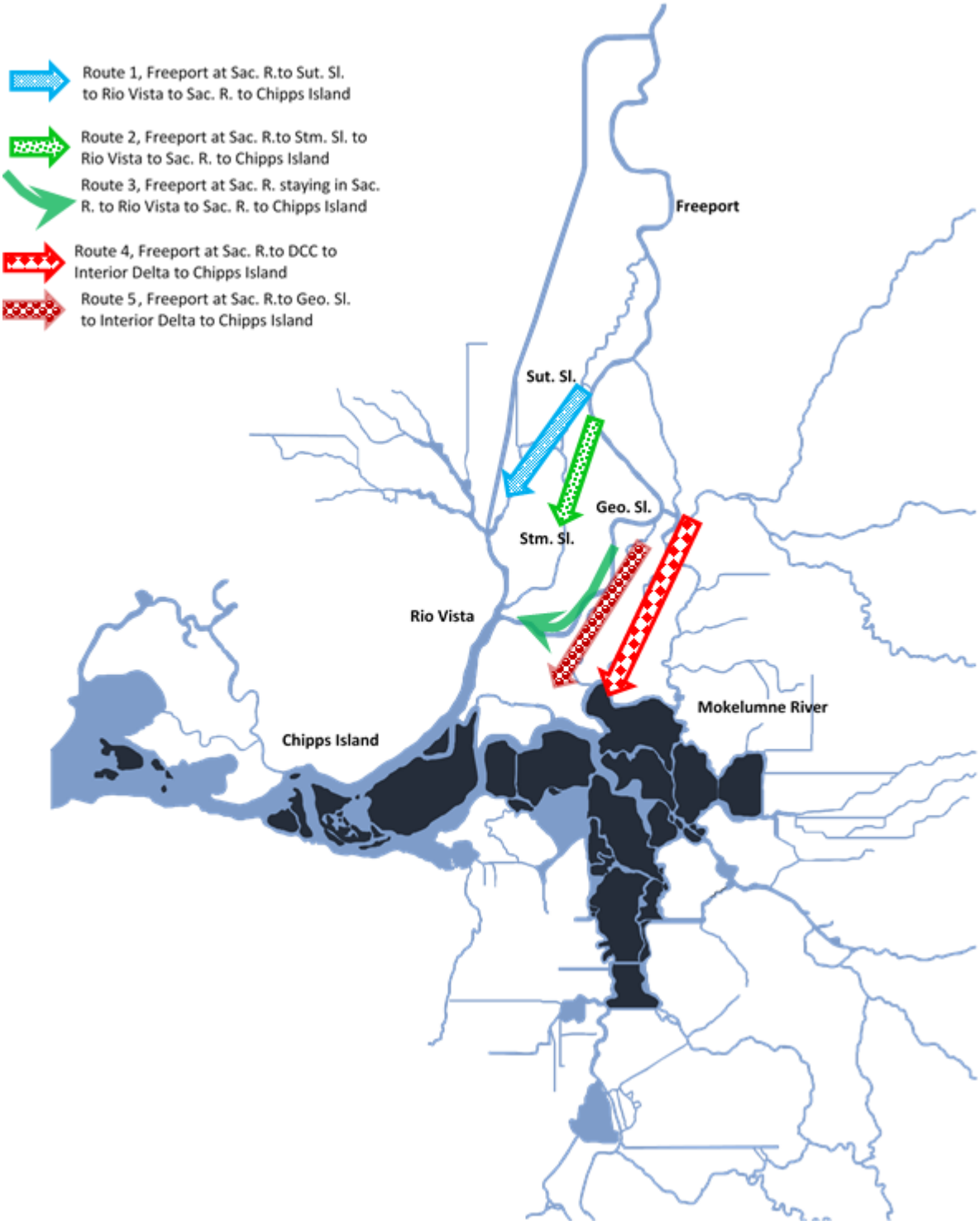

Note: Sac R. = Sacramento River, Sut. Sl. = Sutter Sough, Stm. Sl. = Steamboat Slough, Geo. Sl. = Georgiana Slough.

1.3 Comparison of ECO-PTM with STARS

STARS (**S**urvival **T**ravel Time **a**nd **R**outing **S**imulation) is a simulation model that predicts daily survival, travel time, and routing of juvenile salmon migrating through the Delta using daily Sac. R. flows at Freeport and Delta Cross Channel operations as covariates (see https://oceanview.pfeg.noaa.gov/shiny/FED/CalFishTrack/). The model is based on the Bayesian analysis of acoustic-tagged late-fall Chinook salmon data (Perry et al. 2018) and currently is limited to evaluating the juvenile salmon migration and survival through the Delta under historical Delta conditions. With the same period of historical simulations, STARS can be used to evaluate the performance of ECO-PTM with the comparison of the simulation results from both models.

Simulations under historical conditions were conducted with both STARS and ECO-PTM for the same time period. STARS used historically observed daily DCC operations and flows at Freeport in Sac. R. while ECO-PTM used the 15-minute-timestep historical simulation from DSM2 Hydro. With the observed data, STARS produced daily fish survival rates from Freeport to Chipps Island for the period of 1/1/1991 to 6/30/2016 (every day except for the non-migration season of July through September). A total of 6984 daily survival rates were produced by STARS. For each daily survival rate from the STARS simulation, ECO-PTM performed a corresponding simulation with particle releases on that particular day. For the simulation, the model released 9600 particles at a location near Freeport. To capture the daily tidal variation, 9600 particles were released over a period of 24 hours (100 particles every 15 minutes). The simulation started 10 days prior to the first 100 particle release and continued 150 days after the completion of the release of all 9600 particles to allow fish particles to pass through the Delta. The survival rate from Freeport to Chipps Island was calculated at the end of each simulation. The comparison of the survival rates from the two models are shown in Figures 1-2 and 1-3. The green and blue lines represent the STARS results. Two green lines indicate the upper and lower bound of 90 percent confidence interval. The blue line is mean survival rates. The ECO-PTM simulated survival rates were plotted with the red line. As shown in Figures 1-2 and 1-3, the simulation results from ECO-PTM and STARS closely agree except for a few periods when flows were relatively low and other factors, such as tides, could dominate fish migration and survival. This is because STARS is only sensitive to Freeport inflow and DCC operations, while ECO-PTM accounts for the complex Delta hydrodynamics by using the

fine-scale hydrodynamic simulation by DSM2 Hydro. When the two models differ, the survival rates simulated by ECO-PTM still mostly fall within the 90 percent confidence interval of the STARS simulation.

Figure 1-2 Comparison of Survival Rate STARS vs. ECO-PTM 1991–2001

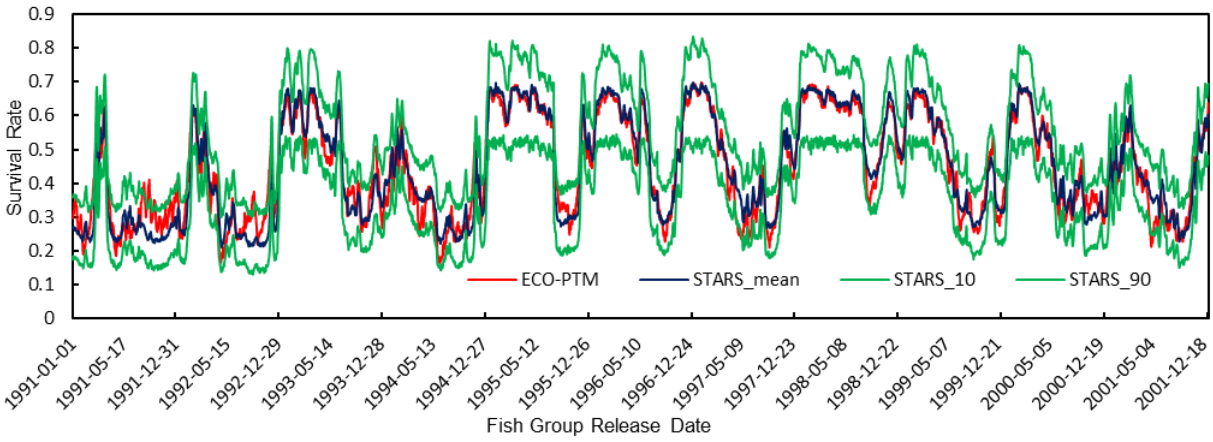

Figure 1-3 Comparison of Survival Rate STARS vs. ECO-PTM 2002–2016

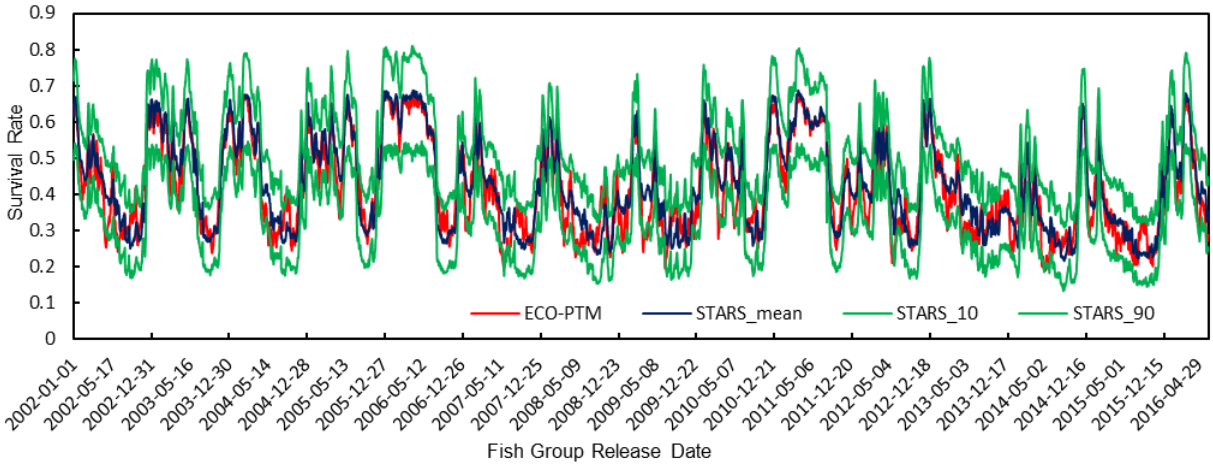

1.4 ECO-PTM Applications

With the performance of historical simulations (baseline) examined, ECO-PTM was applied to evaluate the effectiveness of non-physical barriers. DWR is analyzing the use of non-physical barriers to guide fish to more favorable survival routes. There are five routes for fish migration from Freeport to Chipps Island as shown in Figure 1-1. Route 2 via Stm. Sl. and Route 3 remaining in the main stem of Sac. R. are considered better routes for survival than the routes entering the interior Delta (Route 4 and Route 5). To guide fish to the more favorable routes, DWR is considering installing a non-physical barrier at each of the two junctions in Sac. R., at Stm. Sl. and at Geo. Sl. The barrier at the Stm. Sl. junction could guide fish to a shorter route to Rio Vista, and the one at the Geo. Sl. junction could prevent fish from entering the interior Delta. Although USGS expert opinion and the DWR 2011–2012 field studies (California Department of Water Resources 2012, 2013) indicate that the barriers at both junctions could help fish achieve a higher survival rate, a quantitative assessment is needed to comprehensively assess the benefits of the non-physical barriers prior to installation.

ECO-PTM was employed to perform the assessment task. Because the non-physical barriers do not significantly affect Delta hydrodynamics, the same historical hydrodynamic simulation used in Section 3 was used for this task. With a 15-minutes timestep, the historical hydrodynamic simulation covers a period from 1990–2017, which includes seven critically dry, five dry, four below normal, four above normal, and eight wet water years. The 28-year hydrodynamic simulation has a good representation of the Delta hydrodynamics and its variations.

To simulate the functions of the barrier, which is to increase or reduce the routing probability into the branch (either Stm. Sl. or Geo Sl.), ECO-PTM was programed to allow users to input a percentage either to increase or to reduce route probabilities based on the historical routing probability calculation.

Based on USGS expert opinion and the 2011–2012 field studies (California Department of Water Resources 2012, 2013), three management scenarios were created to simulate the effectiveness of a non-physical barrier:

Scenario 1. Adding a constant 30 percent to calculated Stm. Sl. routing probability;

Scenario 2. Multiplying calculated Geo. Sl. routing probability by constant 50 percent;

Scenario 3. Combining Scenarios 1 and 2.

Addition was used instead of multiplication in Scenario 1 because the routing probability to Stm. Sl. is very small during low Sac. R. flow periods. If this low calculated number was multiplied by a percentage, the final routing probabilities would still be very small, which would be counter to the assumption that the barrier increases the routing probability. The simulations were only conducted for the months from January to April, the migration period for the winter run Chinook salmon.

The results of the simulations for the three scenarios are summarized in Tables 1-1 and 1-2 and Figures 1-4 to 1-9. The survival benefits brought by the barriers were measured according to the survival rate differences between the baseline and the alternative scenarios. The median survival benefits are about 2 percent to 3 percent (Table 1-1); however, the survival rates and the survival benefits varied significantly depending on Delta flow conditions. Survival benefits varied from -3 percent to 7 percent while survival rates varied from 19 percent to 75 percent.

Sac. R. inflows significantly affected the survival rates. The effect depended on the flow rates. The higher the inflows, the higher the survival rates and the less variations in the survival rates. But when the inflow increases to about 35,000 to 40,000 cfs, the further increases of inflows did not lead to further increases in the survival rates. Figures 1-4 to 1-6 shows fish survival rates from Freeport to Chipps Island vs. Sac. R. inflows. When Sac. R. inflows are less than 20,000 cfs (at the low-flow end), the survival rates varied from 20 percent to 60 percent. This is because fish survival during the low-flow periods could be dominated by factors other than Sac. R. inflows.

The barrier benefits also varied with the flow, thus with different months and water year types. The inflow range of 30,00–40,000 cfs provides more benefits than other flow ranges. In addition, wet months or years show fewer survival benefits and variations while drier months and years have more (Figures 1-7 to 1-9). The simulations also indicated that two barriers at both the Stm. Sl. and Geo. Sl. junctions yielded slightly more survival benefits than a single barrier.

Table 1-1 Survival Benefits (Survival Rate Increase from Baseline)

A. Scenario Georgiana Slough - 50%

Months	Max	Median	Min
January	5%	2%	-1%
February	5%	2%	-1%
March	6%	2%	-2%
April	7%	2%	-1%
All Months Combined	6%	2%	-1%

B. Scenario Steamboat Slough + 30%

Months	Max	Median	Min
January	5%	2%	-1%
February	5%	2%	-1%
March	5%	2%	-2%
April	5%	1%	-3%
All Months Combined	5%	2%	-2%

C. Scenario Georgiana Slough + 50% + Steamboat Slough + 30%

Months	Max	Median	Min
January	6%	3%	0%
February	7%	3%	0%
March	7%	3%	0%
April	7%	3%	-1%
All Months Combined	7%	3%	0%

Table 1-2 Survival Rates for Three Scenarios

A. Scenario Georgiana Slough - 50%

Months	Max	Median	Min
January	75%	57%	23%
February	74%	58%	28%
March	75%	55%	22%
April	74%	48%	19%

B. Scenario Steamboat Slough + 30%

Months	Max	Median	Min
January	75%	57%	23%
February	74%	58%	28%
March	74%	55%	22%
April	72%	47%	17%

C. Scenario Georgiana Slough - 50% + Steamboat Slough + 30%

Months	Max	Median	Min
January	76%	58%	24%
February	76%	59%	29%
March	76%	56%	24%
April	74%	49%	19%

Figure 1-4 Survival Rates from Freeport to Chipps Island vs. Daily Flows at Freeport (Scenario 1)

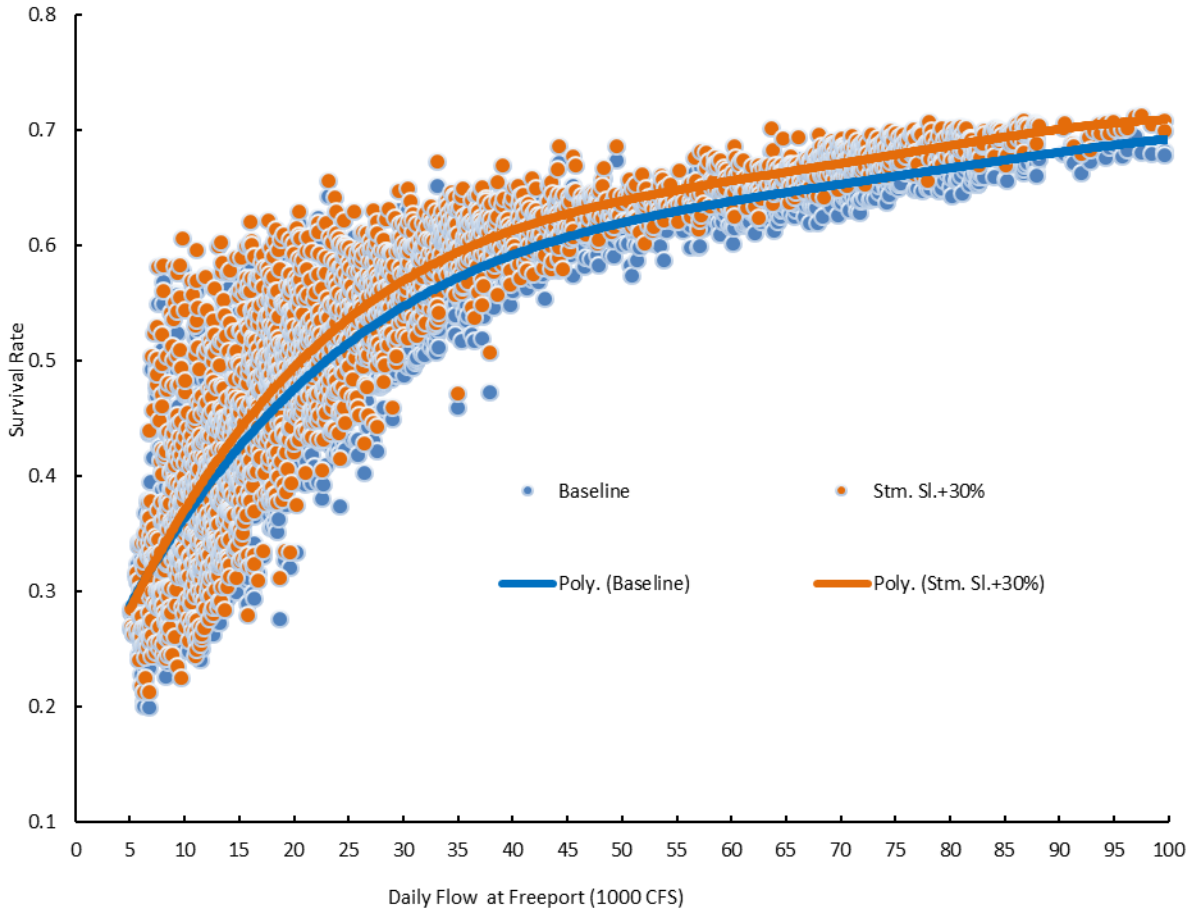

Note: The polynomial trendlines are generated by Excel.

Figure 1-5 Survival Rates from Freeport to Chipps Island vs. Daily Flows at Freeport (Scenario 2)

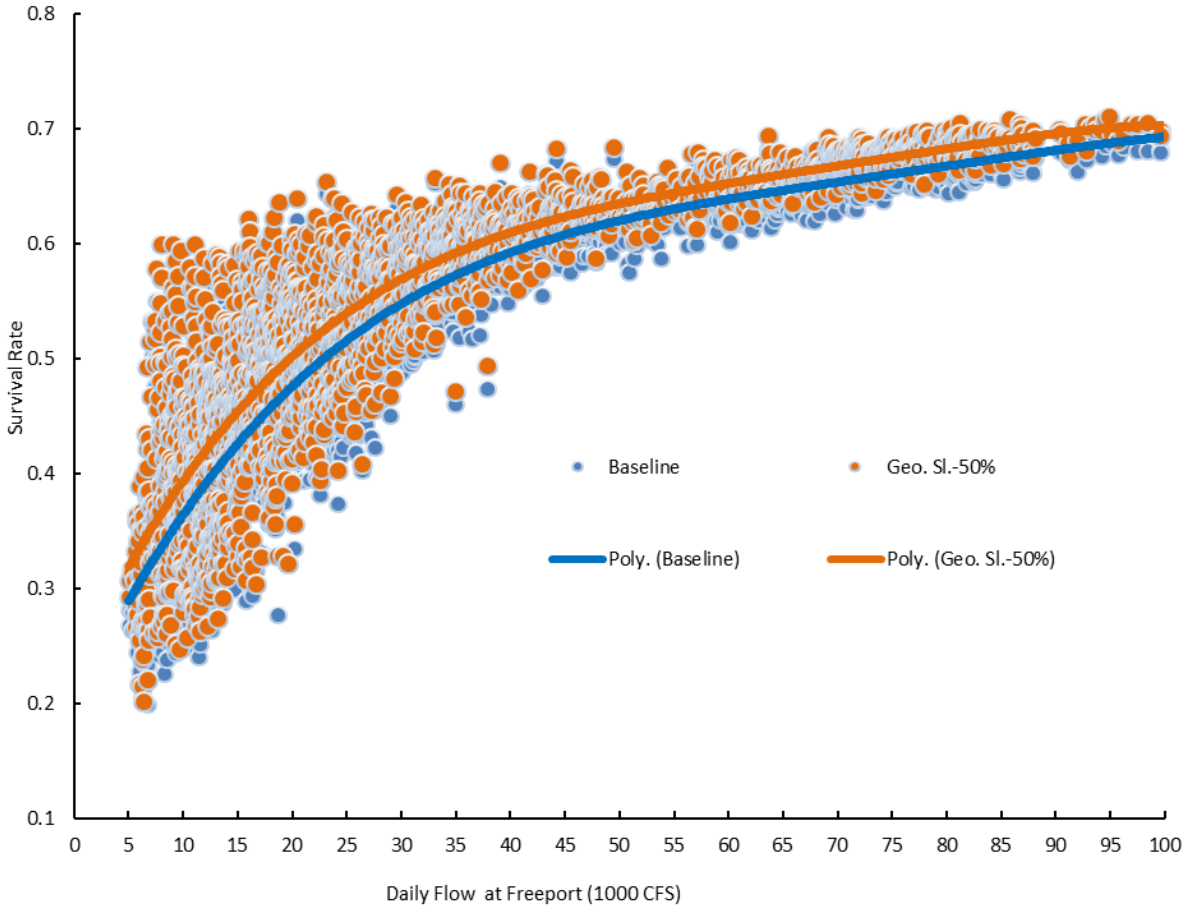

Note: The polynomial trendlines are generated by Excel.

Figure 1-6 Survival Rates from Freeport to Chipps Island vs. Daily Flows at Freeport (Scenario 3)

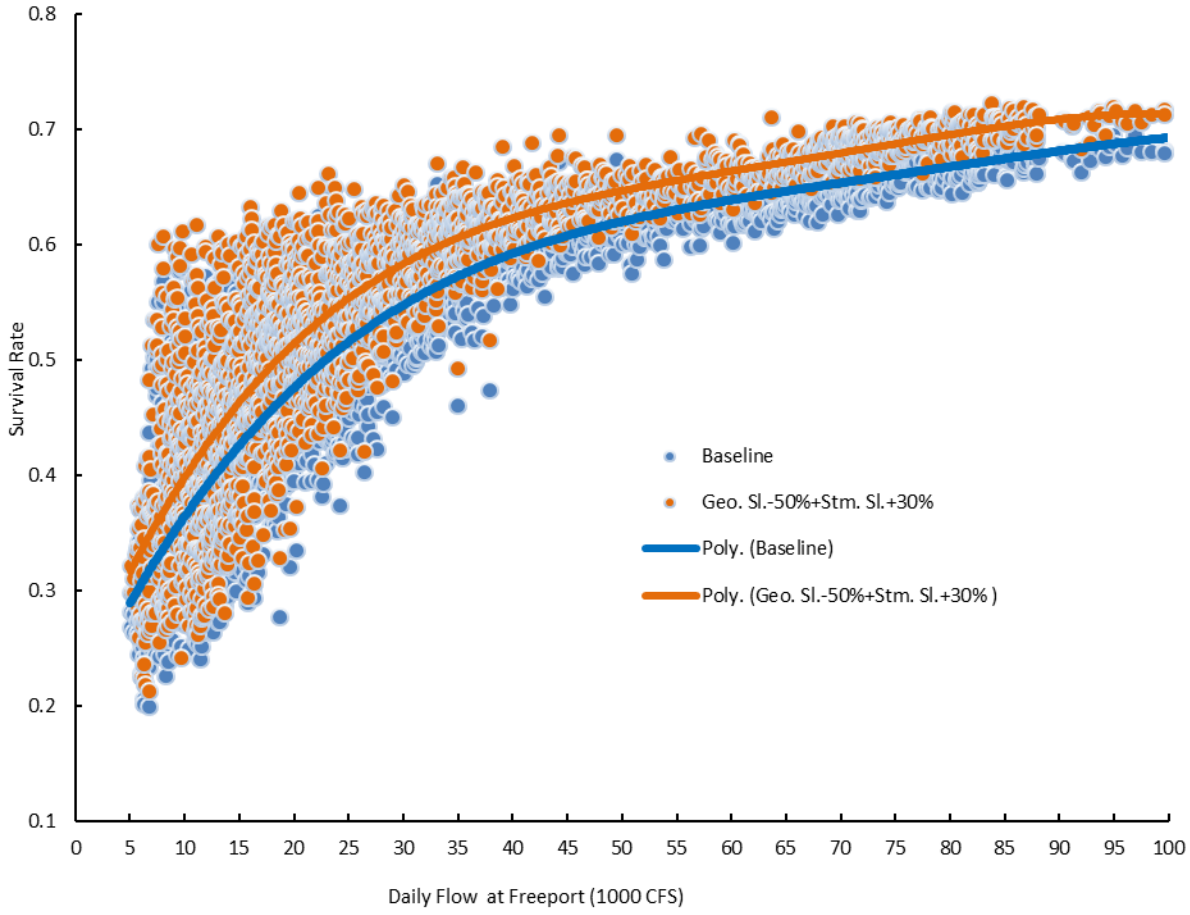

Note: The polynomial trendlines are generated by Excel.

Figure 1-7 Survival Benefits Wet vs. Critical Years (Scenario 1 — Baseline)

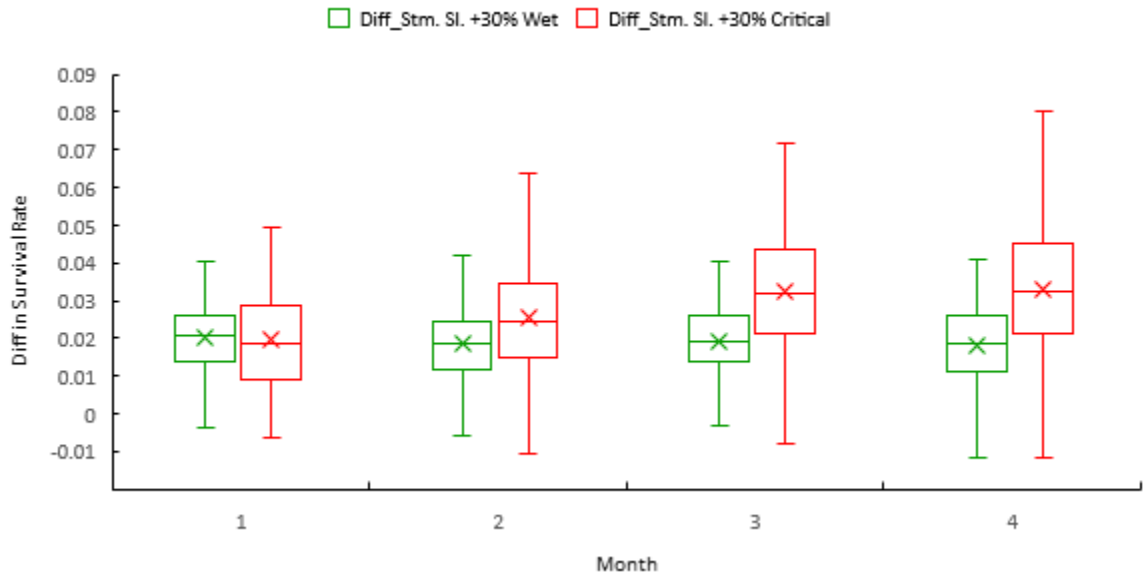

Note: Stm. Sl. = Steamboat Slough.

Figure 1-8 Survival Benefits Wet vs. Critical Years (Scenario 2 — Baseline)

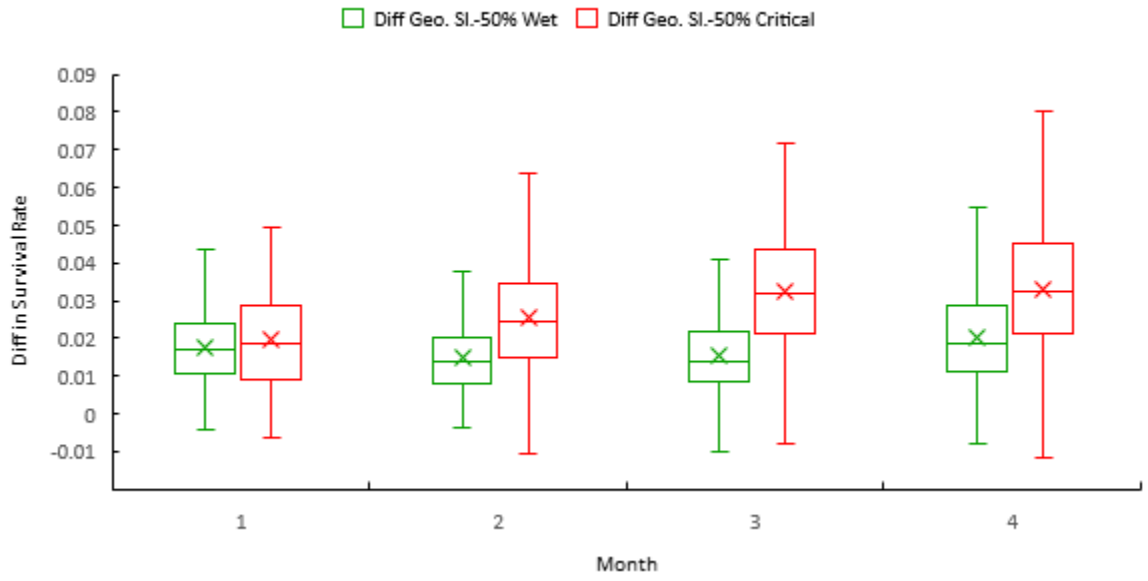

Note: Geo. Sl. = Georgiana Slough.

Figure 1-9 Survival Benefits Wet vs. Critical Years (Scenario 3 — Baseline)

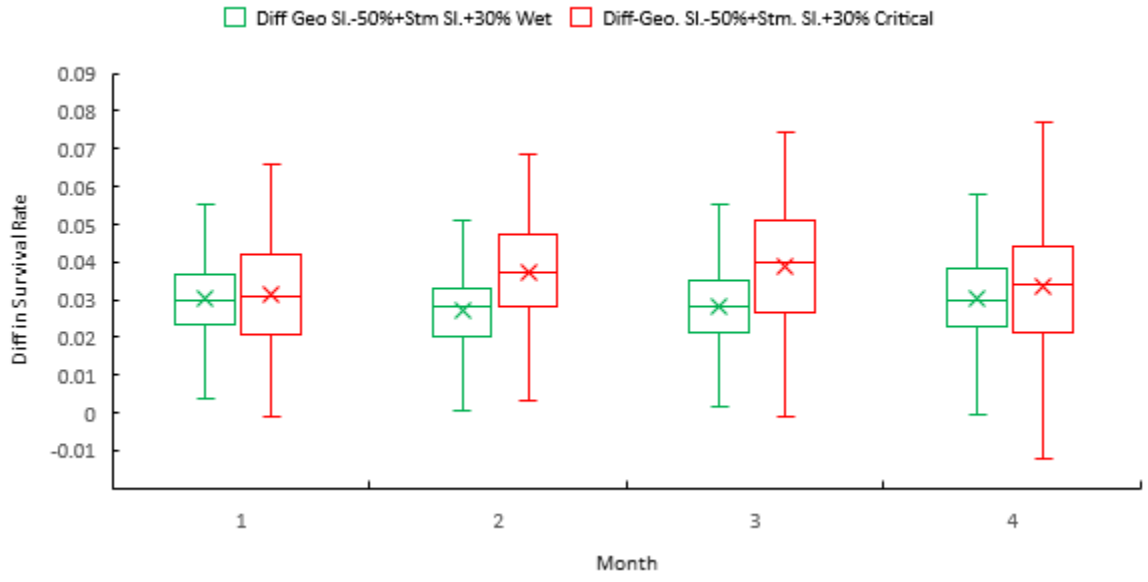

Note: Geo. Sl. = Georgiana Slough, Stm. Sl. = Steamboat Slough.

1.5 Conclusion and Future Work

ECO-PTM can be an effective tool for evaluating management actions, thus helping adaptive water resources management decision making. The model attaches fish-like behaviors to individual neutrally buoyant particles so juvenile salmon migration and survival through the Delta can be more accurately simulated. The swimming behavioral parameters were calibrated with tag data using novel mathematical methods to match simulated juvenile salmon travel times with those observed. The simulated travel times then were utilized by the routing and survival modules, which were developed by fitting statistical models to the tag data to calculate routing and survival probabilities.

To verify the model's performance, the simulated survival rates from ECO-PTM were compared to those from an independently developed and peer-reviewed statistical model, STARS. Both models performed simulations that covered a period of twenty-five years and included a broad spectrum of hydrodynamic conditions from critically dry to wet years. The simulation results from the two models closely agreed with each other. Unlike STARS, which is sensitive only to daily Delta inflows and DCC operations, ECO-PTM can be used for evaluating more complex management actions.

The model was applied to evaluate the benefits of non-physical barriers at the crucial Delta junctions on the Sac. R. The simulations indicated that the non-physical barriers could bring fish survival benefits; however, the simulated survival rates and the barrier benefits vary depending on Delta conditions. This suggests that it may be more cost effective to target the management actions at specific flow conditions, certain water year types, or months to achieve an optimal solution.

Currently, ECO-PTM has been mainly calibrated for the north Delta from Freeport to Chipps Island and for Late-Fall Chinook Salmon. In the future, ECO-PTM will be improved by conducting more calibration and validation, especially for the South Delta region and for other salmon populations. Formal code review and testing processes are planned and will be started soon. After the review and testing processes are completed, the model will be released. The release date is planned for late 2019.

1.6 Acknowledgments

We would like to thank co-contributors Russell Perry, Adam Pope, and Dalton Hance at USGS and Jason Romine at USFWS for their contribution to this project. USGS developed the behavioral sub-models and helped formulate the ECO-PTM implementation algorithms of the sub-models. Furthermore, they also helped in reviewing the simulation results and solve the sub-model implementation issues found during the review process.

We would also like to thank Ryan Reeves, Bill McLaughlin, Robert Trang, and Khalid Ameri, DWR program managers and colleagues for their support and suggestions. They offered management perspectives and assistance on developing simulation scenarios. In addition, they are thanked for their edits and comments which greatly improved the manuscript. Special thanks to Khalid Ameri who helped to create the tables for the chapter.

Gratitude and appreciation are extended to Steve Lindley and his group in NOAA Fisheries, Doug Jackson at QEDA Consulting for the collaboration at the early stage of the project, and Aaron Blake in USGS for his suggestions.

1.7 References

California Department of Water Resources. 2012. 2011 Georgiana Slough Non-Physical Barrier Performance Evaluation Project Report. Bay-Delta Office. Sacramento, CA.

California Department of Water Resources. 2013. 2012 Georgiana Slough Non-Physical Barrier Performance Evaluation Project Report. Bay-Delta Office. Sacramento, CA.

Perry RW, Pope AC, Romine JG, Brandes PL, Burau JR, Blake AR, Ammann AJ and Michel CJ. In press. "Flow-mediated effects on travel time, routing, and survival of juvenile Chinook salmon in a spatially complex, tidally forced river delta." Canadian Journal of Fisheries and Aquatic Sciences. DOI: doi: 10.1139/cjfas-2017-0310.

Perry RW, Buchanan RA, Brandes PL, Burau JR and Israel JA. 2016. "Anadromous salmonids in the Delta: new science 2006–2016." San Francisco Estuary and Watershed Science, 14(2). Retrieved from https://escholarship.org/uc/item/27f0s5kh.

Perry RW, P L Brandes, JR Burau, PT Sandstrom, and JR Skalski. 2015. "Effect of tides, river flow, and gate operations on entrainment of juvenile salmon into the interior Sacramento–San Joaquin River Delta." Transactions of the American Fisheries Society. 144: 445-455. DOI: 10.1080/00028487.2014.1001038.

Romine JG, Perry RW, Burau JR, Stumpner P, and Blake A. 2017. Effects of tidally varying river flow on entrainment of juvenile salmon into Sutter and Steamboat Sloughs. Manuscript submitted for publication.

Methodology for Flow and Salinity Estimates in the Sacramento-San Joaquin Delta and Suisun Marsh

40th Annual Progress Report
June 2019

Chapter 2
DSM2-simulated 2015 Historical Flows using DCD-based Channel Depletions

Authors: Bob Suits, Lan Liang, and Wenli Yin
Delta Modeling Section
Bay-Delta Office
California Department of Water Resources


DEPARTMENT OF WATER RESOURCES
STATE OF CALIFORNIA

Contents

Figures

Tables

2 DSM2-simulated Historical Flows using DCD-based Channel Depletions

2.1 Introduction

In 2018 the Delta Modeling Section released the beta version of its Delta Channel Depletion (DCD) model. This model is based on the Delta Evapotranspiration of Applied Water Model (DETAW) and differs from the Delta Island Consumptive Use Model (DICU) in several significant ways (Liang and Suits 2017). While DSM2-simulated EC under DICU and DCD estimated channel depletions are presented in this report, simulated in-Delta flows are not. This chapter compares DSM2-simulated flows using DICU- and DCD-generated channel depletions to measurement-based flows in 2015 — a recent year when channel depletions (and historic hydrologic conditions) would likely have had a greater influence on in-Delta flows. Also presented is a brief analysis of using measurement-based and DSM2-simulated flows to estimate total channel depletions in several south Delta regions.

2.2 Delta Hydrology and Geometry in 2015

2.2.1 Key Boundary Conditions in 2015

In-Delta flows (usually considered in Delta studies) include Old and Middle River flows (OMR) as well as flows in the south Delta where circulation and water levels may be of concern. Average flows in both OMR and the south Delta can be highly influenced by San Joaquin River inflow and export operations of State and federal facilities. In the south Delta, agricultural diversions, seepage, and drainage can also contribute to localized circulation patterns. In 2015, the fourth year of the 2012–2016 drought, San Joaquin inflows and exports at the State Harvey O. Banks (Banks) and federal C.W. Bill Jones (Jones) pumping plants were very low for an extended period (Figures 2-1 and 2-2). During such conditions, diversions and returns of agricultural water use may play a greater role in south Delta flow splits and circulation patterns. Consequently, errors in estimated channel depletions should be more evident in the hydrodynamic modeling of the south Delta in 2015 when compared with the conditions of higher San Joaquin River inflow and exports from the Banks and Jones pumping plants.

Figure 2-1 Key Boundary Conditions in the South Delta for 2015

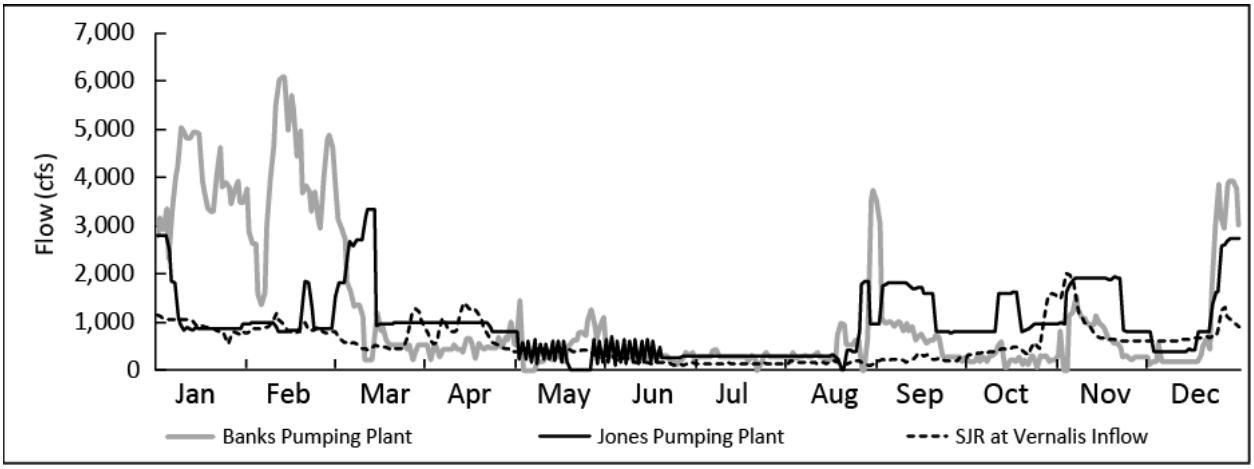

Figure 2-2 Key Boundary Conditions in the South Delta for March 15 – August 24, 2015

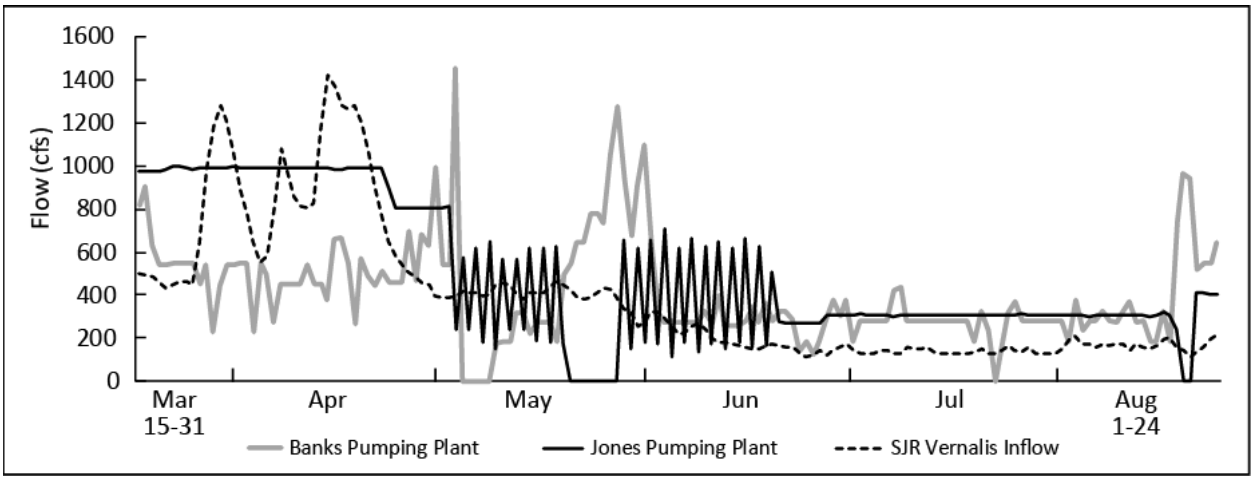

2.2.2 Measurement-based In-Delta Flows in 2015

Calculated actual flows in 2015 are available through the California Data Exchange Center (CDEC) and DWR's Water Data Library (WDL). These values are based on a localized sampling of velocity that has been calibrated to flow based on simultaneously measured water levels. Data accessed through CDEC has not been checked for possible errors, and both CDEC and WDL datasets may have spatial or temporal gaps. For the purpose of this report, CDEC and WDL reported flows are collectively referred to as "reported flows." Reported flows are later contrasted with DSM2-simulated

flows. In addition to flow at Old River at Bacon Island and Middle River, reported flows at 18 locations in the south Delta were used for this analysis (Figure 2-3). All flow data are at a 15-minute interval except for HRO (Banks Pumping Plant) and TRP (Jones Pumping Plant) which are daily average flow. Flows are often processed to 14-day running average values in order to reduce the tidal signal.

Figure 2-3 Locations Where Reported Flow Data Are Available in the South Delta for 2015

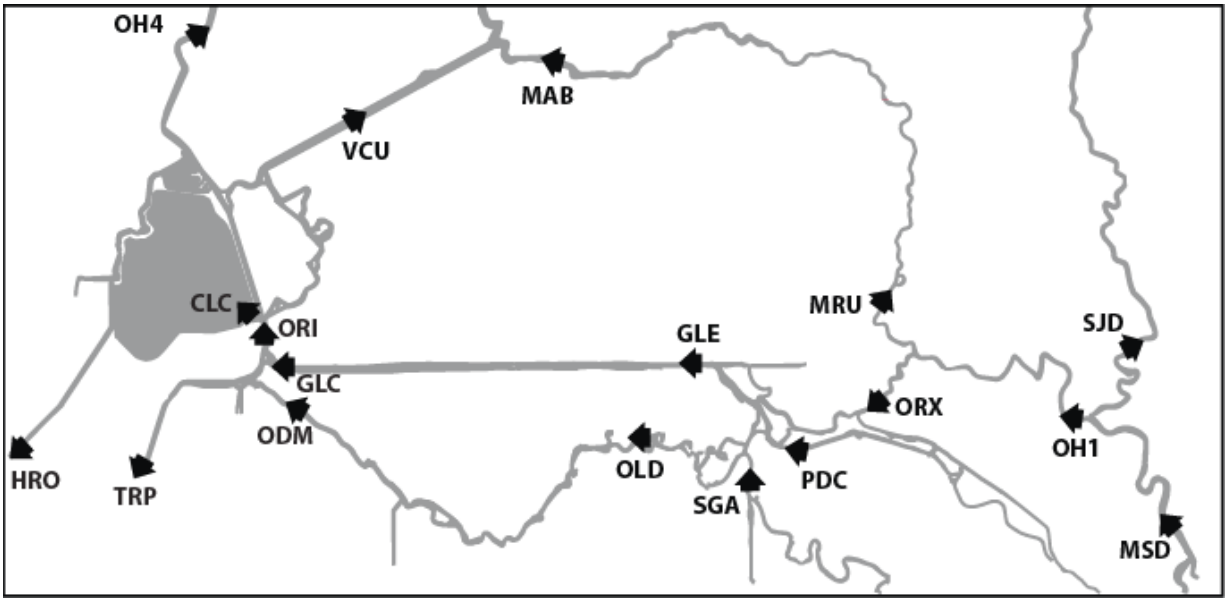

Reported in-Delta flows can be checked for accuracy by calculating a water balance at flow splits. This was done at four locations in the south Delta (Figure 2-4). One error in this analysis is not accounting for losses and gains between reported flows stemming from agriculture diversions and drainage.

Figure 2-4 Locations Where a Water Balance is Calculated Using Reported Flow for 2015

	Location	Flow Check		Location	Flow Check
1	SJR/Old River	MSD : (OH1+SJD)	3	East GLC/Old R	(ORX+PDC+SGA) : (GLE+OLD)
2	Old R/Middle R	OH1 : (MRU+ORX)	4	West GLC/Old R	TRP : (ODM+GLC+ORI)

Figures 2-5 through 2-8 show the 14-day the running average of the reported flows at the locations shown in Figure 2-4. For this analysis, obvious reported flow data errors were removed, and missing data were filled by simple interpolation.

There is good closure of reported flows at the San Joaquin River/Old River and Old River/Middle River flow splits (Figures 2-5 and 2-6). Over July and August, the average OH1 flow is 14 cfs lower than (MSD-SJD) flow and 33 cfs lower than the (ORX-MRU) flow.

Figure 2-5 Reported Flow at San Joaquin River/Old River Flow Split for 2015

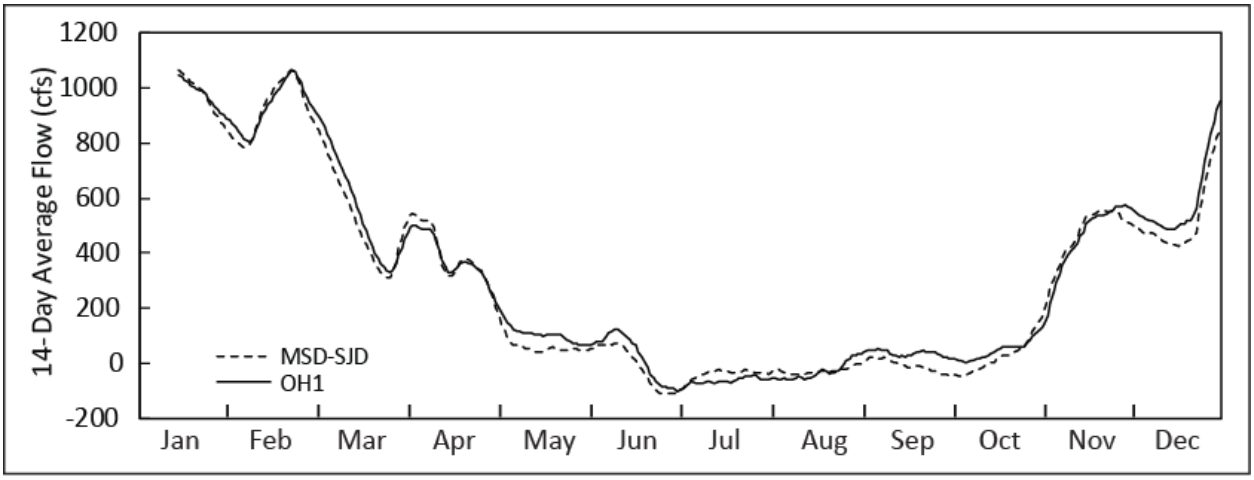

The reported flows at the Old River/East Grant Line Canal split show a difference of about 200 cfs for July through October (Figure 2-7). Some of this difference can be attributed to some channel depletion in between ORX and OLD/GLE, but how much is unclear. A similar graph created from a DSM2 simulation of 2015 using DCD channel depletions shows a difference of about 50 cfs from July through September (Figure 2-8).

Figure 2-6 Reported Flow at Old River/Middle River Split for 2015

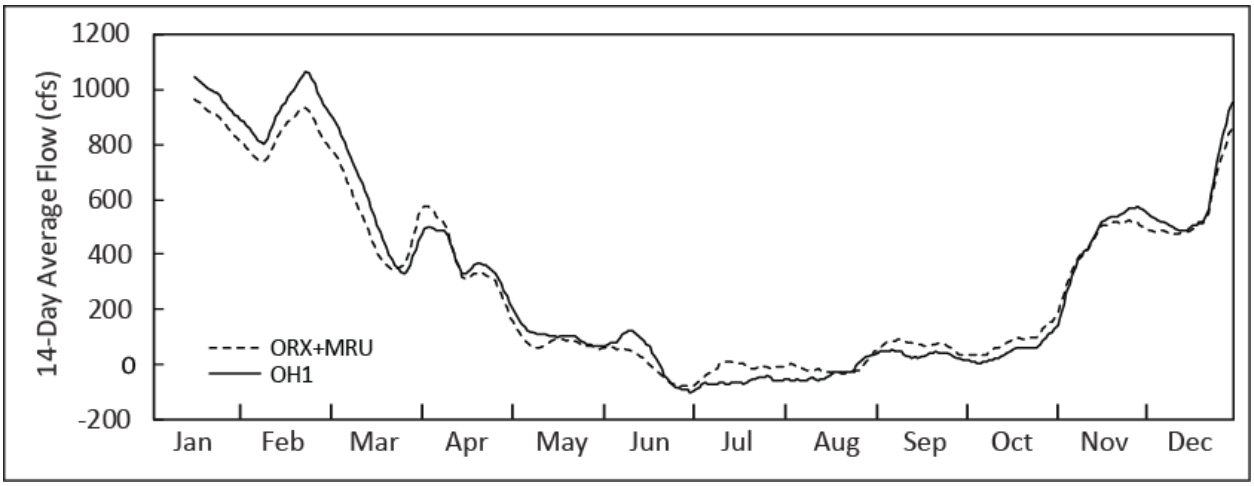

Figure 2-7 Reported Flow at Old River/East Grant Line Canal Flow Split for 2015

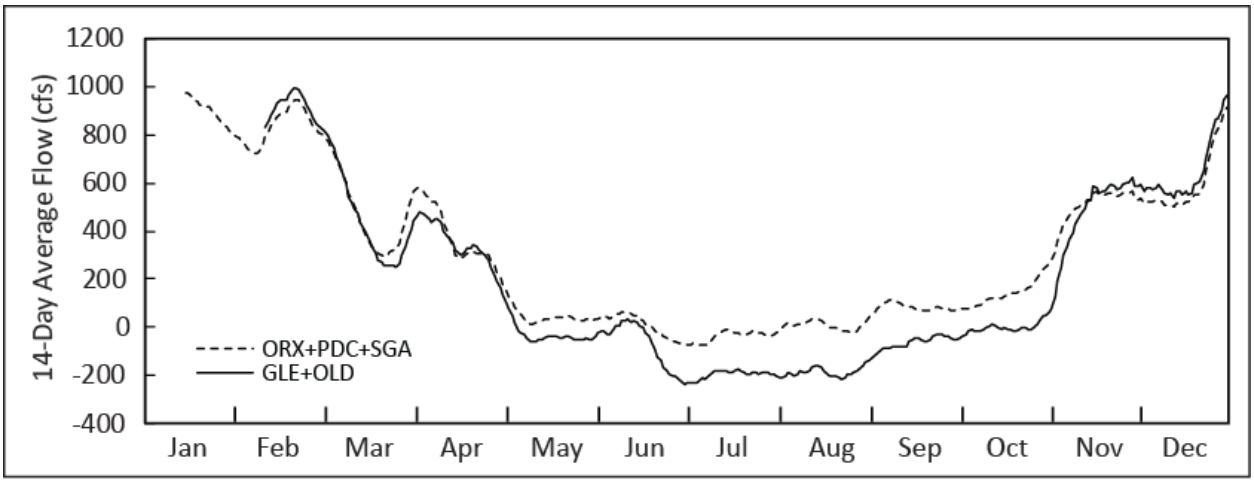

Figure 2-8 DSM2+DCD-Simulated Flow at Old River/East Grant Line Canal Flow Split for 2015

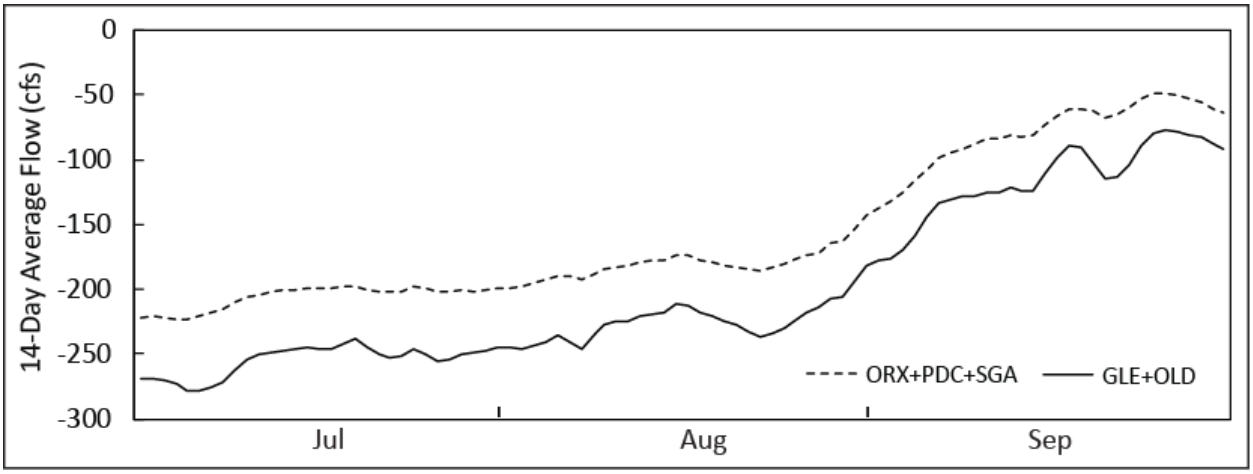

The difference in 2015 reported flows around the west end of Grant Line Canal is greater, particularly in July and August when the difference between Jones Pumping Plant pumping and the combined flows at ORI, GLC, and ODM is about 500 cfs (Figure 2-9). Assuming some net channel depletion, the combined flows entering the region should be higher than TRP. As is discussed in Sections 2.3.1 and 2.3.3, the reported flow at GLC is suspect and the likely source of much of the differences in the flows. The DSM2 simulation with DCD shows the combined (ORI+GLC+ODM) flow to be about 50 cfs higher than TRP (Figure 2-10), which is much more reasonable.

Figure 2-9 Reported Flow at Old River/West Grant Line Canal Flow Split for 2015

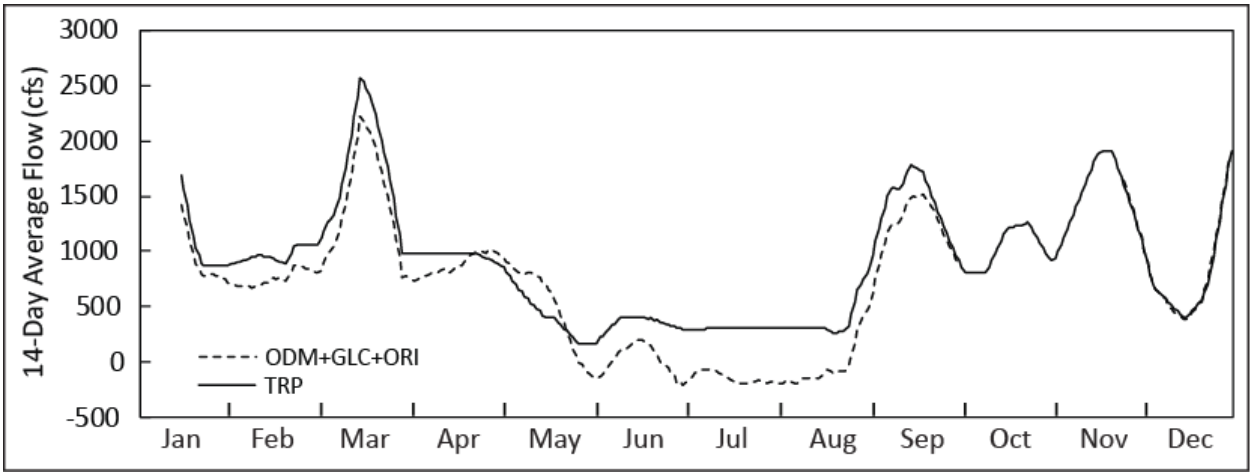

Figure 2-10 DSM2+DCD-Simulated Flow at Old River/West Grant Line Canal Flow Split for 2015

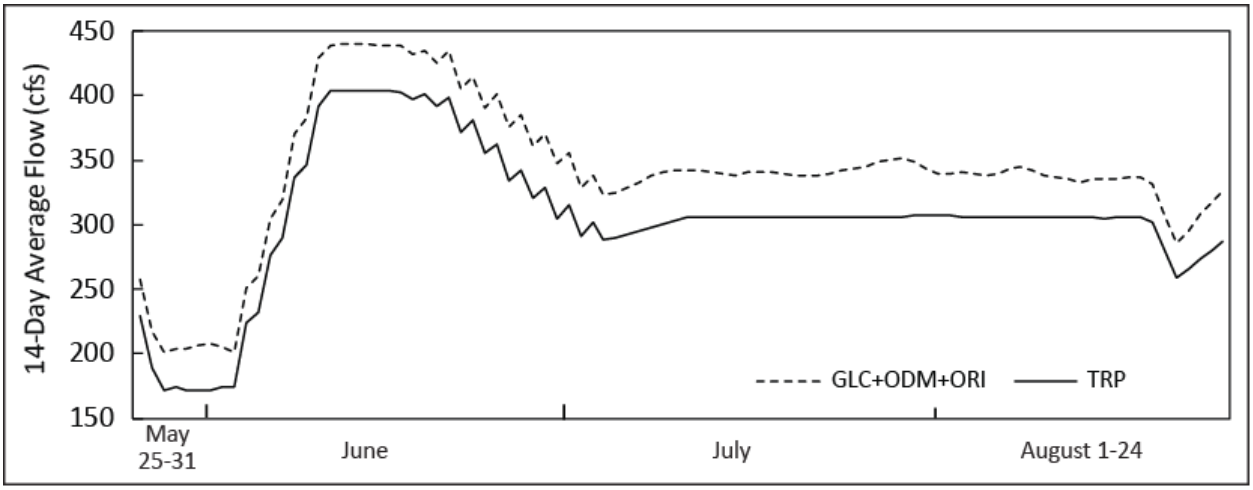

2.2.3 DICU and DCD Estimated Net Delta Channel Depletion Values for 2015

As mentioned above, channel depletions calculated by DICU and DCD models can substantially differ. DCD-based channel depletions tend to be lower than DICU values during the irrigation season and higher during the winter (Liang and Suits 2017). Figure 2-11 shows the channel depletions calculated by the two models for April–November 2015 and their difference. DICU calculates monthly values while DCD calculates daily values. The average DCD net Delta channel depletion in July 2015 is over 1,000 cfs less than that calculated by DICU. This would correspond to a difference of about 500 cfs in the south Delta in July 2015 if one assumes that 65 percent of net Delta channel depletions occur in the combined central and south Delta per DWR's model DAYFLOW (California Department of Water Resources). A difference of 500 cfs in July of 2015 is significant considering the low San Joaquin River inflow and limited pumping at Banks and Jones pumping plants.

Figure 2-11 Comparison of DICU and DCD Estimates of Total Net Delta Channel Depletion for April–November 2015

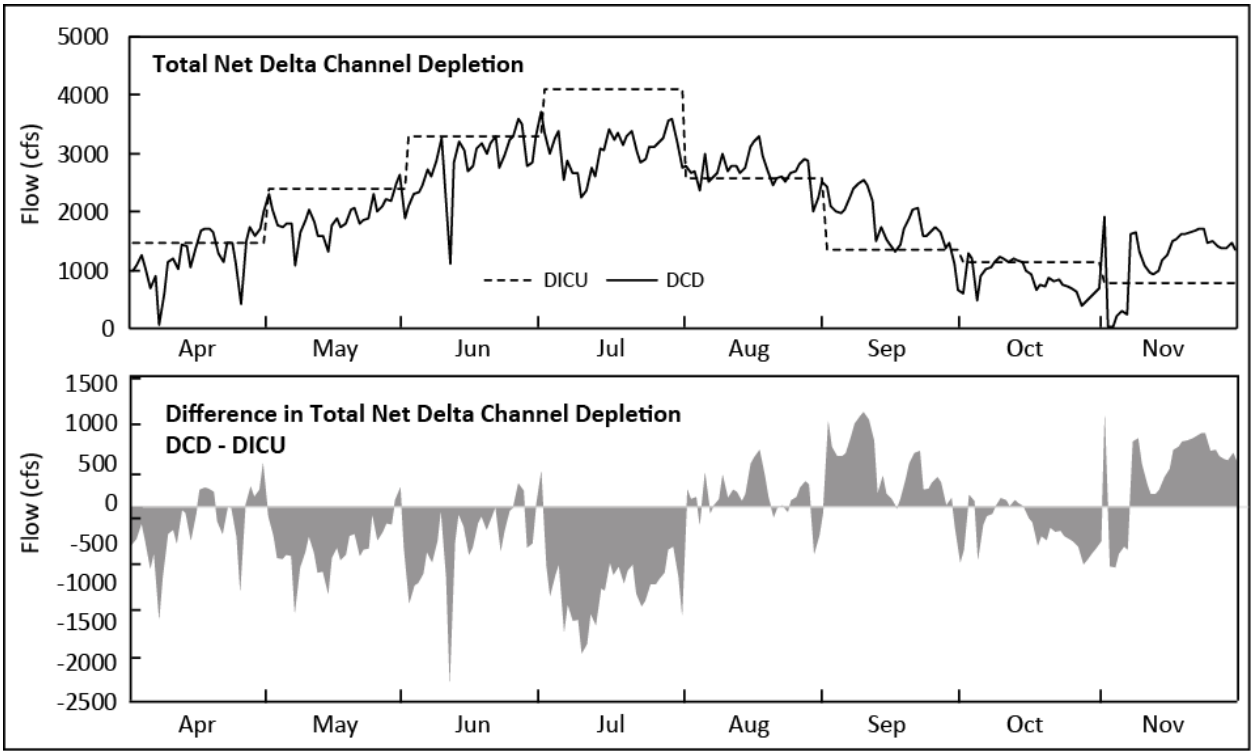

2.2.4 Temporary Barriers Schedule in 2015

In 2015, all three temporary agriculture barriers and the spring and fall Head of Old River barriers were installed (Table 2-1). Flows down Old River from the San Joaquin River are strongly influenced by the installation of the Old River at Head barrier and when the Grant Line Canal Barrier is completely closed. South Delta water levels and circulation resulting from the installation and operation of all the temporary barriers are simulated each year by DSM2 for DWR's Temporary Barrier Project.

Table 2-1 Installation, Operation, and Removal of Temporary South Delta Barriers in 2015

A. Installation

Barrier	Started	Closed	Completed
Old River at Tracy	16 Mar.	3 Apr.	8 Apr.
Middle River	27 Mar.	31 Mar.	2 Apr.
Grant Line Canal	30 Mar.	17 Apr.	18 Jun.
Old River at Head (Spring)	16 Mar.	3 Apr.	8 Apr.
Old River at Head (Fall)	3 Sep.	13 Sep.	17 Sep.

B. Operation

Barrier	Weir Raised 1 foot	Weir Notched
Old River at Tracy	-	8 Sep.
Middle River	4 Jun.	8 Sep.
Grant Line Canal	-	-
Old River at Head (Spring)	-	-
Old River at Head (Fall)	-	-

C. Removal

Barrier	Started	Breached	Completed
Old River at Tracy	30 Oct.	4 Nov.	19 Nov.
Middle River	19 Nov.	20 Nov.	30 Nov.
Grant Line Canal	29 Oct.	4 Nov.	8 Jun.
Old River at Head (Spring)	27 May	1 Jun.	18 Nov.
Old River at Head (Fall)	12 Nov.	12 Nov.	18 Nov.

2.3 Validation of DSM2-Simulted Flows for 2015

Historical 2015 hydrodynamic Delta conditions were simulated by DSM2 using both DICU- and DCD-based channel depletions. Simulated and reported flows were compared at the Old and Middle River (OMR) stations and at the 15 in-channel locations shown in Figure 2-3. Comparisons are based on 14-day running average flow for time plots and specific period-average flows for flow schematics.

2.3.1 Reported and DSM2-Simulated Flow at Specific Locations in the South Delta

As shown in the following figures, DSM2-simulated flow at some locations match reported flow well and at other locations it substantially deviates. Negative flows indicate upstream flow. Suspected errors in reported data complicate the analysis. There is no obvious pattern of DSM2 better matching reported data in the south Delta under DICU or DCD estimated channel depletions.

DSM2-simulated flow at Mossdale agrees well with the reported flow during the very low flow period of July through September 2015 (Figure 2-12); however, the simulated flow in May is about 300 cfs higher than the reported data. The DSM2 simulations use the reported flow at Vernalis as a boundary condition. As Figure 2-13 shows, the reported flow at Vernalis and Mossdale show about the same differences in flow as those between simulated flow and reported flow at Mossdale. Mossdale is about 13 miles downstream of Vernalis and such large differences in flow between the two locations are not expected.

Figure 2-12 Reported and DSM2-Simulated Flow at Mossdale for 2015

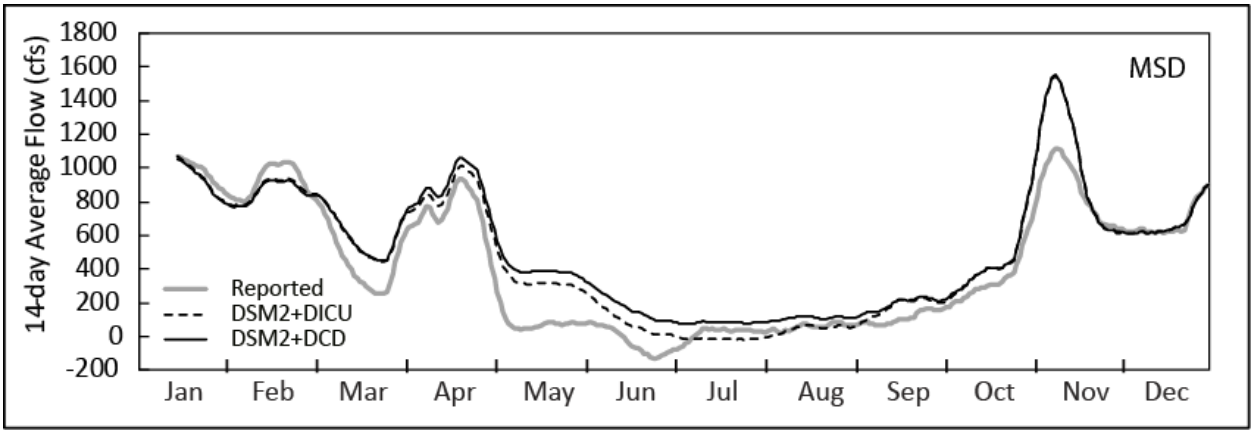

Figure 2-13 Reported Flow at Vernalis and Mossdale for 2015

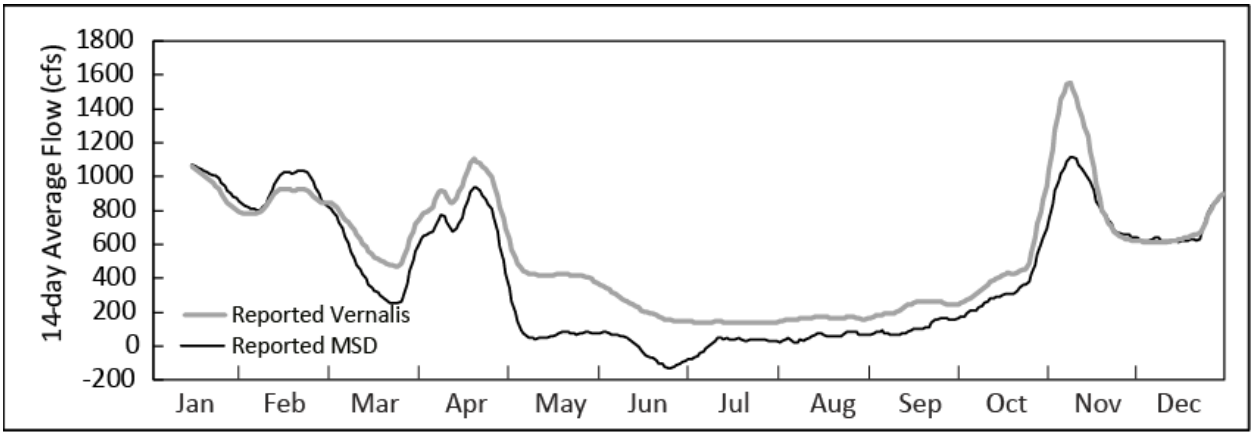

Figure 2-14 Reported and DSM2-Simulated Flow at Old River at SJR above Dos Reis for 2015

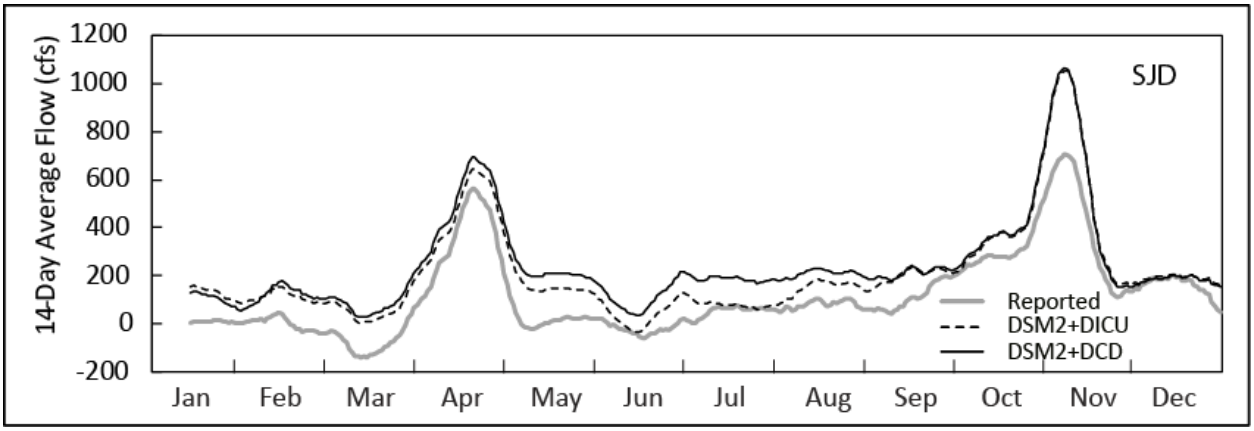

Figure 2-15 Reported and DSM2-Simulated Flow at Old River at Head for 2015

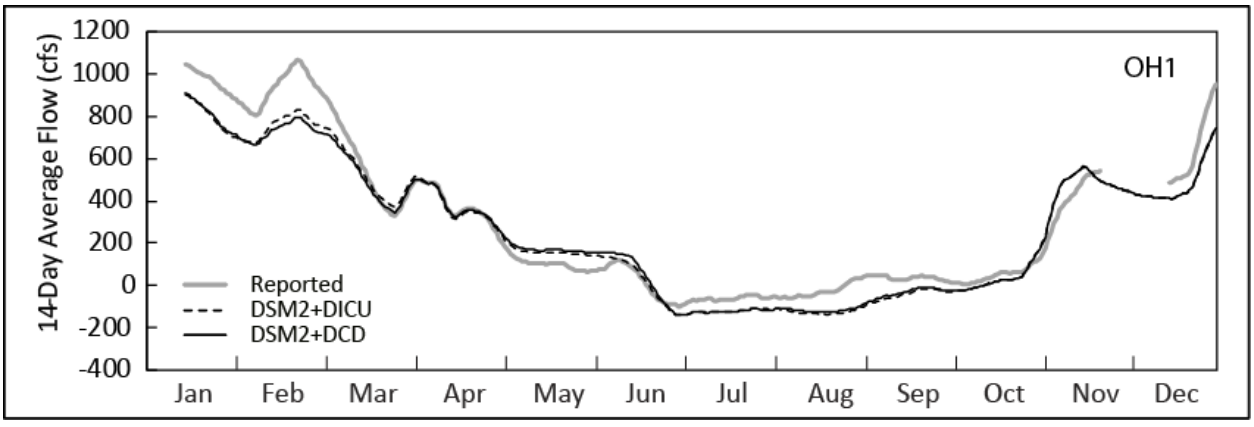

The reported flows in Middle River (MAB and MRU) substantially differ from DSM2-simulated flows (Figure 2-16 and 2-17). The pattern of differences in flow is consistent with a scenario of actual channel depletion in Middle River between MAB and MRU being higher than that estimated by DICU or DCD. Higher channel depletions in Middle River would result in more negative or upstream flows at MAB and more positive or downstream flows at MRU.

The reported MAB flow in July 2015 shows an obvious error the second half of July (Figure 2-17). The reported and DSM2-simulated 15-minute flow and daily average flow at MAB during this period are shown in Figures 2-18 and 2-19. Reported flow at MAB ceases to show upstream tidal flow during this period. Either the reported flow is in error or the DSM2-simulation fails to capture some phenomenon. One possibility would be for the water levels downstream of the barrier site being so low as to prevent upstream flow over the Middle River weir. Though, as shown in Figure 2-20, the stage just downstream of the barrier site shows that the water levels were maintained during this period.

Figure 2-16 Reported and DSM2-Simulated Flow at Middle River at Undine Road for 2015

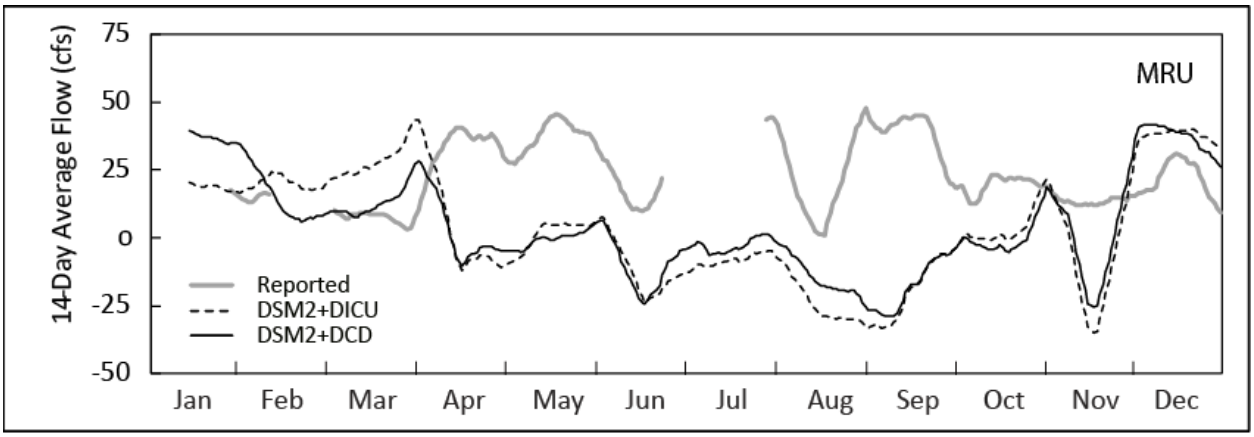

Figure 2-17 Reported and DSM2-Simulated Flow at Middle River above Barrier for 2015

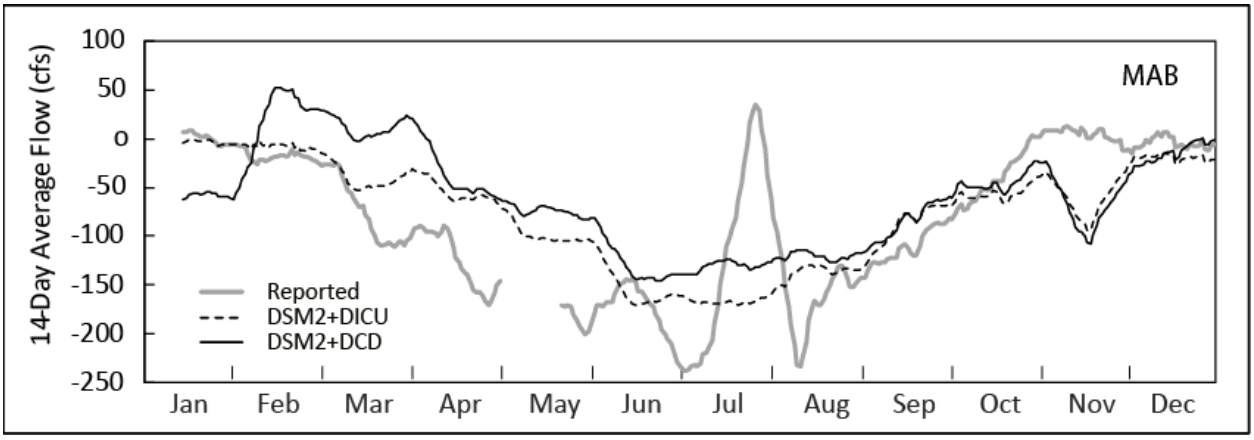

Figure 2-18 Reported and DSM2-Simulated 15-Minute Flow at MAB in July of 2015

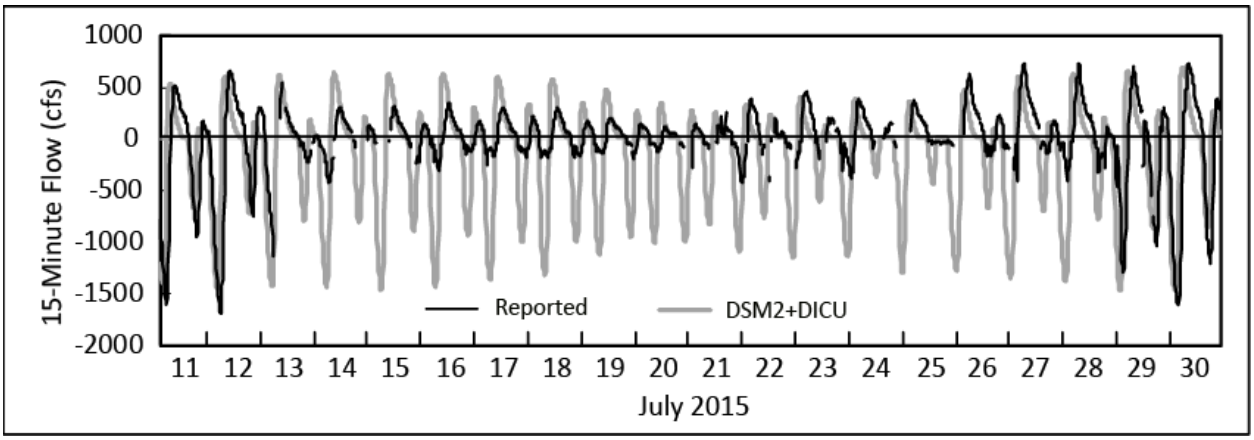

Figure 2-19 Reported and DSM2-Simulated Daily Average Flow at MAB in July 2015

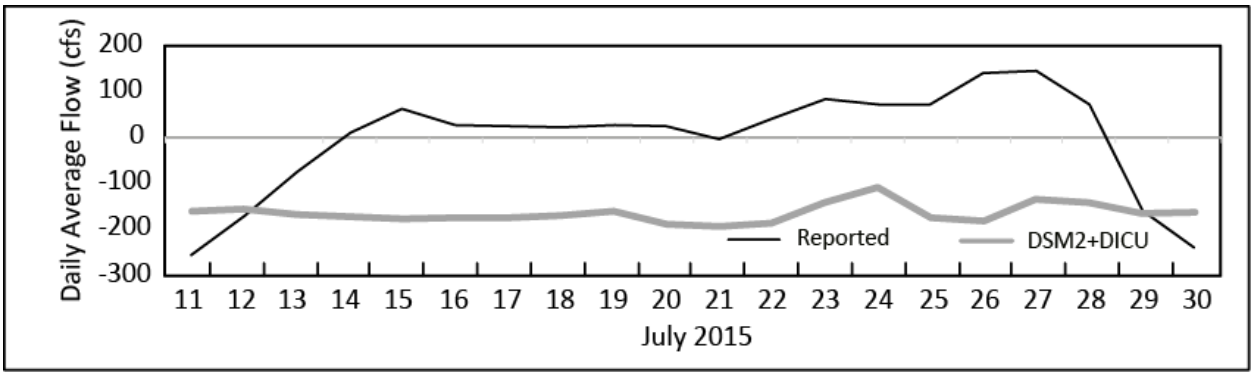

Figure 2-20 Reported Stage at Middle River downstream of Barrier in July of 2015

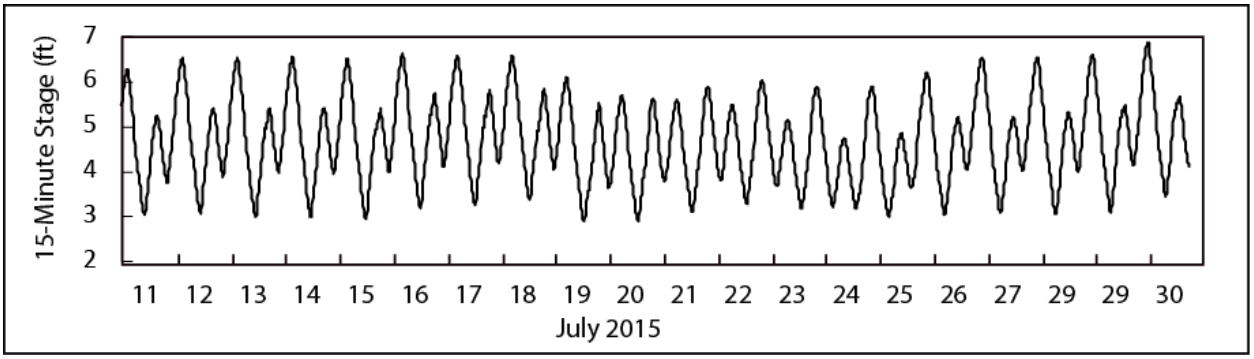

While the reported and DSM2-simulated flow at ORX match well (Figure 2-21), the reported flow in Old River at OLD and ODM are substantially less in the upstream direction when compared with DSM2-simulated flow when the Old River barrier is installed and operating (Figures 2-22 and 2-23). Such large differences have not been seen in simulations of previous years.

DSM2-simulated flow seems to have well matched reported flow at ORI, OH4, and VCU, with the DSM2 simulation with DCD better matching reported flow in July and August (Figures 2-24, 2-25, 2-26). This is readdressed from another perspective in Section 2.4 when discussing channel depletion estimates based on reported flow.

At the east end of Grant Line Canal at GLE, the DSM2-simulation matches the reported flow fairly well, particularly the DSM2 simulation with DICU (Figure 2-27). Nevertheless, at GLC the reported flow substantially deviates from the simulated flow (Figure 2-28). The reported flow in July and August of 400 to 600 cfs in the upstream direction is not realistic and this data is suspect.

In Paradise Cut at PDC, the reported flow during the irrigation season varies from 20 to 100 cfs, while the DSM2 simulations show virtually no net flow (Figure 2-29). It is likely that the DSM2 simulations fail to account for some source water flowing into Paradise Cut during this period. In contrast, the reported flow in Sugar Cut shows about 50 cfs more in the upstream direction in July and August than does the simulated flow (Figure 2-30). This would correspond to DSM2 underestimating the channel depletion in Sugar Cut.

Figure 2-21 Reported and DSM2-Simulated Flow at Old River Above Doughty Cut for 2015

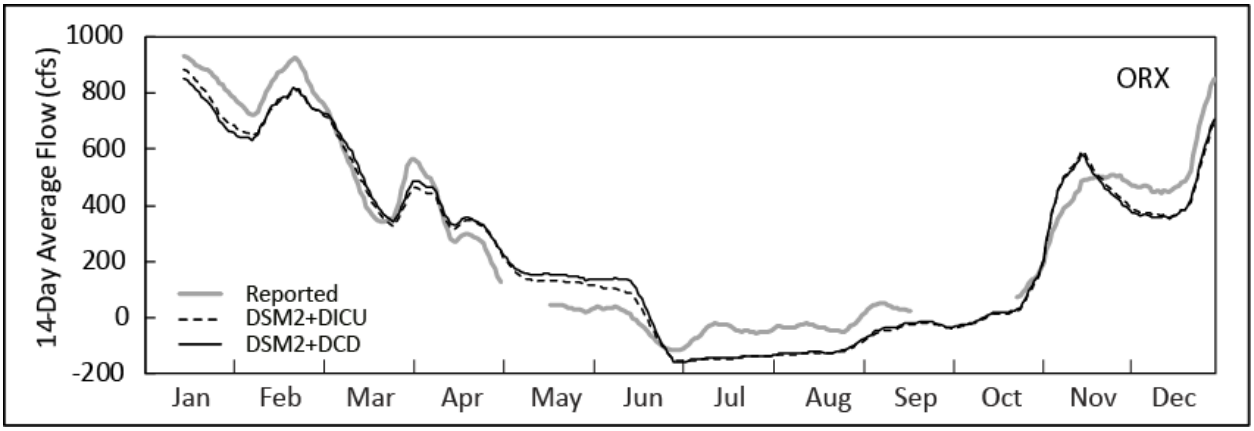

Figure 2-22 Reported and DSM2-Simulated Flow at Old River at Tracy Road for 2015

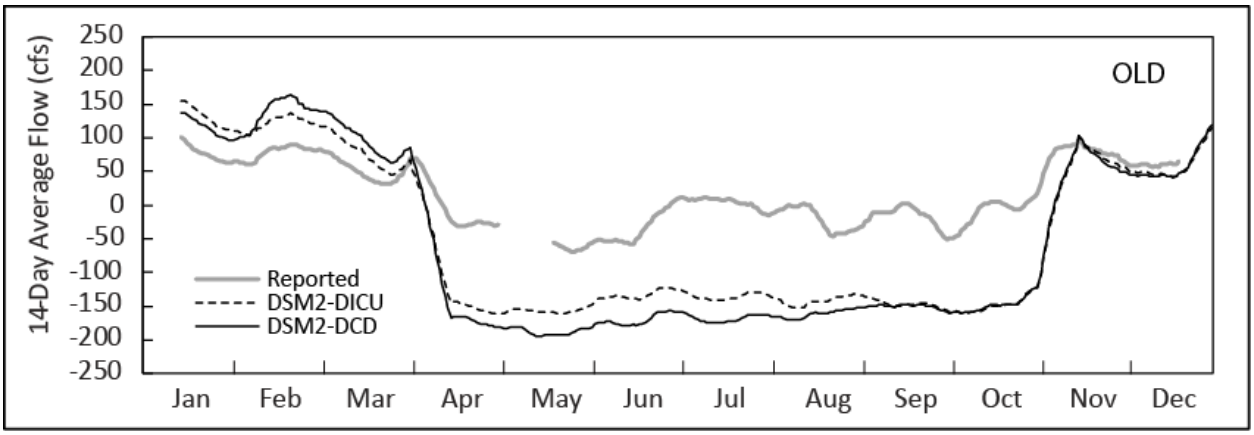

Figure 2-23 Reported and DSM2-Simulated Flow at Old River Above Barrier for 2015

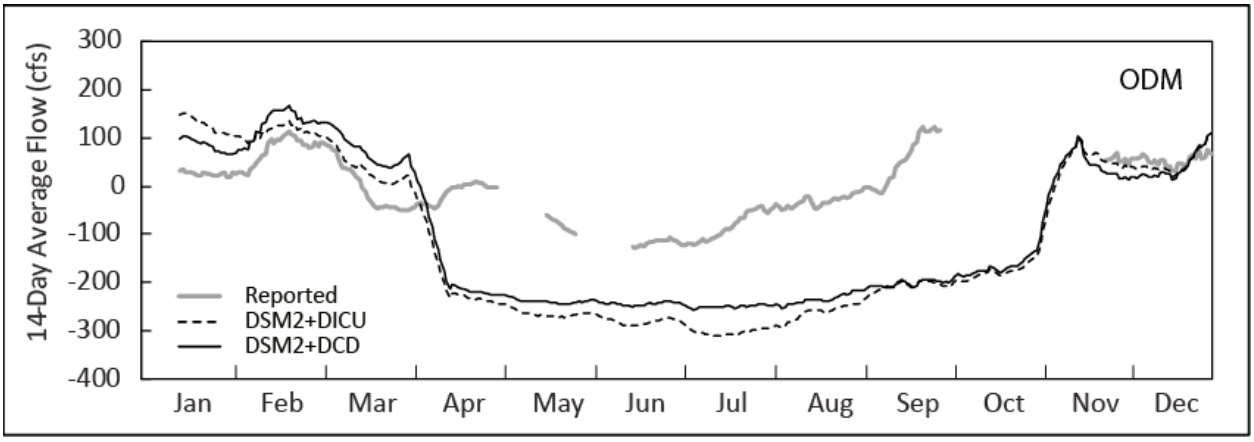

Figure 2-24 Reported and DSM2-Simulated Flow at Old River near Clifton Court Forebay for 2015

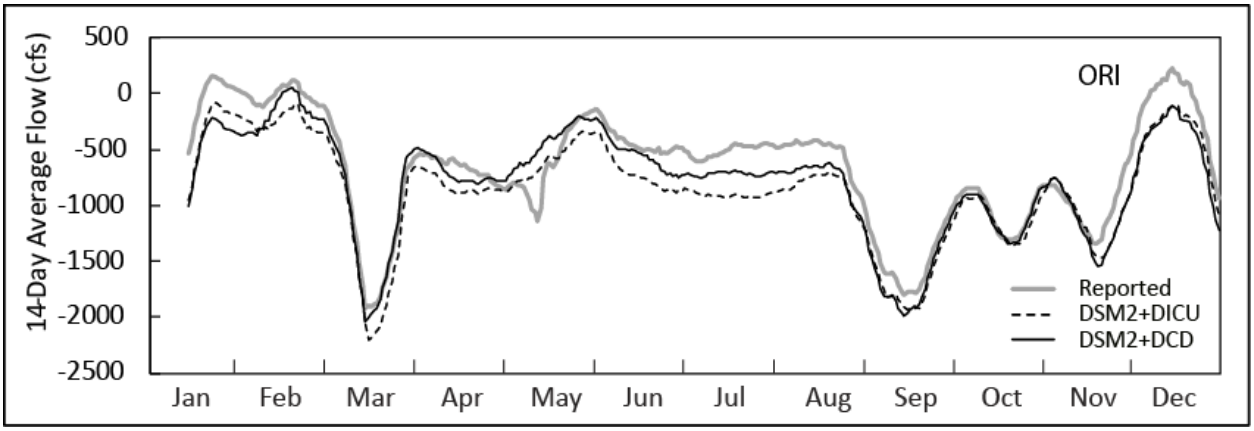

Figure 2-25 Reported and DSM2-Simulated Flow at Old River at Highway 4 for 2015

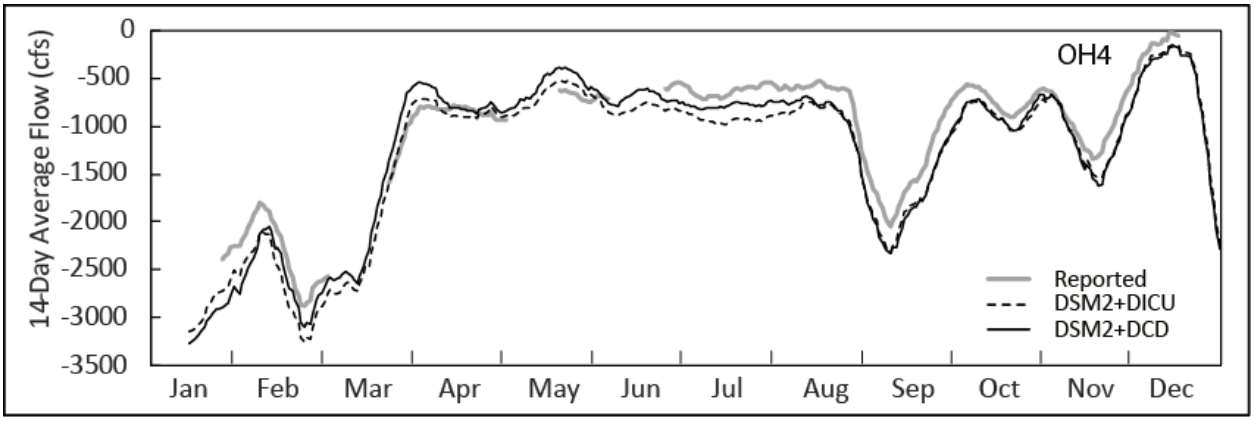

Figure 2-26 Reported and DSM2-Simulated Flow at Old River at Victoria Canal for 2015

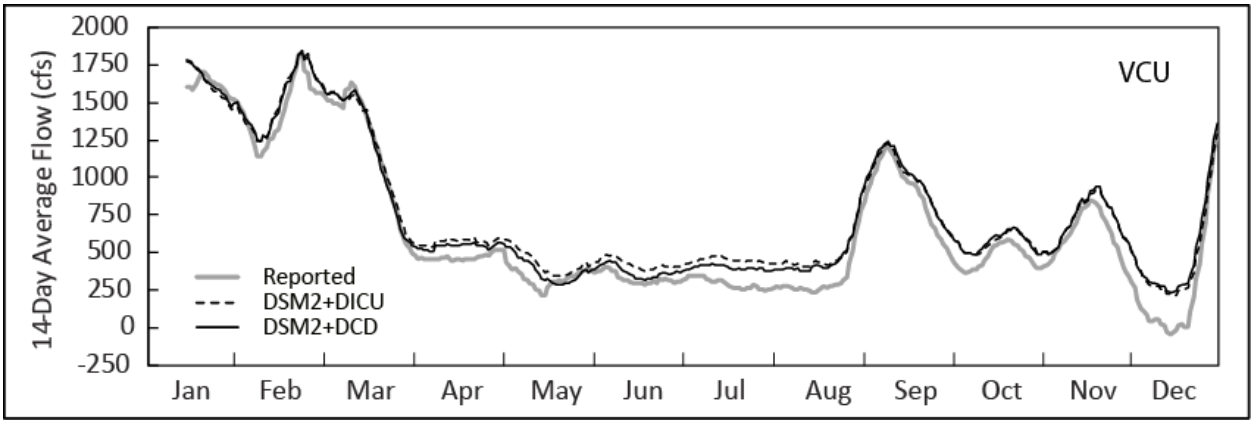

Figure 2-27 Reported and DSM2-Simulated Flow at Grant Line Canal East for 2015

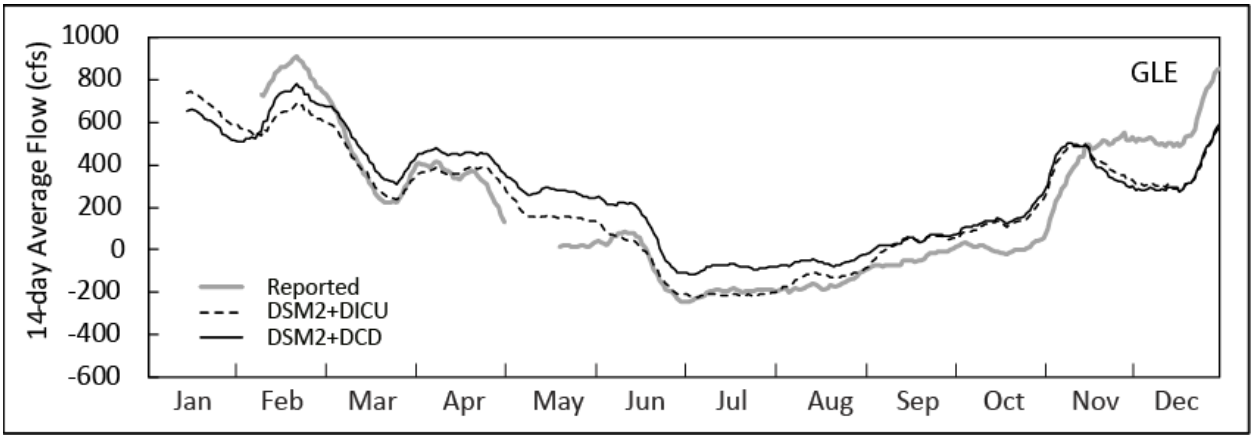

Figure 2-28 Reported and DSM2-Simulated Flow at Grant Line Canal West for 2015

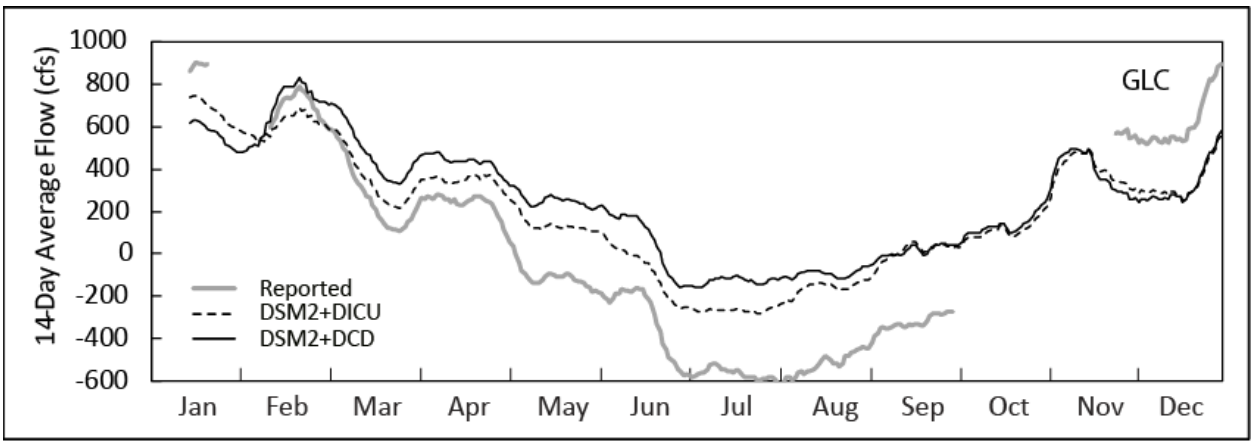

Figure 2-29 Reported and DSM2-Simulated Flow at Old River at Paradise Cut for 2015

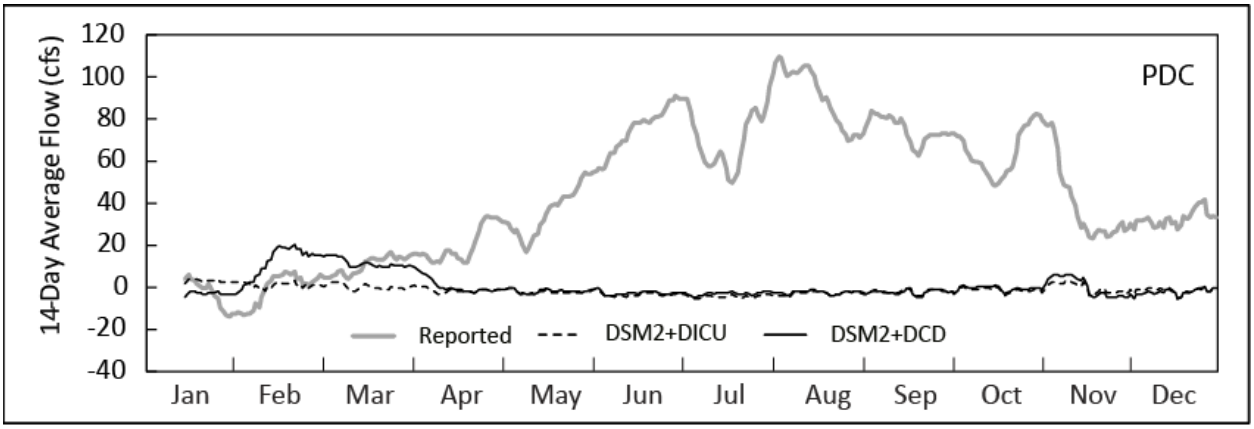

Figure 2-30 Reported and DSM2-Simulated Flow at Old River at Sugar Cut for 2015

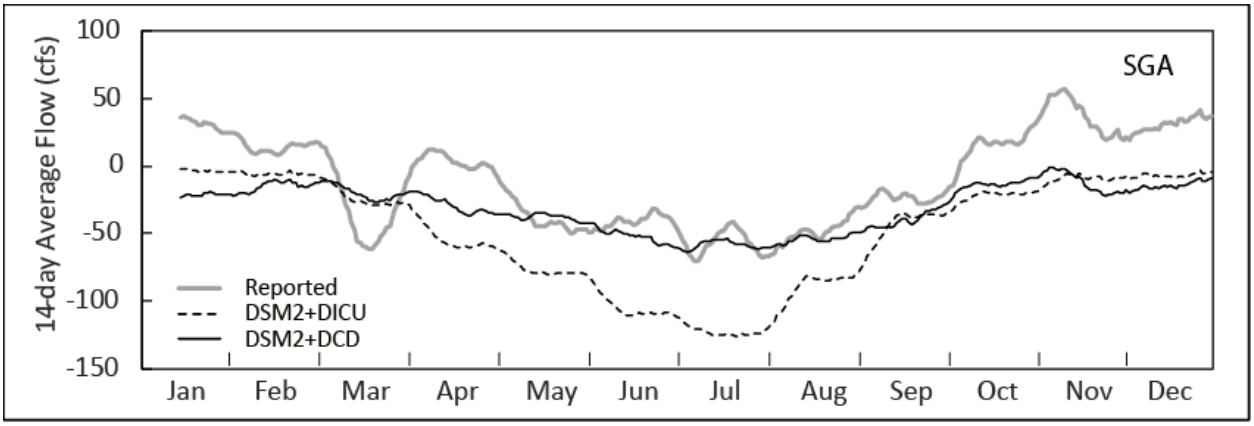

2.3.2 Reported and DSM2-Simulated Flow in Old and Middle Rivers (OMR)

Flow was simulated at the two OMR stations, Old River at Bacon Island (OBI) and Middle River (MDM), and is shown in Figures 2-31 and 2-32. Negative flow again indicates net flow upstream. DSM2 under DICU and DCD tended to underestimate the net flow upstream at OBI by about 250 to 300 cfs and overestimate negative flow at MDM by about 0 to 150 cfs. The combined reported and simulated OBI and MDM flow is shown in Figure 2-33, and the difference between combined simulated and reported OBI and MDM flow is shown in Figure 2-34.

The DSM2 simulation of OBI and MDM flow under both DICU and DCD channel depletion estimates match the reported flow well enough to be meaningful. DSM2 with DICU tracked closer to the estimates reported at OBI, while DSM2 with DCD tracked closer to the estimates reported at MDM.

Figure 2-31 Reported and DSM2-Simulated Flow at Old River at Bacon Island for 2015

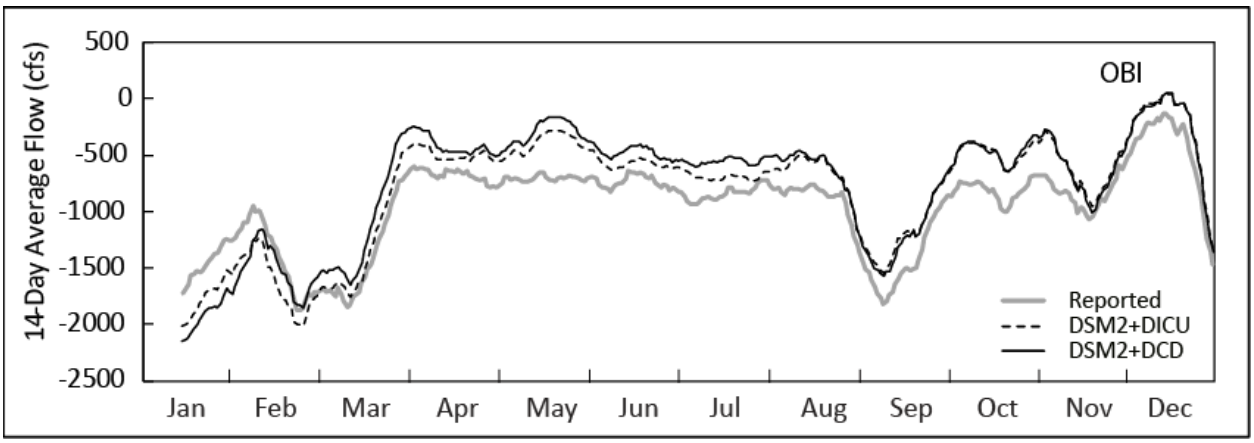

Figure 2-32 Reported and DSM2-Simulated Flow at Middle River at MDM for 2015

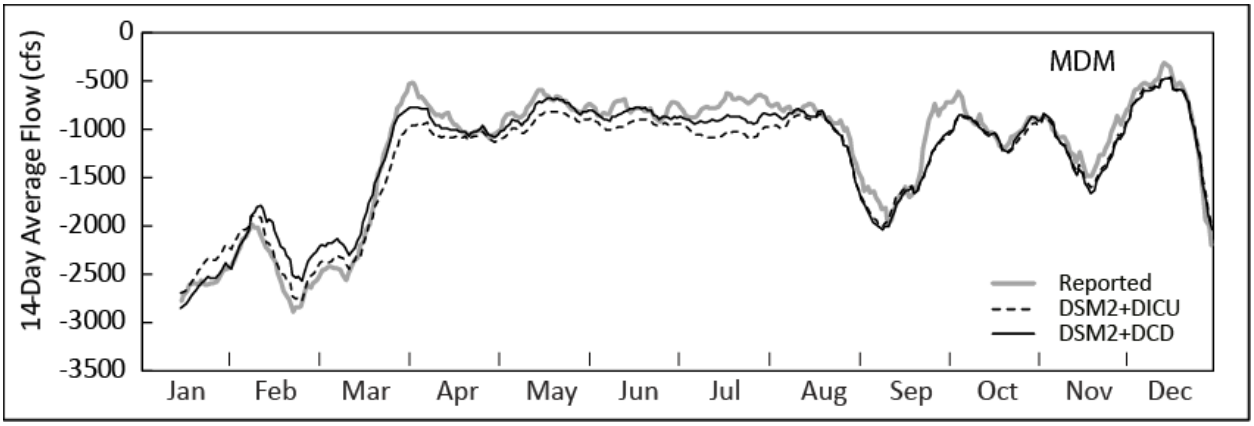

Figure 2-33 Reported and DSM2-Simulated Combined OBI and MDM Flow for 2015

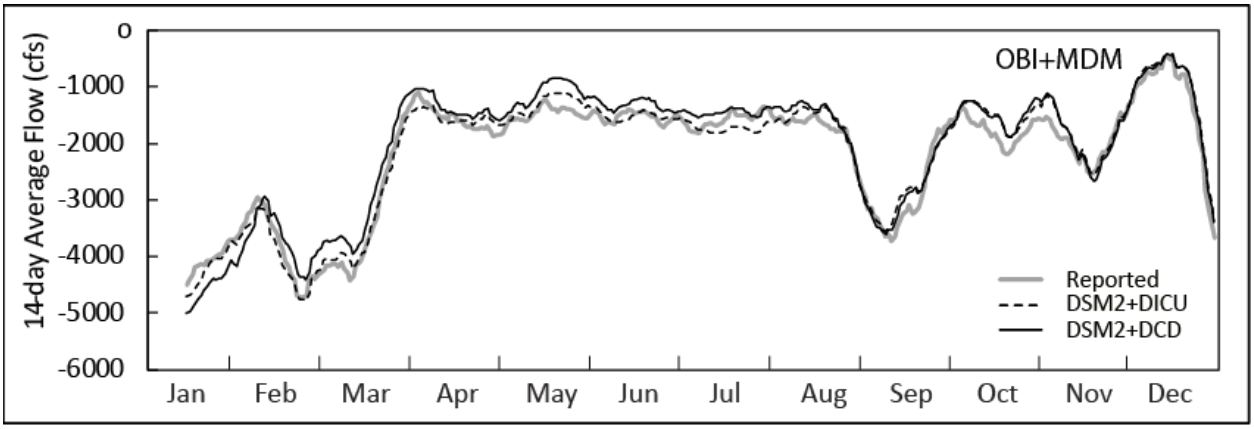

Figure 2-34 Difference Between Reported and DSM2-Simulated Combined OBI and MDM Flow for 2015

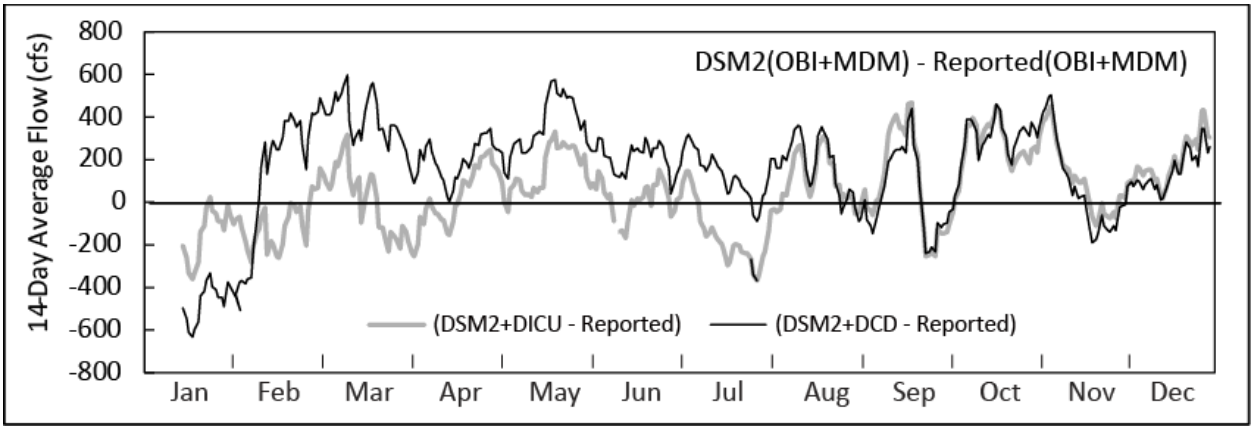

2.3.3 Circulation Patterns Based on Reported and DSM2-Simulated Flows in the South Delta

One of the difficulties in characterizing the meaningfulness of DSM2 historical condition simulations is the high variability of the factors that drive Delta hydrodynamics. How well a model reproduces historical conditions in the south Delta will always depend, at least somewhat, on the San Joaquin River inflows, State and federal water operations, the installation and operation of temporary barriers, and agricultural diversions and returns. Some conditions are less challenging to reproduce than others. For example, circulation patterns in the south Delta under high San Joaquin River inflows and no barriers tend to be well reproduced by DSM2. Under low-flow

conditions, errors in reported flow complicate any attempt to compare circulation patterns based on reported flow with those based on DSM2 simulations.

To present circulation patterns in a schematic format, average flows are found over specified periods of time when conditions that influence circulation are fairly constant: each barrier either completely installed or completely removed and fairly constant San Joaquin River inflows and water exports. The duration of these periods can vary. Since channel depletions change monthly in DICU, the longest period for which a circulation pattern is shown is one month.

Four periods were evaluated for this report: July 1–31, August 1–24, September 2–11, and September 15–30 (Figures 2-35 to 2-38). In all four periods all three temporary agriculture barriers were fully installed and operating and San Joaquin River inflow and the south Delta exports were low. The circulation patterns for the two DSM2 simulations are very similar in September but show some differences in July and August with the DCD-based simulation showing less flow up Grant Line Canal and Old River above the barrier when compared with the DICU-based simulation. But these differences are small when compared with those based on comparing DSM2 results against reported flow.

The DSM2 simulations with DICU and DCD consistently show substantially less flow up Grant Line Canal than is indicated from reported flows. But, as mentioned before, the reported flow at GLC seems in error. If reported flow at both GLC and GLE are correct, then about 280 cfs is consistently lost between GLE and GLC, and this is not realistic. The two DSM2 simulations show substantially more flow up Old River above the barrier compared to reported flows.

The overall impression of the flow schematics for July through September 2015 is that the DSM2 simulations fail to reproduce well the general circulation indicated by reported flow. Nevertheless, the uncertainty in the accuracy of at least some of the reported flow make assessment problematic at this time.

Figure 2-35 Period-Average Reported and DSM2-Simulated Flows for July 1–31, 2015

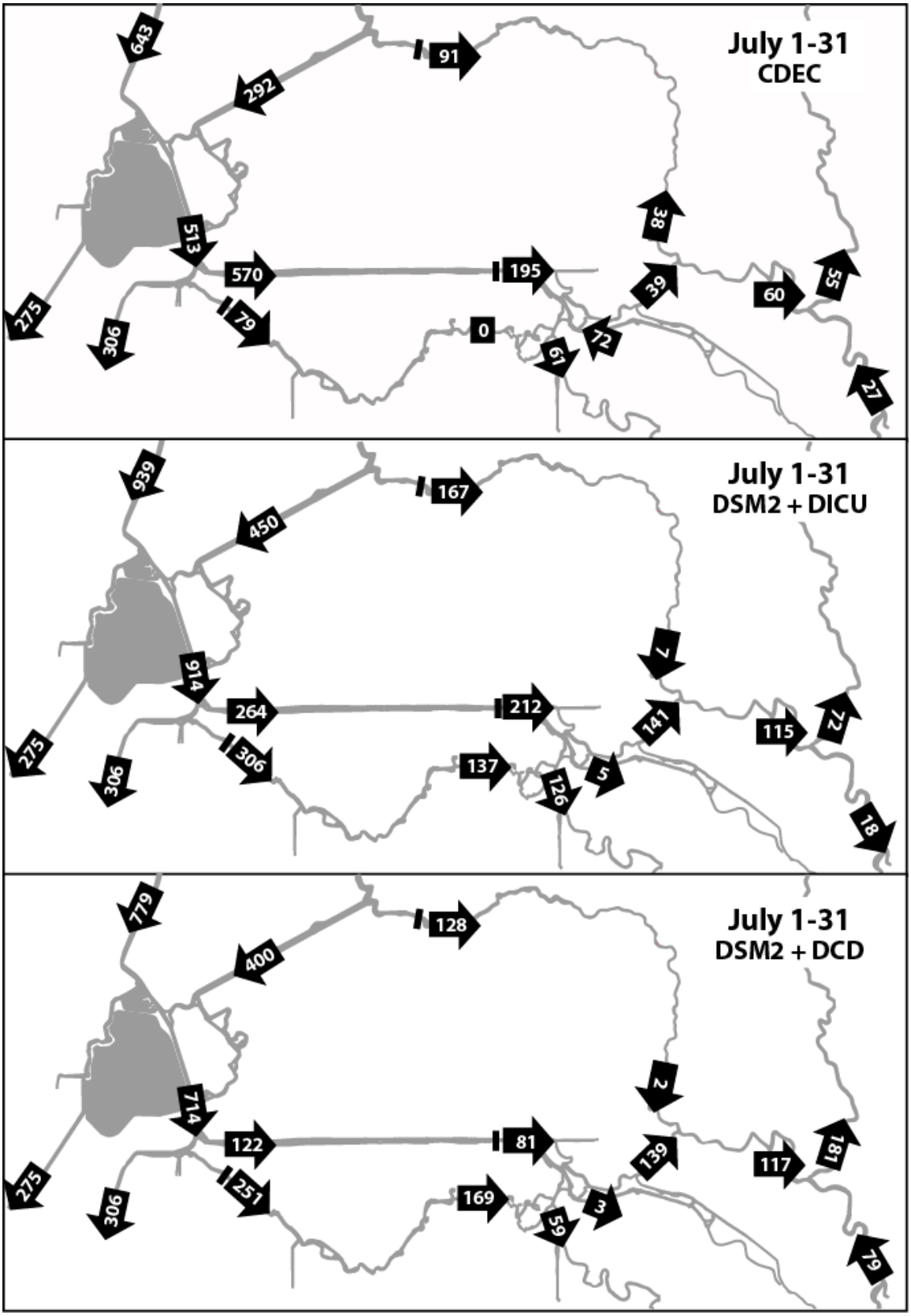

Figure 2-36 Period-Average Reported and DSM2-Simulated Flows for August 1–24, 2015

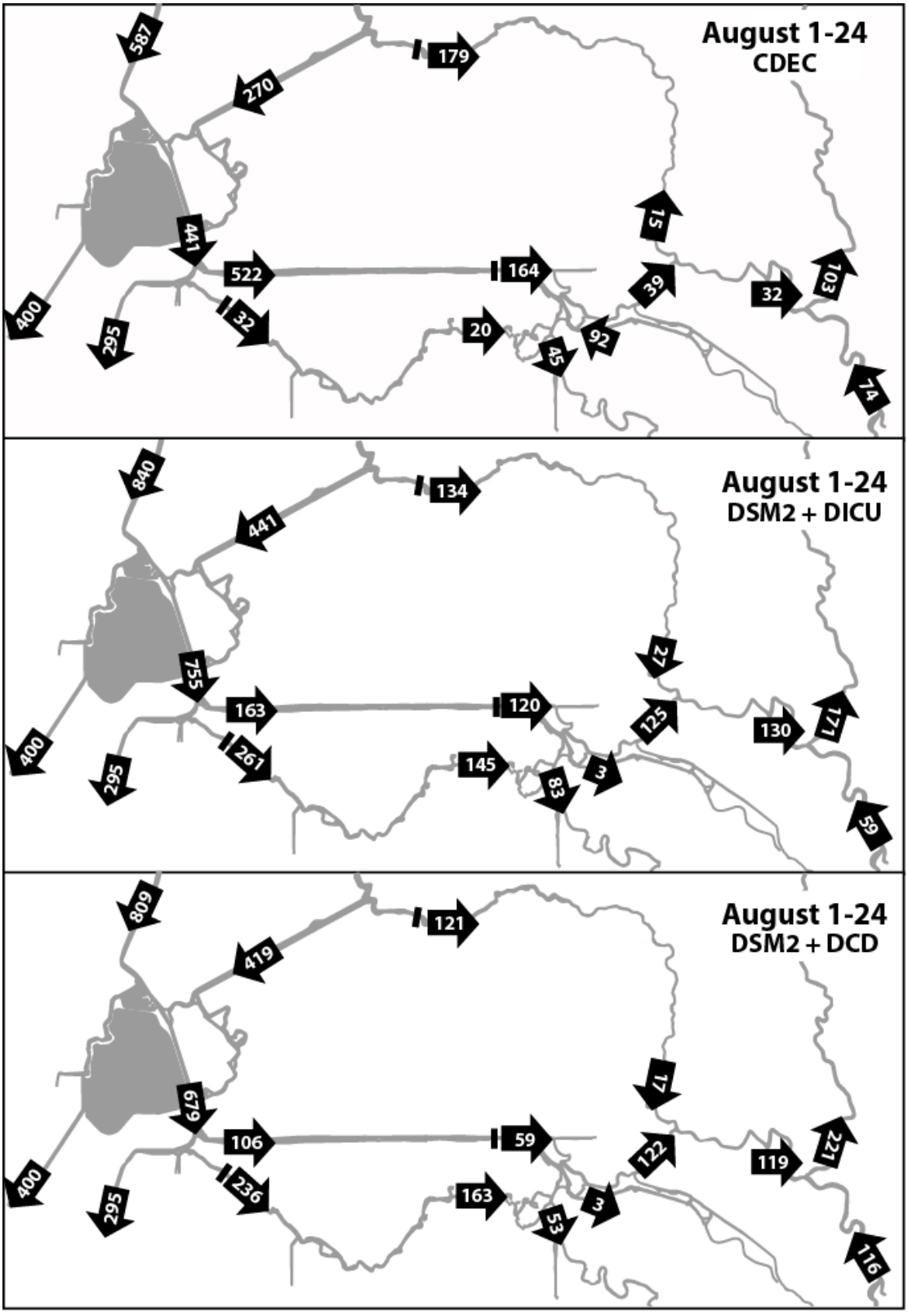

Figure 2-37 Period-Average Reported and DSM2-Simulated Flows for September 2–11, 2015

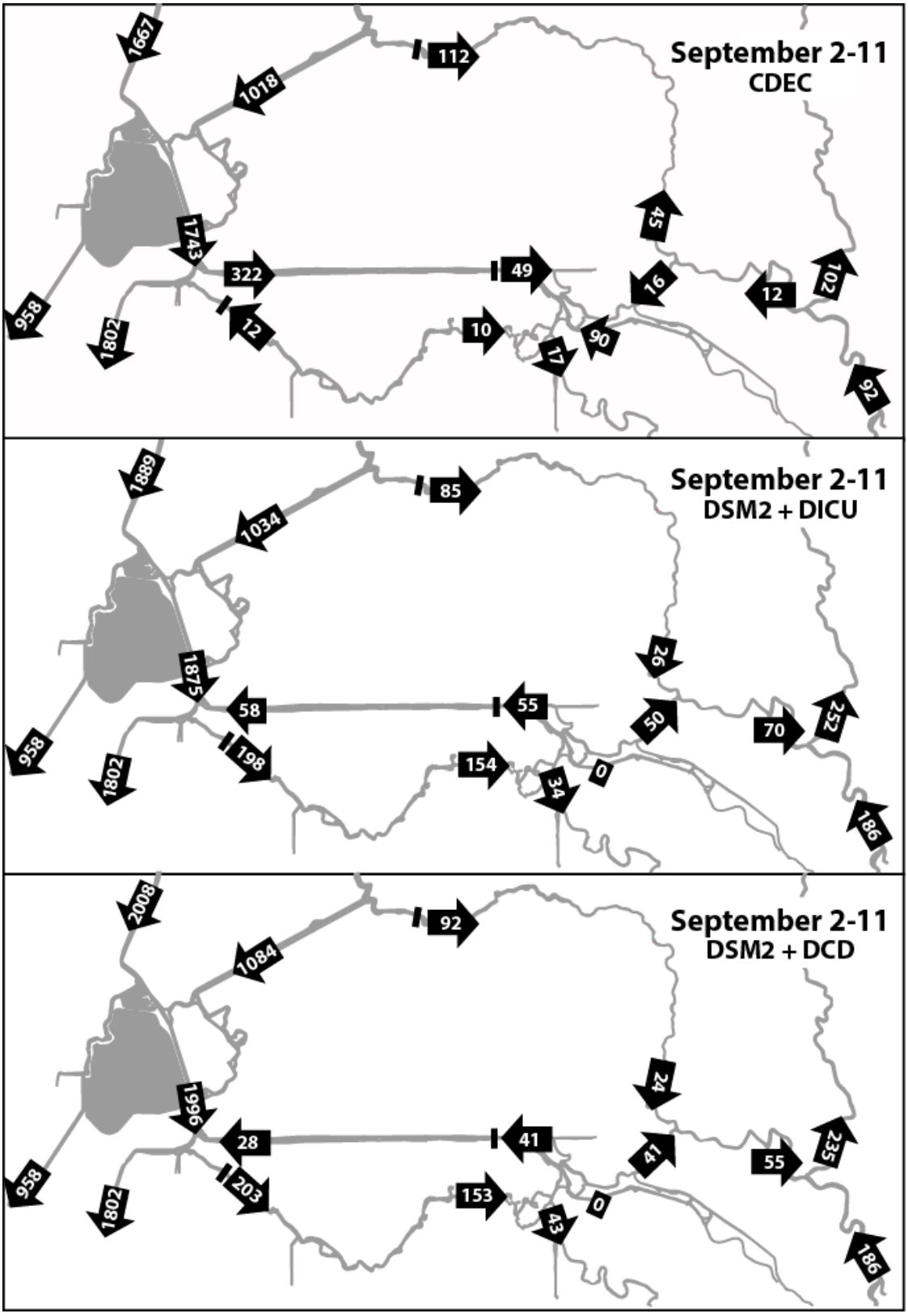

Figure 2-38 Period-Average Reported and DSM2-Simulated Flows for September 15–30, 2015

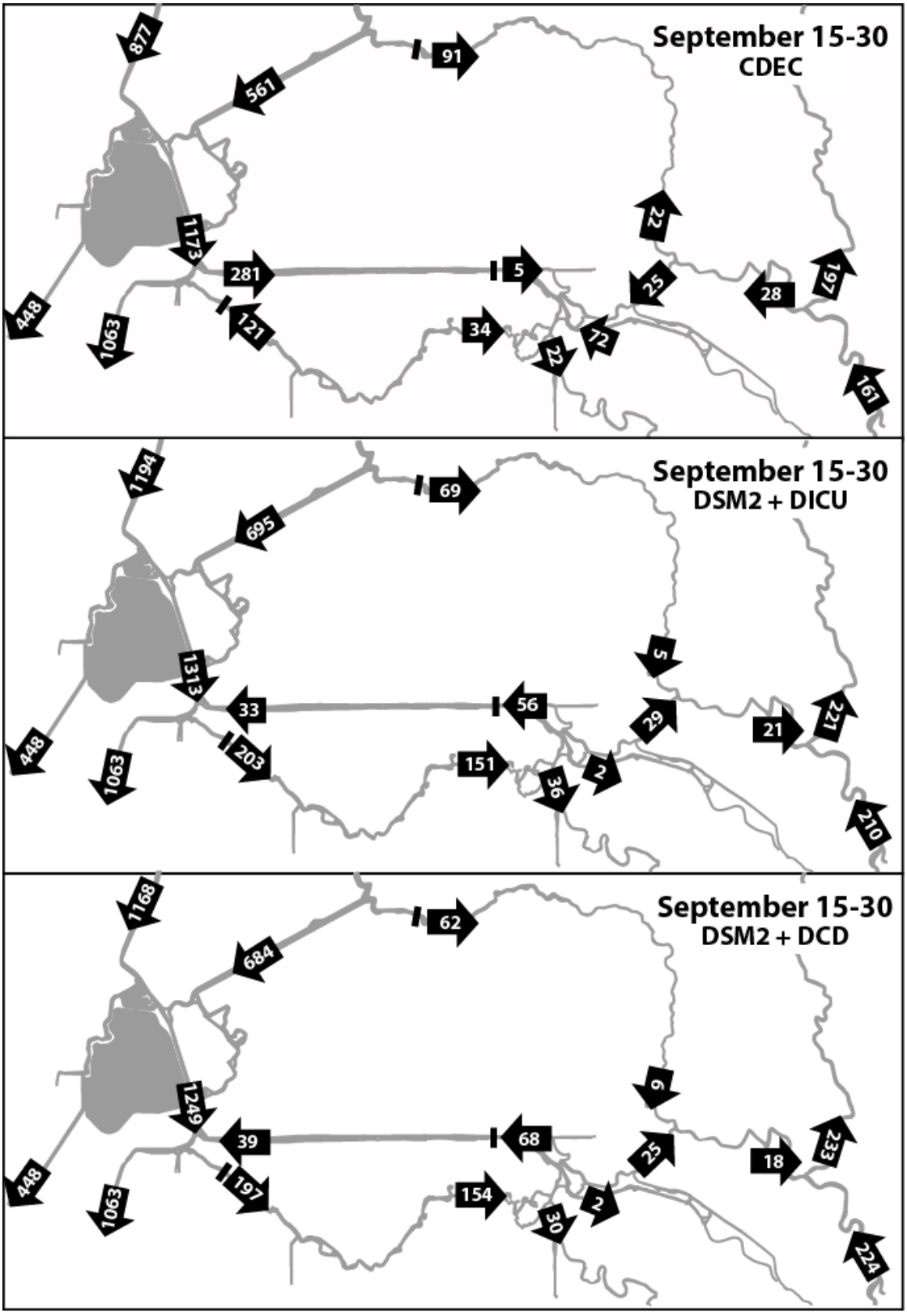

2.4 Estimating Delta Channel Depletions in the South Delta by Reported and DSM2-Simulated Flows Using DICU and DCD

The reported flows were used to estimate channel depletion over seven regions in the south Delta (Figures 2-39 and 2-40). For reference, these values were compared to one based on DSM2-simulated flows at the same locations.

Figure 2-39 Smaller Regions in South Delta Channel Where Depletion is Estimated for 2015

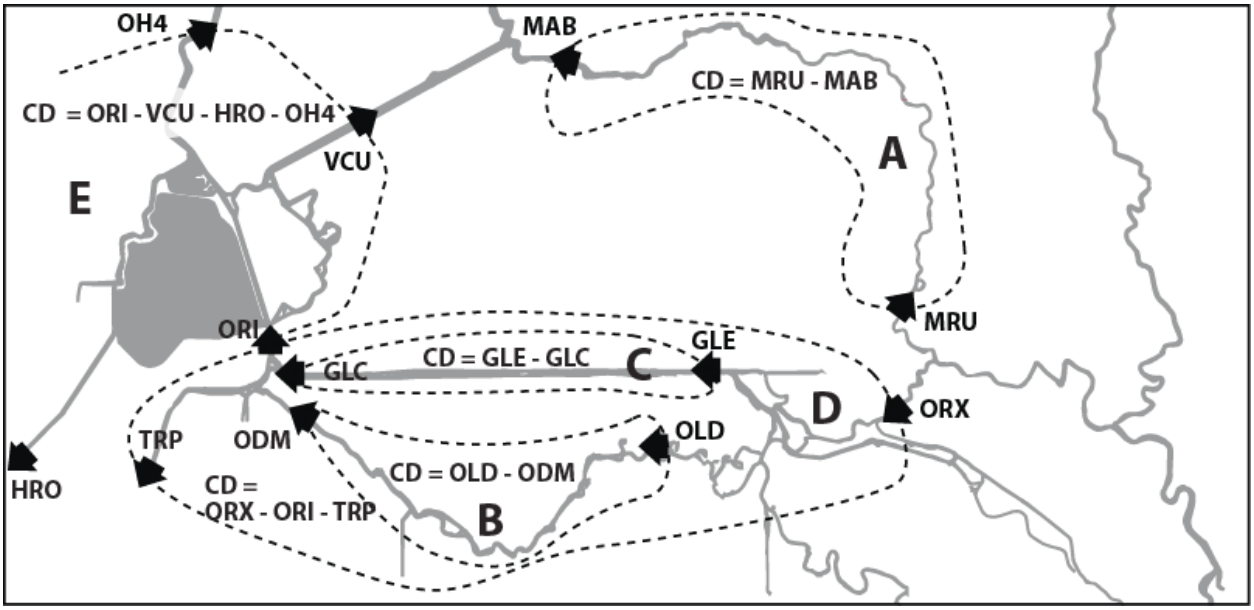

Figure 2-40 Larger Regions in South Delta Channel Where Depletion is Estimated for 2015

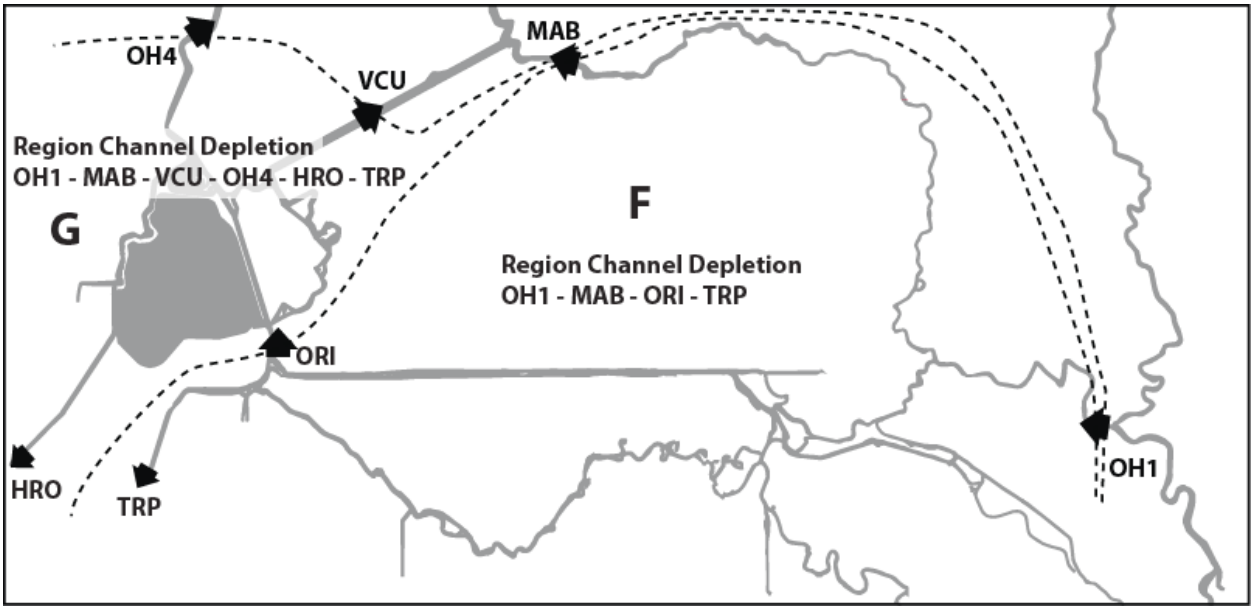

Despite the suspected error in reported flow at MAB in the second half of July, it does appear that in general, the reported flow-based estimate of channel depletion in Middle River is higher than that based on the DSM2 simulation based on both DICU and DCD (Figure 2-41). The suspected errors in reported flows at ODM and GLE in 2015 limit the meaningfulness of the estimates of channel depletion based on this year's reported flows in Old River and Grant Line Canal (Figures 2-42 and 2-43).

Figure 2-41 Estimated Channel Depletion in Middle River (Region A) for 2015

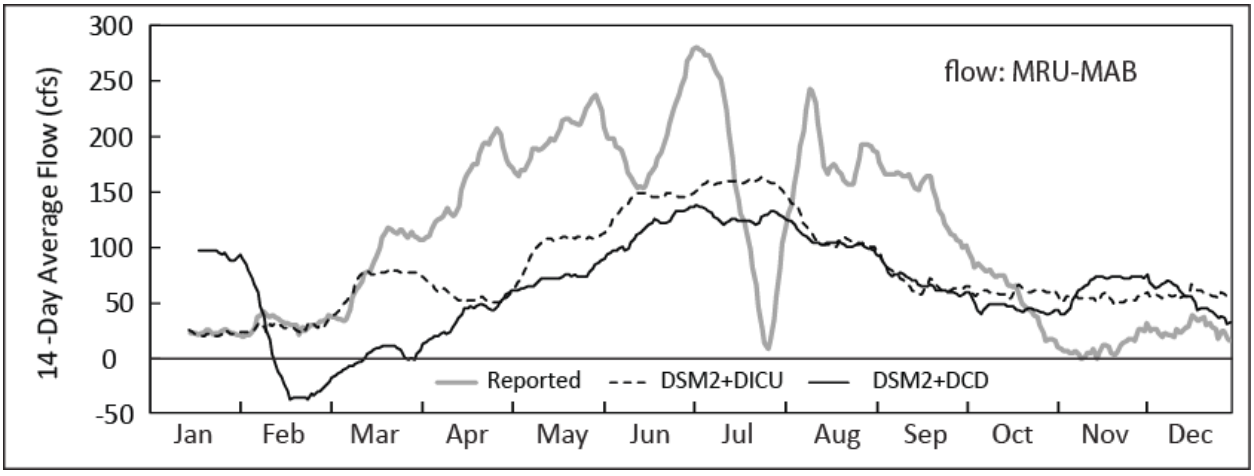

Figure 2-42 Estimated Channel Depletion in Old River (Region B) for 2015

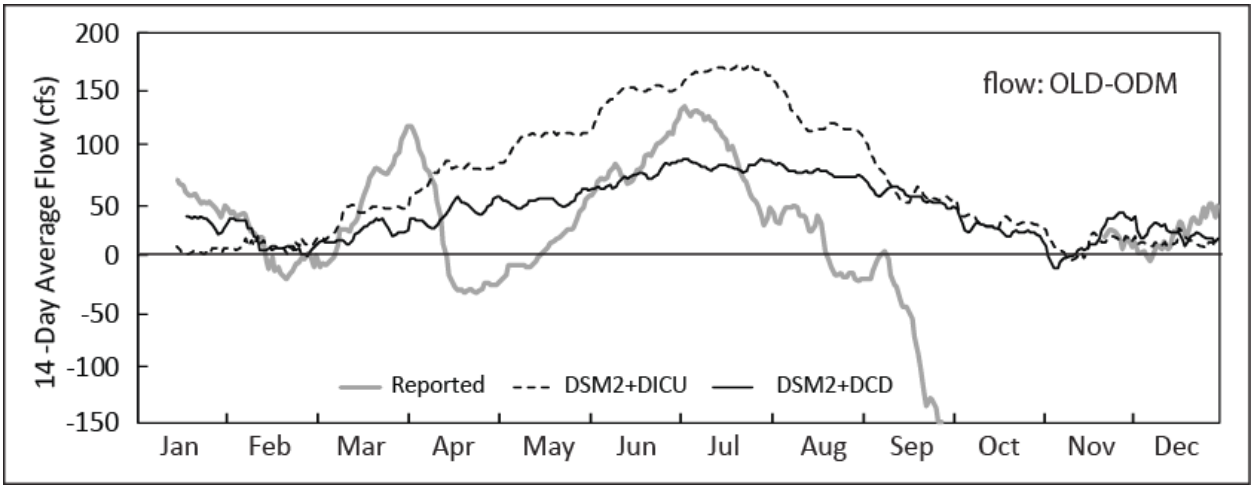

The channel depletion estimates for Region D (Old River and Grant Line Canal) are calculated by the ORX-ORI-TRP flows. Negative ORI flows indicate upstream flow into the control area. Channel depletion calculations for this region avoid the use of reported flows at GLC and ODM. Channel depletion estimates for this region based on reported flows do show peak depletions in July, but also show a fairly constant depletion from April through October. More variation over this period is usually expected. DSM2-simulated flows yield higher channel depletion estimates than do reported flows in Region D, with DCD-based DSM2-simulated flows yielding better matching depletion estimates than do DICU-based DSM2-simulated flows (Figure 2-44).

The channel depletion estimates for Region E (Old River and Victoria Canal) are calculated by flows (ORI-VCU-OH4-HRO). The depletion estimates based on DSM2-simulated flows matched the estimates based on reported flows in April, June, and July but deviated in August through November when channel depletion based on reported flows was as low as -200 cfs (Figure 2-45). A negative value for channel depletions indicates a net gain of water and would typically be seen in winter periods of rain. A gain of 200 cfs in Region E in August and September is not likely. The reported flows at OH4 and VCU deviated the most from DSM2-simulated flows and are a likely source of much of the error.

Figure 2-43 Estimated Channel Depletion in Grant Line Canal (Region C) for 2015

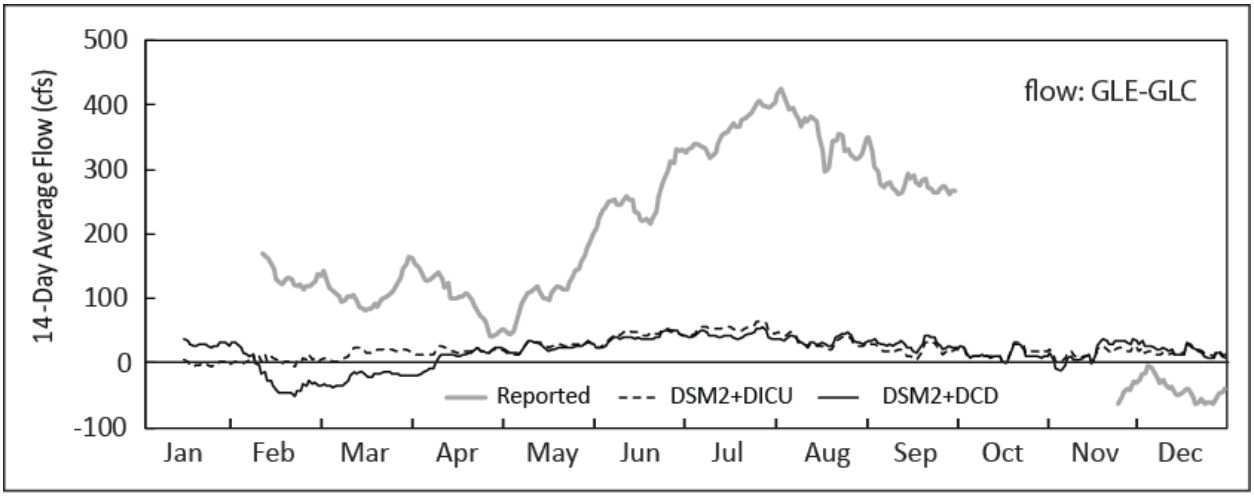

Figure 2-44 Estimated Channel Depletion in Old River + Grant Line Canal (Region D) for 2015

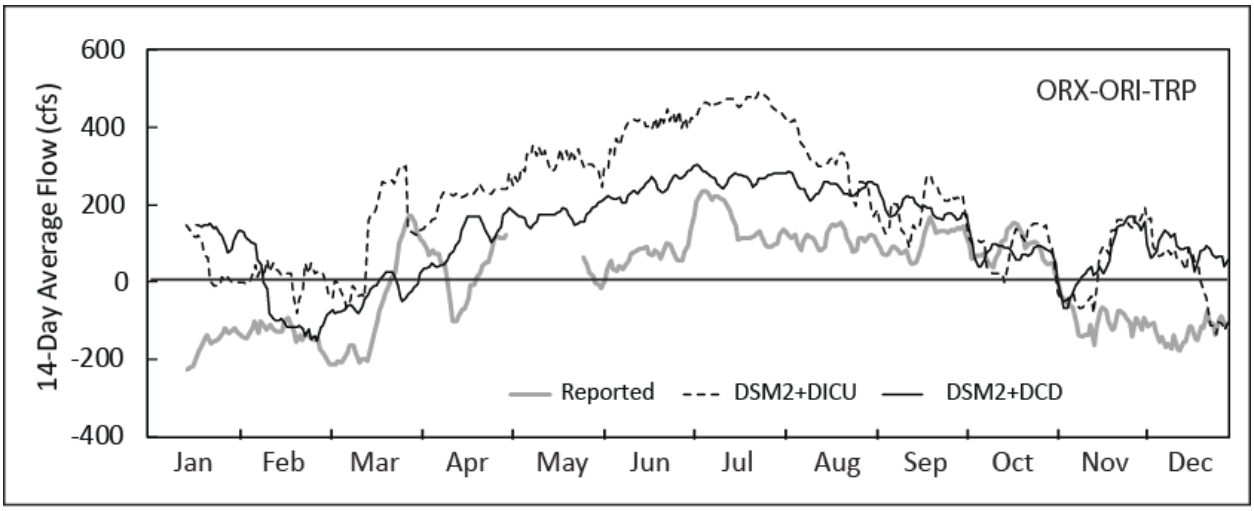

The channel depletion estimate for Region F (OH1-MAB-ORI-TRP) was based on reported flows that match fairly well with those based on the DSM2 simulation with DCD, with the exception of July (again likely a result of MAB reported flow errors) and November through December (Figure 2-46). The channel depletion estimate that was based on the DSM2 simulation with DICU exceeds the other two estimates by 100 to 350 cfs from April through mid-August, but then closely follows in September and October.

The channel depletion estimate for Region G (OH1-MAB-VCU-OH4-HRO-TRP) that was based on reported and DSM2-simulated flow does not match as well for Region F, particularly from August through December (Figure 2-47). The error in reported MAB flow in July drives the channel depletion estimate down as before, and depletion estimates based on DSM2-simulated flow with DICU were again higher than those based on DSM2 with DCD. Figure 2-48 shows the channel depletions from Region F and G for 2015 based on reported flows. The channel depletion in Region F should be less than that for Region G during the irrigation season since Region F is a subregion of G. Nevertheless, the Region F channel depletion estimate using reported flows exceeds that for Region G from mid-August through October. This error is likely based on the reported flows at VCU and OH4. The channel depletion in Region G during the winter is more negative than for Region F, as is expected, as rain falls over a larger area. For comparison, channel depletion based on DSM2-simulated flow for DICU and DCD is shown in Figures 2-49 and 2-50.

Figure 2-45 Estimated Channel Depletion in Old River + Victoria (Region E) for 2015

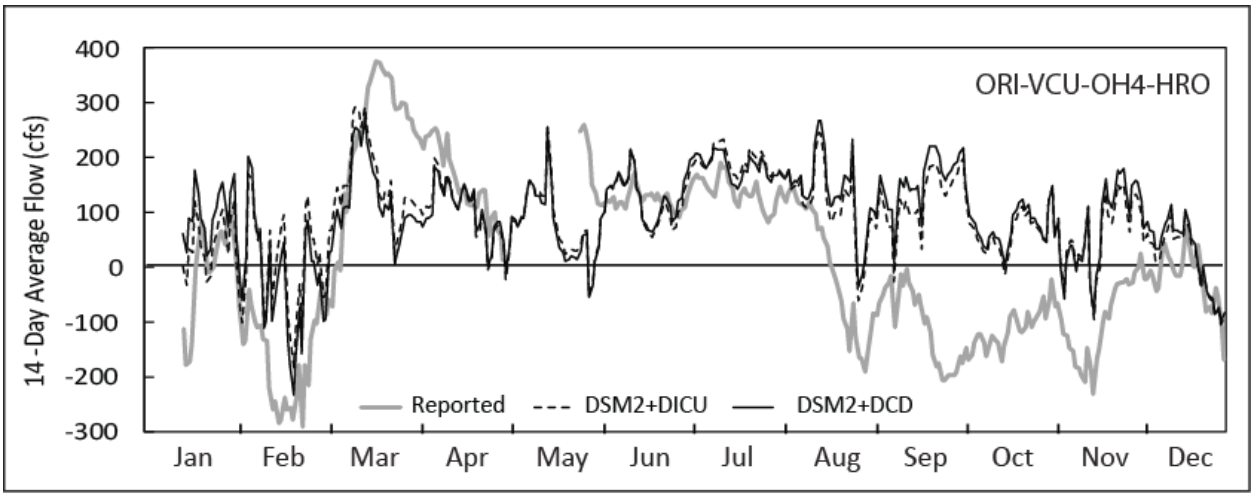

Figure 2-46 Estimated Channel Depletion in South Delta without Clifton Court (Region F) for 2015

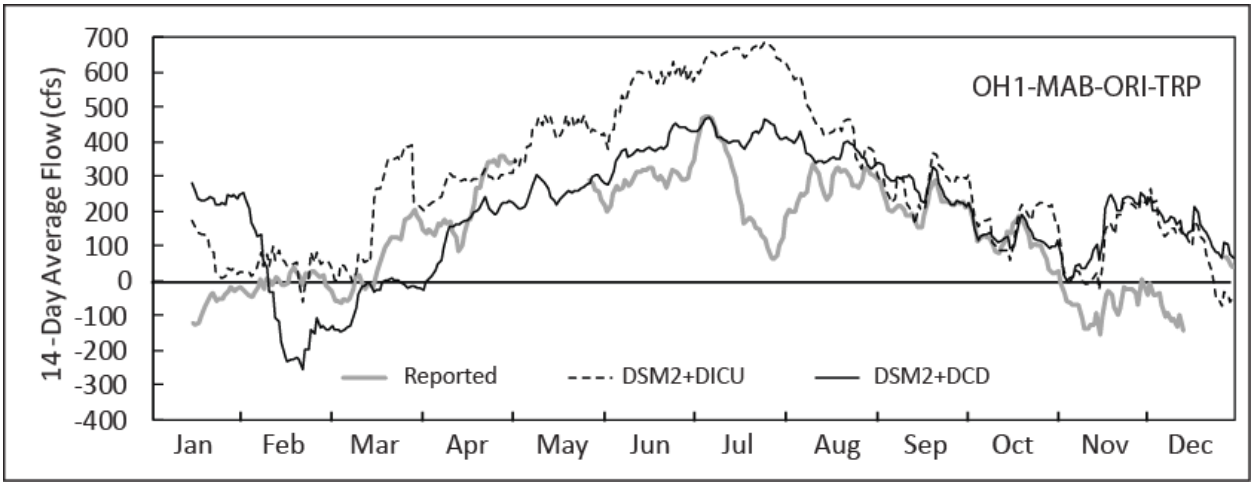

Figure 2-47 Estimated Channel Depletion in South Delta with Clifton Court (Region G) for 2015

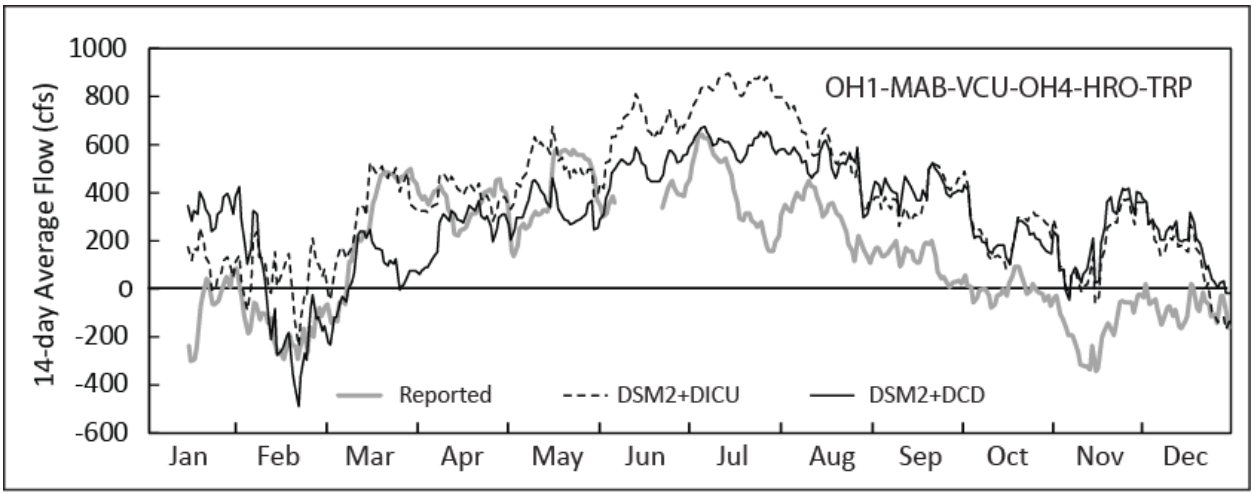

Figure 2-48 Channel Depletion in Regions F and G Based on Reported Flows for 2015

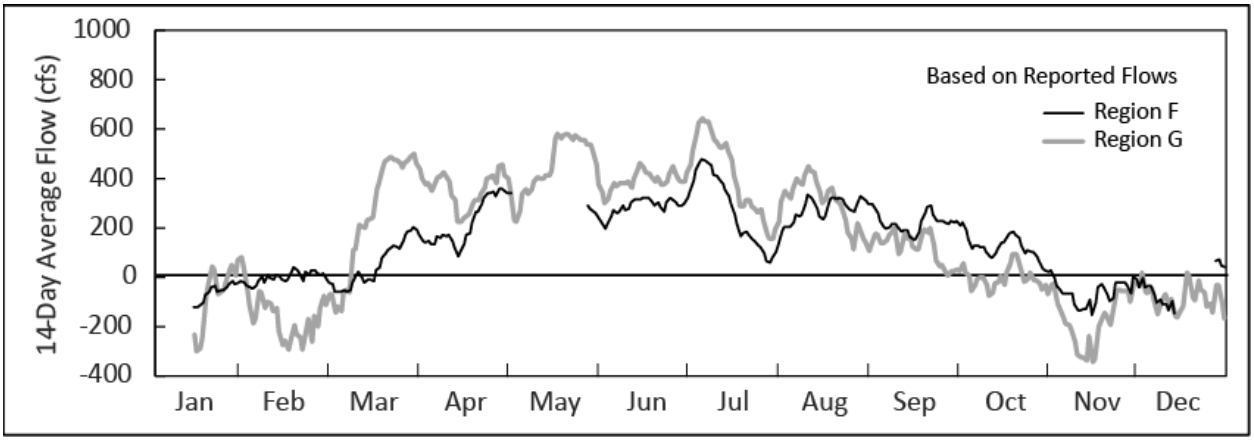

Figure 2-49 Channel Depletion in Regions F and G Based on DSM2 Simulation with DICU for 2015

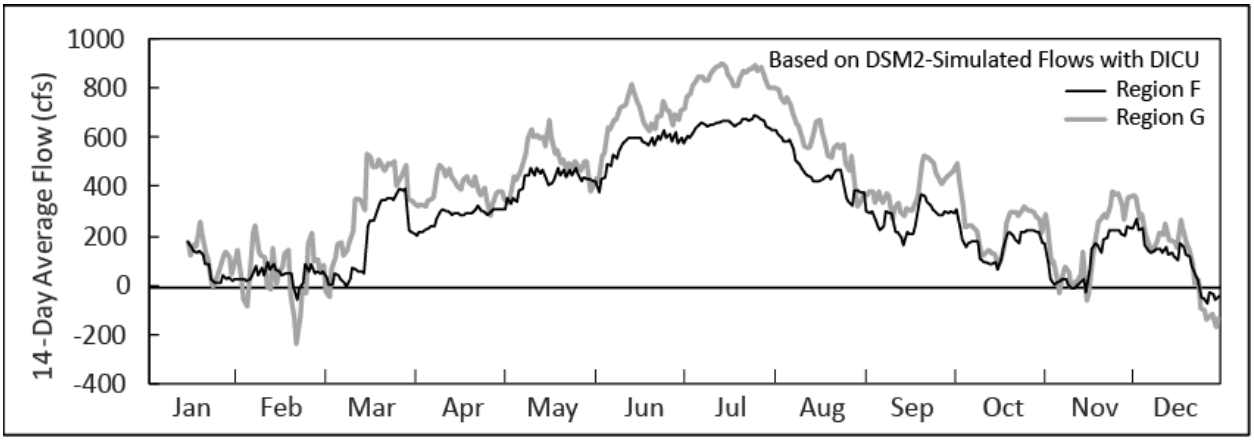

Figure 2-50 Channel Depletion in Regions F and G Based on DSM2 Simulation with DCD for 2015

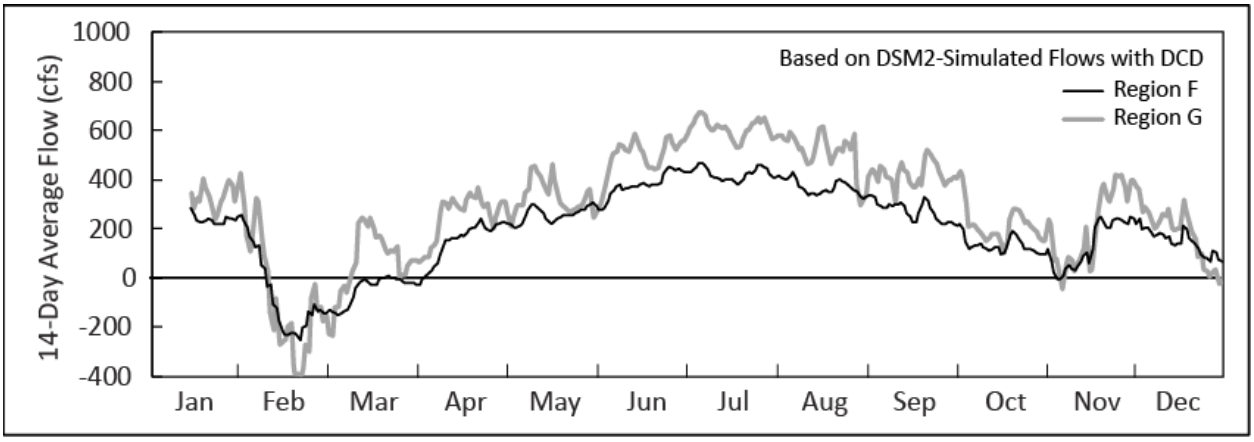

2.5 Conclusion

DSM2 simulation of flows in the south Delta and OMR stations generally replicated the reported flow for 2015. Where reported and simulated flow deviated widely, the reported flow was suspect. At specific locations, flows based on DSM2 simulations under DICU and DCD are generally close, with flow under DCD less than DICU in the upstream direction during the corresponding irrigation season. This is consistent with DCD estimating less channel depletion in the south Delta so there is less draw upstream to the area.

South Delta flow schematic results based on reported and DSM2-simulated flows under the conditions experienced in 2015, such as low pumping and low San Joaquin River inflow, are mixed. This is partly because of errors in reported flow at CLC and ODM. More work is needed in this area, perhaps repeating this analysis for other years during the 2012–2016 drought.

The reported and simulated flows in Middle River (MAB and MRU) are consistent with the notion that both DICU and DCD underestimate channel depletion in Middle River. Similarly, reported and simulated flow in Paradise Cut are consistent with assertions that DICU and DCD fail to account for drainage into Paradise Cut.

Using reported flows to estimate channel depletion in the south Delta has some promise, at least for larger areas such as Region F. There needs to be

a better understanding of how the reported flows values are generated, namely their accuracy under lower flow conditions, because the kinds of errors seen in 2015 were not evident in earlier years. Simulated flows should be able to help identify problems in reported flows on a near real-time basis in the future.

2.6 References

California Department of Water Resources. *DAYFLOW: An Estimate of Daily Average Delta Outflow*. Sacramento (CA): Division of Environmental Services. 25 pp. Viewed online at: https://water.ca.gov/-/media/DWR-Website/Web-Pages/Programs/Environmental-Services/Compliance-Monitoring--Assessment/Dayflow/Files/Publications/Current-Dayflow-Documentation.pdf.

Liang L and Suits R. 2017. "Chapter 3: Implementing DETAW in Modeling Hydrodynamics and Water Quality in the Sacramento-San Joaquin Delta." In: Methodology for Flow and Salinity Estimates in the Sacramento-San Joaquin Delta and Suisun Marsh. 38th Annual Progress Report to the State Water Resources Control Board. Sacramento (CA): California Department of Water Resources. Bay-Delta Office.

Methodology for Flow and Salinity Estimates in the Sacramento-San Joaquin Delta and Suisun Marsh

40th Annual Progress Report
June 2019

Chapter 3
2018 Suisun Marsh Salinity Control Gates Pilot Study: Water Cost Analysis

Authors: Yu Zhou, Minxue He, Nicky Sandhu
Delta Modeling Section
Bay-Delta Office
California Department of Water Resources


DEPARTMENT OF WATER RESOURCES
STATE OF CALIFORNIA

Contents

Figures

Tables


DEPARTMENT OF WATER RESOURCES
STATE OF CALIFORNIA

3 2018 Suisun Marsh Salinity Control Gates Pilot Study: Water Cost Analysis

3.1 Introduction

The Delta Smelt Resiliency Strategy (California Natural Resources Agency 2016) calls for summer operation of the Suisun Marsh Salinity Control Gates (SMSCG) to reduce salinity and improve habitat in the Suisun Marsh during summer months in above normal (AN) and below normal (BN) water years. To better understand the benefits and impacts of this operation, the California Department of Water Resources (DWR) conducted a pilot project to operate the SMSCG during August 2018. To support the pilot project, the Delta Modeling Section (DMS) of DWR's Bay-Delta Office was tasked with: (1) assessing potential influence of the operation on salinity at key Delta water quality compliance locations via Delta Simulation Model II (DSM2); and (2) estimating water cost to maintain salinity within the compliance standards. This chapter summarizes the results and findings of DMS' analysis.

3.2 Approach

3.2.1 Suisun Marsh Salinity Control Gates Operations

The SMSCG facility, installed by DWR in 1988, is located on Montezuma Slough in the Suisun Marsh (Figure 3-1). The facility consists of three 36 foot (ft)-wide radial gates, one 20 ft-wide boat lock, and flashboards totaling 120 ft in width. This facility is typically operated from October to May (control season), as needed, to reduce salinity in the marsh. During the control season, the flashboards remain installed so that there is no flow passing through them. The boat lock is operated, when needed, to allow vessels to pass. Operation of the gates is triggered when salinity measurements at salinity compliance locations within the marsh are expected to exceed salinity targets set by Water Right Decision 1641 (D1641) as well as the Biological Opinions of the National Marine Fisheries Service (NMFS) and the U.S. Fish and Wildlife Service (USFWS). Once triggered, the gates are operated to reduce salinity in the marsh until all of the Marsh objectives are met. When in operation, the gates are open on ebb tides so that fresh water from the Delta can flow into Montezuma Slough and the surrounding marsh; on flood tides, the gates are closed to retain fresher water and reduce more saline water flowing into the marsh. Outside the

control season (June–September), the gates are open, the flashboards are removed, and the boat lock is closed.

Figure 3-1 Location Map of the Suisun Marsh Salinity Control Gates

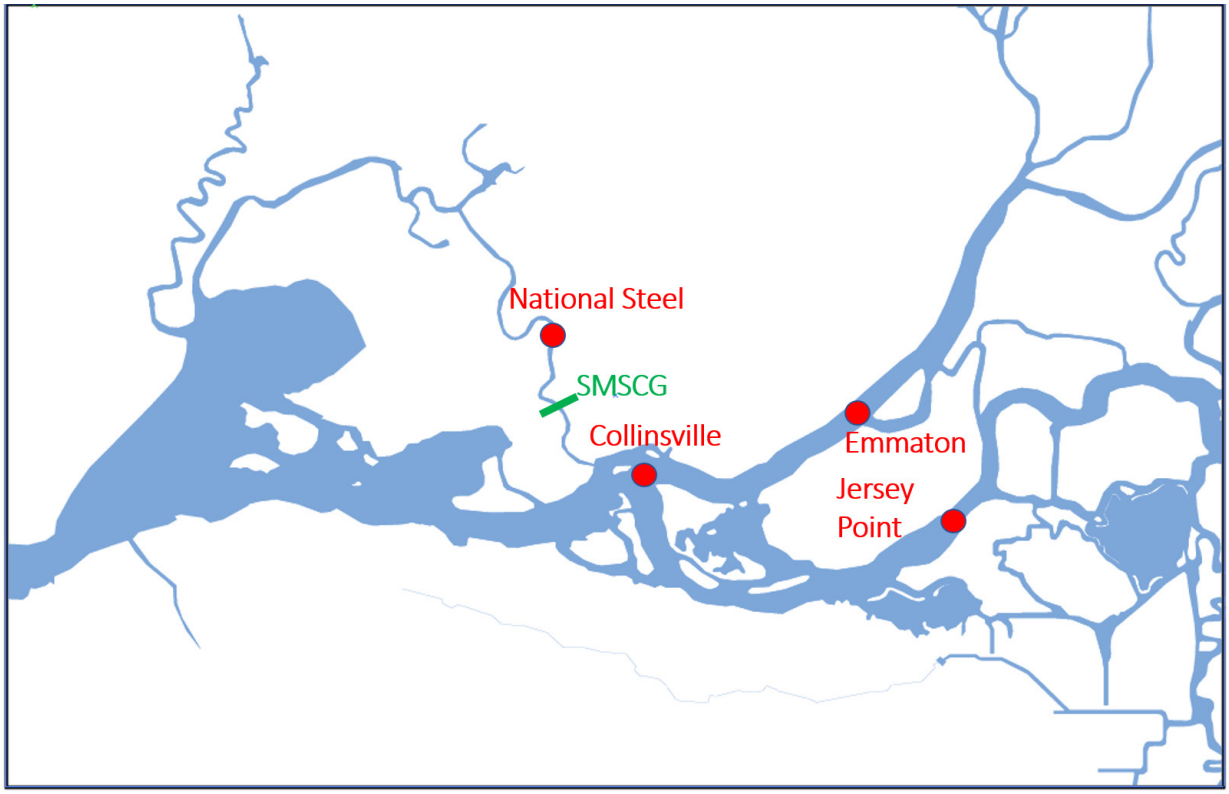

In the pilot project, changes to typical SMSCG operations focused on the non-control period. Specifically, in August, the gates were operated as they typically would be during the control season (Table 3-1). In September, the gates were open; however, the flashboards remained installed and the boat locks were operated. During June–July, operations remained typical.

Table 3-1 Typical and Proposed SMSCG Operations

Season	Period	Radial Gates	Flashboards	Boat Lock
Control Season (Typical)	October–May	Tidally-operated	In place	In operation
Non-Control Season (Typical)	June–September	Open	Removed	Not in operation
Non-Control Season (2018 Pilot Project)	June–July	Open	Removed	Not in operation
Non-Control Season (2018 Pilot Project)	August	Tidally-operated	In place	In operation
Non-Control Season (2018 Pilot Project)	September	Open	In place	In operation

3.2.2 DSM2 Modeling

DSM2 was initially configured in the historical simulation mode to run synthetic gate re-operation scenarios in two representative years: 2005 (above normal) and 2012 (below normal). The results show that the re-operation increases electrical conductivity (EC) at Jersey Point in both years, and the increases show up in mid-August and last until late October. The results also indicate that, in 2005, the re-operation increases EC during September at Collinsville. At other compliance stations, the impacts of gate re-operation are limited and are not likely causing any compliance problems. Based on these historical simulation results, the water quality compliance constraints of the re-operation are mainly the standards at Jersey Point (in both above and below normal years) and Collinsville (above normal years only).

The focus of this study is using the forecasting mode to predict the effects of August SMSCG operation on salinity in the Delta and conduct relevant water cost analysis for the 2018 pilot re-operation project. The model requires three types of inputs in general: hydrology, water quality, and facility operations. Hydrological inputs include boundary inflows, Delta Island Consumptive Use (DICU), and deliveries forecast by DWR Division of Operations and Maintenance (O&M) on a monthly basis. Water quality inputs

are generated in-house using forecasting scripts. Operations of the Delta Cross Channel and Clifton Court Forebay Gate are based on O&M's forecasts as well. Operations of the south Delta Temporary Barriers follow historical operations. Operation of the SMSCG during the non-control period is configured in DSM2 to reflect the proposed changes (Table 3-1).

The following table lists the scenarios covered in this chapter. Each scenario is named after the month when its hydrology forecasts are provided (Table 3-2). Each scenario contains two cases: Base (no gate operation) and Re-operation (gate operation in August). The impact is evaluated in terms of the difference between the Base condition and the Re-operation condition. The control variable is the water cost source (e.g., either additional inflow from Sacramento River at Freeport or export reductions in order to meet standards).

Table 3-2 Study Scenarios Included in This Chapter

Scenarios	Water Year Type	Results in Section	Control Variable
January BN	Below Normal	3.3.1	Sacramento Inflow
January AN	Above Normal	3.3.1	Sacramento Inflow
May	Below Normal	3.3.2	Banks Export
May (no-harm)	Below Normal	3.3.3	Banks Export

3.2.3 Water Quality Standards

After examining water quality and flow standards for the re-operation period, three key standards are considered for this study:

1. D1641 Objective at Jersey Point: maintain electrical conductivity (EC) at Jersey Point below 450 microsiemens per centimeter (µs/cm) from April 1 to June 20, below 740 µs/cm from June 21 to August 15 in below normal years, and below 450 µs/cm from April 1 to August 15 in above normal years.
2. Guidance Standard at Jersey Point: maintain EC at Jersey Point below 1640 µs/cm year-round.
3. Fall distance in kilometers from the Golden Gate Bridge to the point where the salinity on the bottom is about 2 parts per thousand (ppt) (X2): for September and October, NMFS and FWS Biological Opinions of Reasonable and Prudent Alternatives (RPA) stipulates maintaining

monthly X2 no greater than 81km (Collinsville station) for above normal years. This is equivalent to a monthly EC of less than 2640 µs/cm at Collinsville.

These major standards and other less-controlling ones (Net Delta Outflow, EC at Emmaton, etc.) are translated in terms of constraints in the water cost analysis program discussed in the following section.

3.2.4 Water Cost Analysis

A water cost analysis was conducted via a Python program developed by the DMS. The engine of this program is a numerical optimization method called Constrained Optimization by Linear Approximation (COBYLA). This analysis also incorporates mild regularization of solutions in the calibration zone to exclude erratic results. This program runs DSM2 iteratively by adjusting the pre-defined control variable (e.g., a boundary inflow or bank exports) to find an optimal solution (minimal Delta outflow), under the constraints of water quality and flow standards as mentioned in Section 3.2.3.

One critical feature of this approach is that it can provide a robust definition of water cost. Although the amount of water released or exported in a scenario is easy to describe, the quantity of water needed to achieve a particular salinity outcome is not. This cost depends on the nature of the salinity objective as well as the efficiency of the operation. When analyzing operations or proposals with a relatively low incremental water cost, the use of a vague water cost can dominate the calculation. By constraining the solution along the efficient frontier (i.e., looking at "good" operations), there emerges a single water cost, so that the differences in water cost between scenarios such as gate re-operation accurately reflect the incremental effect of the scenarios rather than the vagaries of the approximate water cost. This idea is illustrated by Figure 3-2, which compares the difference between the optimized and non-optimized water cost calculations. For the latter, the amounts of water (in blue dots) required to meet the standards in both cases (Base and Re-operation) are not minimized, and though they are not bad operations, they are haphazard enough to obscure the incremental water cost sought by the analysis. By contrast, the optimized water costs (in red and green dots) are constrained to the red and green lines, eliminating the "wiggle room" and focusing the calculation on the difference between scenarios.

The operations produced by this methodology are an abstraction but reflect O&M real-time operation and strategy in the summer, since they intend to meet the standards while not using too much water (from the historical record pattern) and end up with salinity time series traces that stick close to objectives. In addition to real-time practices, this methodology can also be applied to mid-term and long-term (weeks to months in advance) applications, which is another benefit of the algorithm.

Figure 3-2 Schematic Showing the Logic of Water Cost Analysis Approach

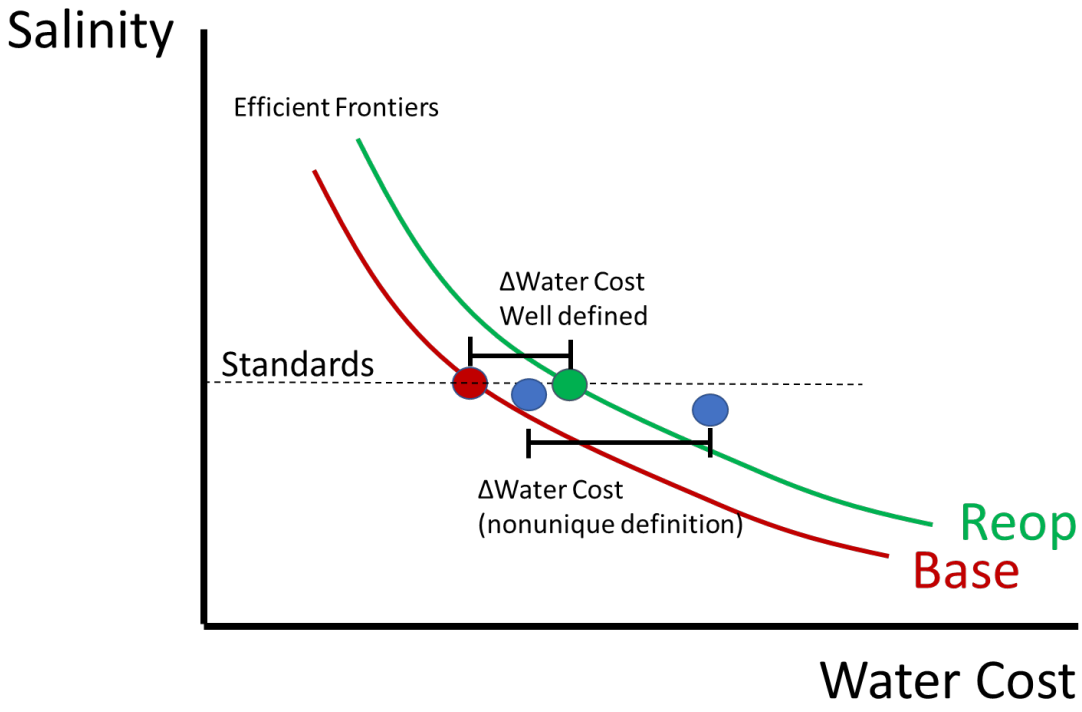

3.3 Results

3.3.1 Below Normal versus Above Normal Conditions

The water cost analysis was conducted with January 2018 hydrology forecasts from O&M, which consists of both below normal (75 percent exceedance probability) year and above normal (50 percent exceedance probability) year forecasts. The Sacramento River inflow was used as the control variable.

Figure 3-3 shows simulated EC at Jersey Point in the below normal year scenario. The 14-day running average (orange line and dash-dot orange line) and tidally filtered EC (surrogate of daily-average, blue line and dash-dot blue line) are illustrated under both base and re-op cases, along with the D1641 objective (dash orange line) and the guidance standard (blue dash line). In both cases, the D1641 standards (April 1–August 15) are not exceeded. From April 1–June 20 and June 21–August 15, the 14-day running average EC is below 450 µs/cm and 740 µs/cm, respectively. The guidance standard is also met in both cases. The tidally filtered EC is consistently less than the 1600 µs/cm threshold through October. The water cost of the re-operation, namely the difference between the amounts of water required to meet water quality standards in base and re-operation cases, is calculated as 29 thousand acre-feet (taf) (daily average 138 cubic feet per second (cfs) during the control period from July 5 to October 17).

Figure 3-3 Simulated EC at Jersey Point Based on 2018 January Below Normal Hydrology Forecasts

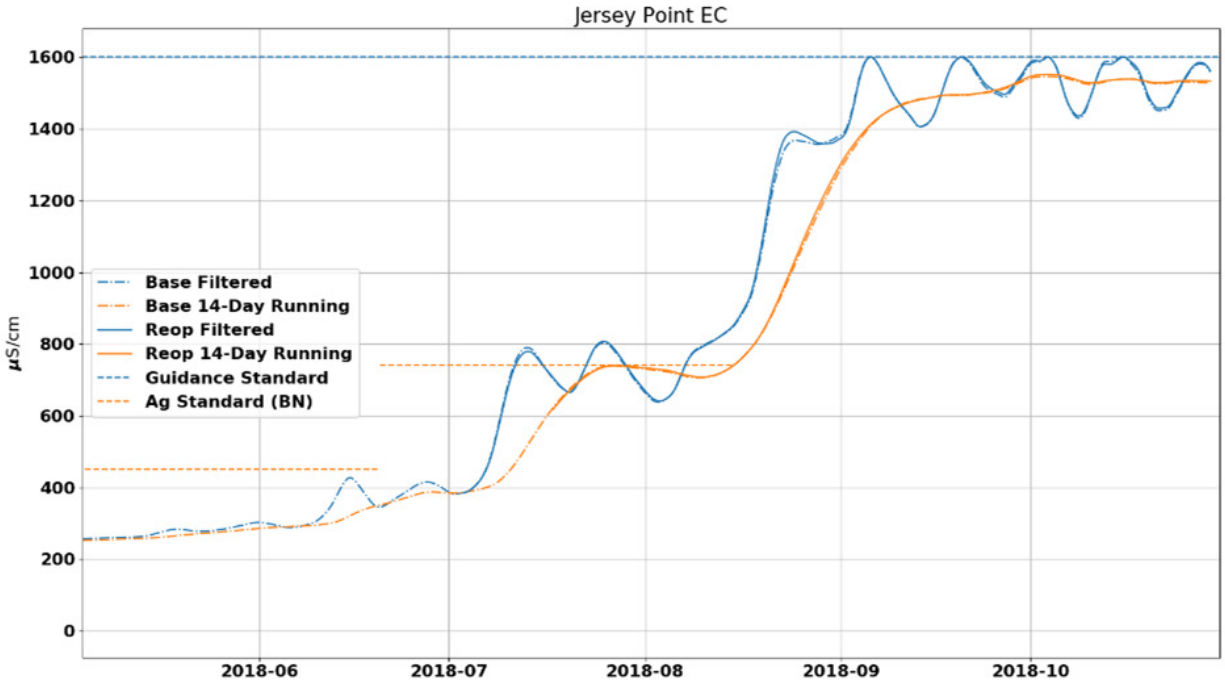

For above normal forecast, EC at Collinsville (RSAC081) is the dominant constraint. In both September and October, the monthly-average EC at Collinsville cannot exceed 2640 µs/cm. A similar water cost analysis was conducted with this and other constraints, including the standards for Jersey Point. Figure 3-4 illustrates the simulated monthly averaged EC (blue line)

up to October along with the standard (red line, only valid for September and October). Both base and re-operation scenarios meet the standard. Even though August EC exceeds 3000 µs/cm, EC values in September and October are maintained below 2640 µs/cm. The corresponding water cost is 33 taf for the control period from July 11 to October 27, with a daily-average flow of 115 cfs.

Figure 3-4 Simulated EC at Collinsville Based on 2018 January Above Normal Hydrology Forecasts

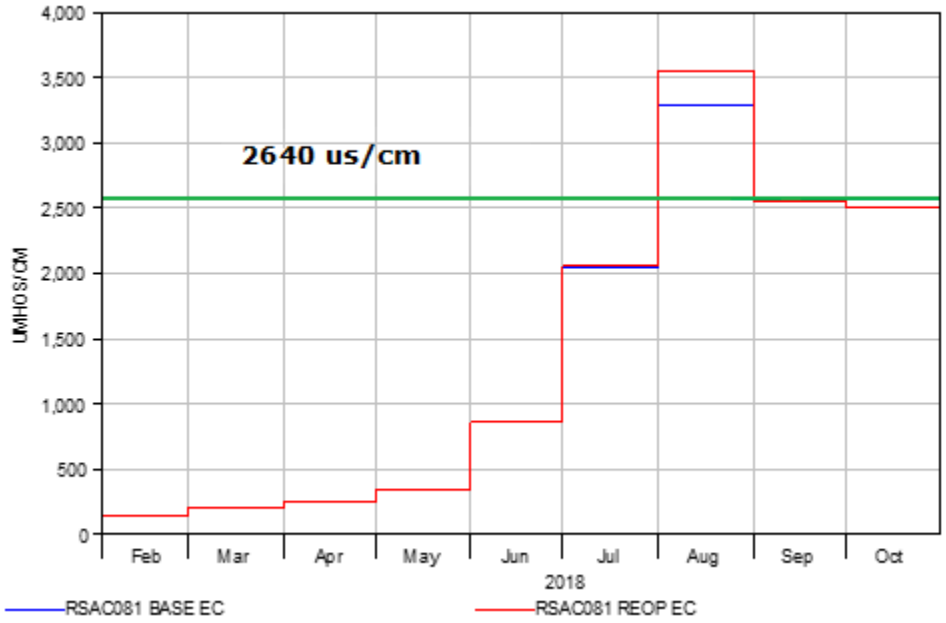

3.3.2 Banks Export as Control Variable

DWR O&M updates the delivery forecasts monthly and water quality forecast seasonally. As summer approaches, the forecasts become more accurate. A similar water cost analysis was conducted based on May hydrology forecasts (below normal year), with O&M DSM2 forecasting configuration using Banks export as the control variable. To fulfill this task, three things were done: (1) the corresponding hydrology boundary inputs were updated, (2) the most recent EC observation at Martinez (downstream boundary of DSM2) was used to generate water quality boundary conditions and initial conditions, (3) the operation of Clifton Court gates was changed to Priority 4 instead of the initial allocation setting to prevent export pumping being limited by gate operations.

Figure 3-5 illustrates the results of this scenario. The figure indicates that simulated EC meets both salinity standards at Jersey Point. The corresponding water cost is 23 taf for the control period from August 1 to September 29 (with the daily average flow of 197 cfs). It should be pointed out that using Banks export as the control variable would affect the water allocation split of the Sacramento River and the San Joaquin River and puts more weight of constraint on Jersey Point EC. It may make a difference in the gross water cost for both base and re-operation cases; however, the incremental water cost (i.e., difference between two cases) resulting from the SMSCG re-operation is essentially the same.

Figure 3-5 Simulated EC at Jersey Point Based on 2018 May Hydrology Forecasts

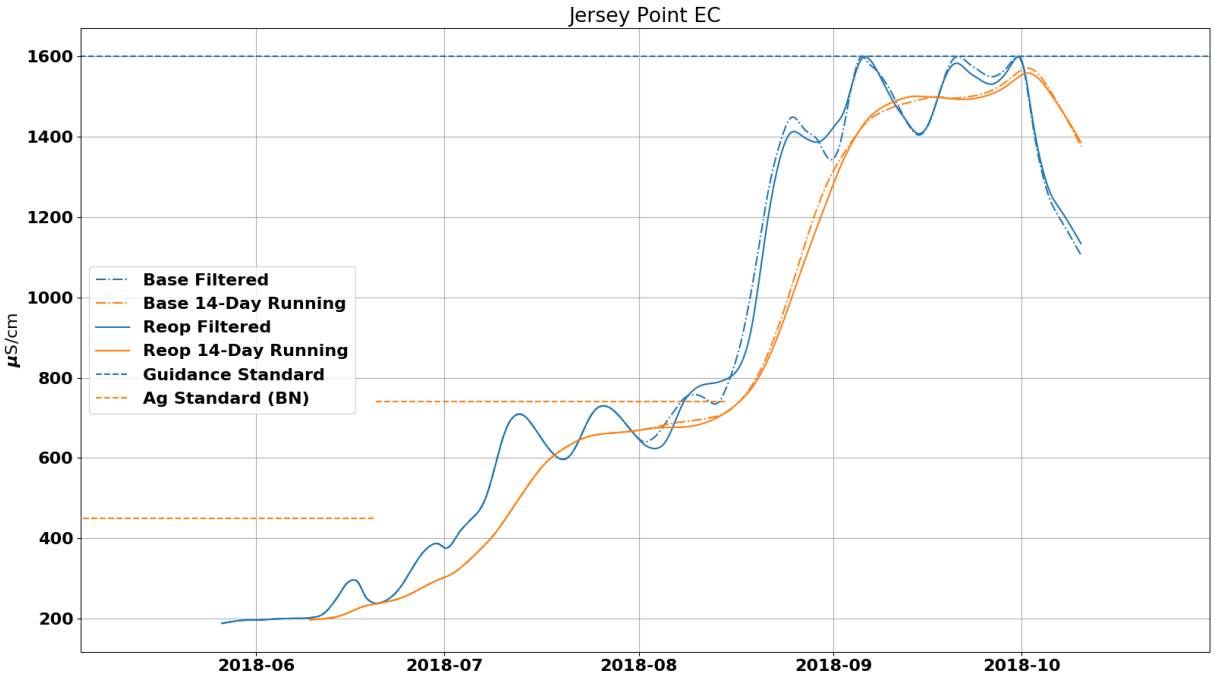

3.3.3 No-harm Scenario

In practice, O&M also runs a "no-harm" scenario in addition to above-mentioned scenarios. The scenario is configured so that the EC remains at or below the base case EC at Jersey Point while including SMSCG re-operation. Water cost analysis was also conducted for such a scenario based on hydrology forecasts in May. The control on salinity was based on export reduction rather than inflow from the Sacramento River. Figure 3-6 illustrates the results of this scenario, using 14-day tidal average EC as the

comparison standard. As shown, EC associated with the re-operation scenario does not exceed its "base" counterpart for the control period from August 1 to September 29. The corresponding water cost is 26 taf, with the daily-average flow being 220 cfs. It is worth noting that the D1641 standard and the guidance standard are still in place as additional constraints on the system.

Figure 3-6 Simulated EC at Jersey Point Based on 2018 May Hydrology Forecasts of the No-Harm Scenario

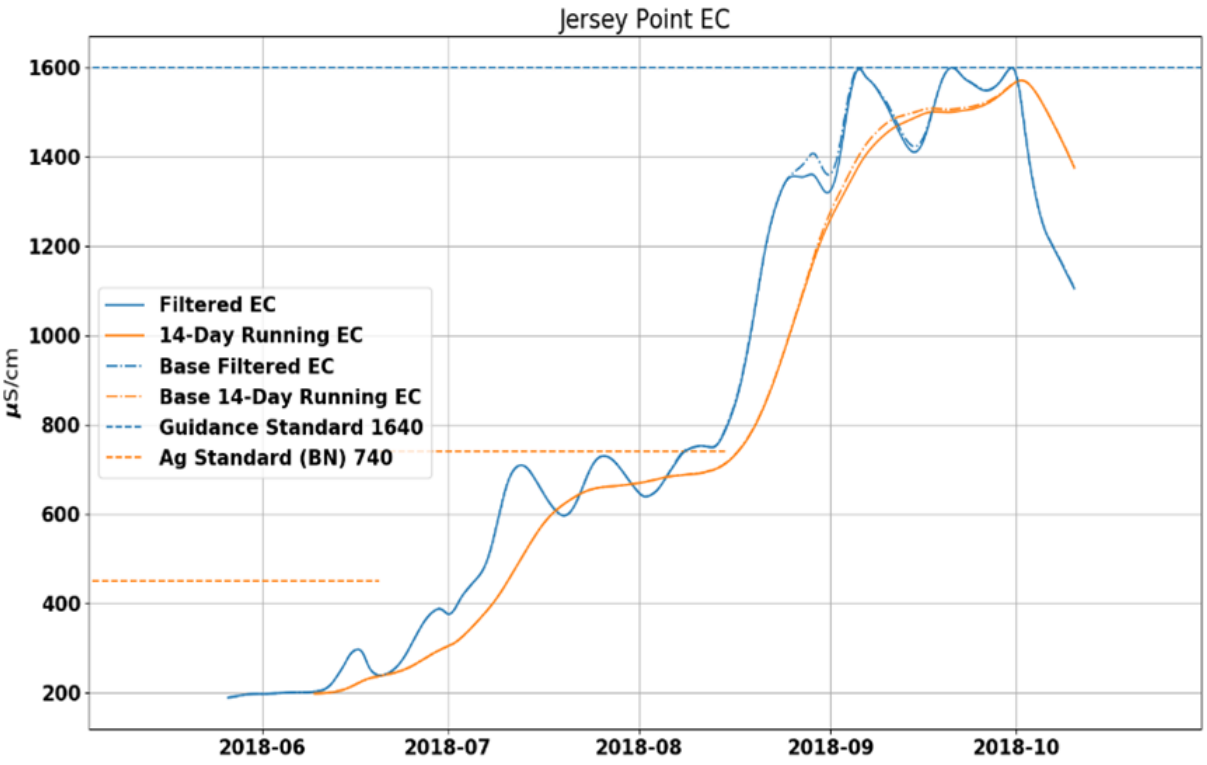

3.4 Summary

Re-operation of the SMSCG was shown to have adverse impacts on Delta salinity in terms of increasing salinity at key compliance locations, including Emmaton and Jersey Point via DSM2 modeling; however, the overall impacts were minor. The water cost of the re-operation was estimated to be less than 33 taf, no matter which water cost source (increased Sacramento River inflow or reduced export) was used or what water year type (above normal or below normal) was forecast. The no-harm scenario had a similar but slightly smaller amount of water cost. After the re-operation, O&M estimated

that the associated water cost was about 37 taf, which is fairly close to what we have forecast.

During this re-operation, field flow and salinity data have been collected. For the next steps, the model will be evaluated against the field data collected and applied in future SMSCG re-operation studies.

3.5 Acknowledgements

This work has been possible as a result of Michal Koller and Ted Sommer (DWR Division of Environmental Services) initiating the project; Eli Ateljevich (DWR Bay-Delta Office) providing the key water cost methodology and project supervision; Bryant Giorgi, Tracy Hinojosa, Siqing Liu, Dan Yamanaka, Ian Uecker (DWR Division of Operations and Maintenance) offering hydrology forecasting data.

3.6 References

California Natural Resource Agency (2016). Delta Smelt Resiliency Strategy July 2016. http://resources.ca.gov/docs/Delta-Smelt-Resiliency-Strategy-FINAL070816.pdf.

Methodology for Flow and Salinity Estimates in the Sacramento-San Joaquin Delta and Suisun Marsh

40th Annual Progress Report
June 2019

Chapter 4
DSM2 Sediment Transport Model (GTM-SED)

Authors: En-Ching Hsu, Jamie Anderson, Prabhjot Sandhu
Delta Modeling Section
Bay-Delta Office
California Department of Water Resources


DEPARTMENT OF WATER RESOURCES
STATE OF CALIFORNIA

Contents

Figures

Tables

4 DSM2 Sediment Transport Model (GTM-SED)

4.1 Introduction

The ability to model sediment and turbidity transport in the Sacramento-San Joaquin Delta (Delta) is vital, in several ways, for effective management of Delta resources. First, the understanding of sediment erosion and deposition in the channel network system provides information for environmental and operational management. Second, turbidity impacts Delta smelt's survival. It affects their feeding success in their larval life stage, their ability to avoid predation, and is a migratory cue. Sediment resuspension elevates turbidity and enhances Delta smelt habitat quality. Third, the ability to model turbidity and suspended sediment transport is essential for the development of a mercury model needed to fulfill the California Department of Water Resources' (DWR) open-water compliance with the Delta Mercury Control Program (2011). For these reasons, the California Department of Water Resources' Delta Modeling Section extended its DSM2 General Transport Model (DSM2-GTM) (Hsu et al. 2016) to include sediment transport (Figure 4-1).

Figure 4-1 Delta Simulation Model 2 With GTM-SED Highlighted

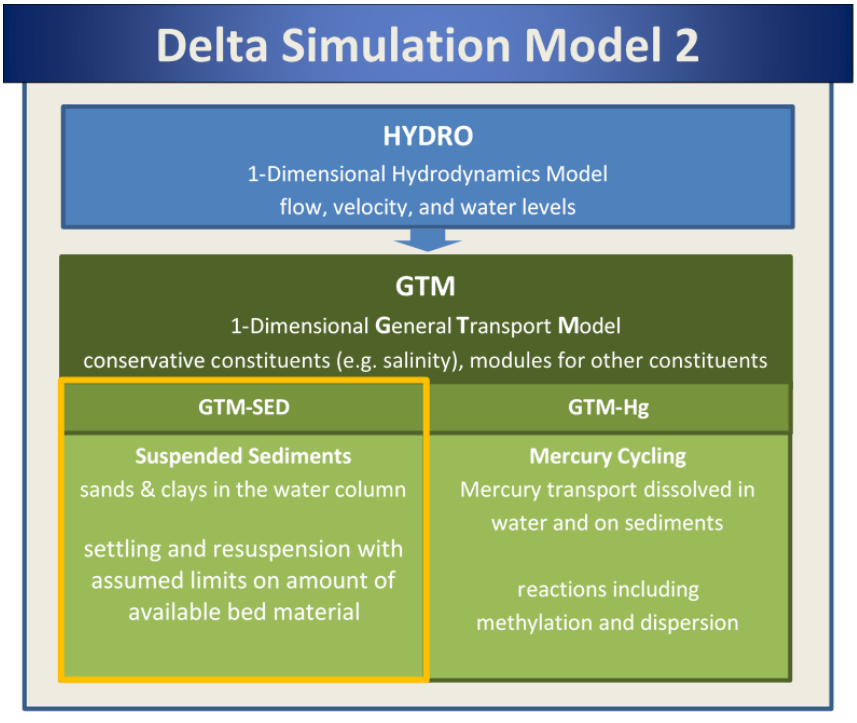

DSM2-GTM employs a fixed (Eulerian) mesh rather than one that moves with flow following virtual parcels of water in a Lagrangian scheme (DSM2-QUAL). That makes it easy to interact with other models, georeferenced data, data assimilation, optimization, and visualization as well as coupling inline to DSM2-HYDRO. It is also more straightforward to extend the new model to new physical processes with sediment, dissolved oxygen, and mercury cycling models.

Sedimentation is a complicated process as it is not a conservative quantity, and in reality, sediment particle sizes change over time. Fine-grained sediment is difficult to quantify, as it interferes with other aspects in estuaries. Numerical modeling has become an increasingly useful tool in cohesive sediment management. The dynamics behind cohesive sediment are mainly empirical since its behavior is affected by numerous parameters that cannot be determined theoretically. This means that field data is still an important aspect of cohesive sediment studies. Details and continuous data play an important role in both model development and calibration. The United States Geological Survey (USGS) has established 15-minute suspended sediment concentration (SSC) networks across the Delta since 2010. Those data are precious and crucial for the success of having a decent estimate of the sedimentation process. This study focuses on suspended sediment, which has long-term continuous data available for calibration and validation. The calibration period for this report is from October 2010 to September 2013, and the current validation period is from October 2013 to September 2016.

This DSM2 Suspended Sediment Transport Model (GTM-SED) has been developed, preliminarily calibrated, and validated. It is an extended module to DSM2-GTM and can be run as a standalone model. This chapter documents the use of data, boundary conditions, model assumptions, methodologies, results of preliminary calibration and validation, further investigations on factors to fine-tune the model, sensitivity analysis, sediment budget analysis, and linkage to the turbidity model. The next chapter (Chapter 5) discusses additional model development for representing the sediment bed.

4.2 Study Area and Data

The study area lies within the Sacramento-San Joaquin Delta. The hydrodynamics of the Delta are driven by climate, upstream reservoir and

gate operations, tides, and local water diversions. DSM2-HYDRO is used to simulate the hydrodynamics in the Delta. As for the sediment data collection, the quality of data is very important for understanding the sedimentation in the Delta and to verify the accuracy of simulation results. There are several data sources available from different agencies. The availability of the 15-minutes continuous suspended sediment data from USGS is the most crucial data source for this model development. The other data sources serve as good references to cover samples before 2010, and as a bonus, some of them contain metadata information.

4.2.1 Sediment Data Availability

(1) USGS — Current/Historical Observations (15-Minute Data)

USGS has 17 continuous measuring stations (Table 4-1) for suspended sediment concentration (SSC). Reported data are derived from backscatter sensors measurements every 15 minutes and are calibrated approximately monthly with bottle samples. Data are available from 2010 to the current date and were obtained from USGS in Sacramento (Wright and Schoellhamer 2005; Morgan-King and Wright 2013). A map of the 15-minute data network and DSM2 grid is shown in Figure 4-2.

(2) USGS — Sediment Portal (Daily Data)

There are more than 40 years of continuous daily suspended sediment concentration data available from Freeport and Vernalis. The locations are mapped and are shown as green dots in Figure 4-2. There are also suspended sediment load data available; however, the data for the interior Delta are discrete and short in time so they are not considered for calibration. The 15-minute sampling at Vernalis is recently established. Therefore, the continuous daily record from this data source is used for the Vernalis boundary.

There are percentages of sand, silt, and clay for each site reported in the metadata file. Those numbers indicate that the sand content is low in the interior Delta (Old River and Middle River) and the Yolo Bypass area. Higher sand content happens upstream of most rivers and streams and at the tidal area toward the ocean. For Freeport, the proportion of sand is 36.2 percent and the proportion of fines is 63.8 percent. For Vernalis, the proportion of sand is 47.9 percent and the proportion of fines is 52.1 percent. The other

information used for calibration is the proportion of sediment composition. Those values are used as initial values to partition sand and fines from suspended sediment concentration; however, those percentages are static values and may not reflect the reality. Further investigation and refinement can be achieved by data sampling and analyses and treating the proportion as a time-variant variable. Another option is to calibrate the percentage and see how well it describes the data.

(3) USGS — Field/Lab Water Quality Data

This site provides discrete data mostly from 2011. Even though the samples are scattered, it is the only place that provides concentrations for bed sediment and suspended sediment with respect to grain sizes. Also, it provides data of loss on ignition, which is an indicator for organic material associated with sediment.

(4) CALFED

There were data collections during the CALFED study period. The data includes total mercury from 1994, methyl mercury from 2000, total suspended solids (TSS), and suspended sediment concentration (SSC) from 1992. These are discrete data and usually two samples are taken in a month.

Table 4-1 Delta Station from USGS 15 Minute Suspended Sediment Data

Station No	Name	USGS	CDEC	Period
11185185	Sacramento River at Mallard Island	MLD	MAL	10/2010–Present
11304810	San Joaquin River Below Garwood Bridge at Stockton	STK	SJG	10/2010–Present
11312676	Middle River at Middle River	MID	MDM	10/2010–Present
11313405	Old River at Bacon Island	OLD	OBI	10/2010–Present
11336680	South Mokelumne River at W Walnut Grove Road	SFM	SMR	10/2010–Present
11336685	North Mokelumne River at W Walnut Grove Road	NFM	NMR	10/2010–Present
11336790	Little Potato Slough at Terminous	LPS	LPS	10/2010–Present
11336930	Mokelumne River at Andrus Island near Terminous	MOK	MOK	10/2010–Present
11337190	San Joaquin River at Jersey Point	JPT	SJJ	10/2010–Present
11447650	Sacramento River at Freeport	FPT	FPT	10/2010–Present
11447903	Georgiana Slough near Sacramento River	GEO	GSS	10/2010–Present
11455165	Miner Slough at Highway 84 Bridge	MIN	HWB	10/2010–Present
11455280	Cache Slough near Hastings Tract	UCS	-	10/2010–Present
11455315	Liberty Island Breach	LIB	LIB	10/2010–Present
11455335	Sacramento River Deep Water Ship Channel	DWS	DWS	10/2010–11/2013
11455350	Cache Slough at Ryer Island	CCH	RYI	10/2010–Present
11455420	Sacramento River at Rio Vista	RIO	SRV	10/2010–Present

Figure 4-2 USGS 15-minutes Suspended Sediment Sampling Network

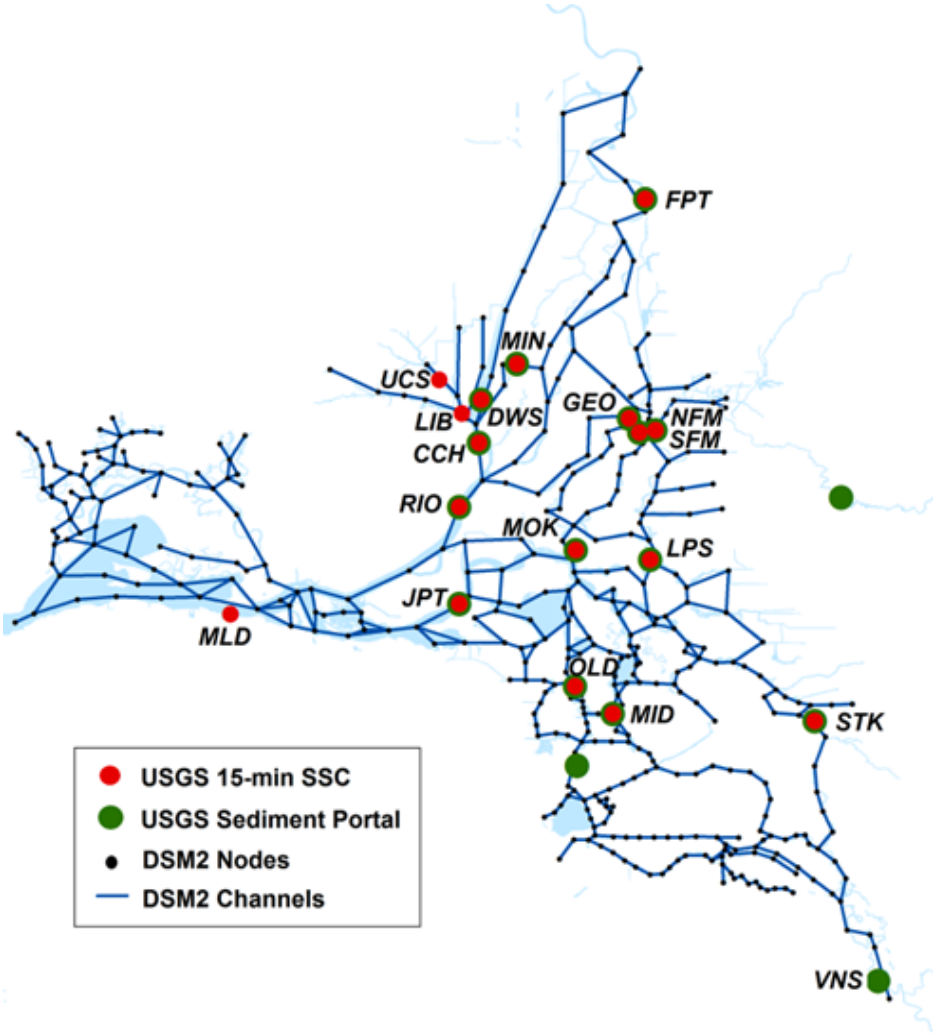

4.2.2 Model boundary condition

(1) Flow and sediment boundaries

Wright and Schoellhamer (2005) used continuous measurements of suspended sediment flux to develop a sediment budget for the Delta for Water Years 1999–2002. During that time period, 85 percent of the sediment that entered the Delta came from the Sacramento River, 13 percent came from the San Joaquin River, and the eastside tributaries supplied the remaining 2 percent. Their findings suggested that the boundary conditions from Sacramento River and San Joaquin River dominate the supply of sediment for the Delta. Those two boundaries should be always included in simulation, and others can be used to increase the accuracy or

accommodate other sources associated with sediment concentration. Aside from the upstream boundaries, GTM-SED also includes the seaside boundary to reasonably capture the sediment variation of a tidal system sloshing back and forth.

The sediment boundaries are Freeport for the Sacramento River, Vernalis for the San Joaquin River, Cache Slough near Hastings Tract for the Yolo Bypass, and Mokelumne River at Walnut Grove Road. As the Freeport location is some distance away from the DSM2 boundary, an 8.5-hour time shift is applied to the boundary data to avoid phase shift. The tidally filtered 15-minute time series for the flow and sediment concentration used for Sacramento River and San Joaquin River boundaries are shown in Figure 4-3 and Figure 4-4, respectively. It can be observed that flow does not have a pattern similar to sediment in terms of relative amplitudes and time to peak. Those two plots suggest that any intent to regress flow and sediment at those two locations may not be appropriate.

Figure 4-3 Boundary Flow and Suspended Sediment Concentration at Freeport

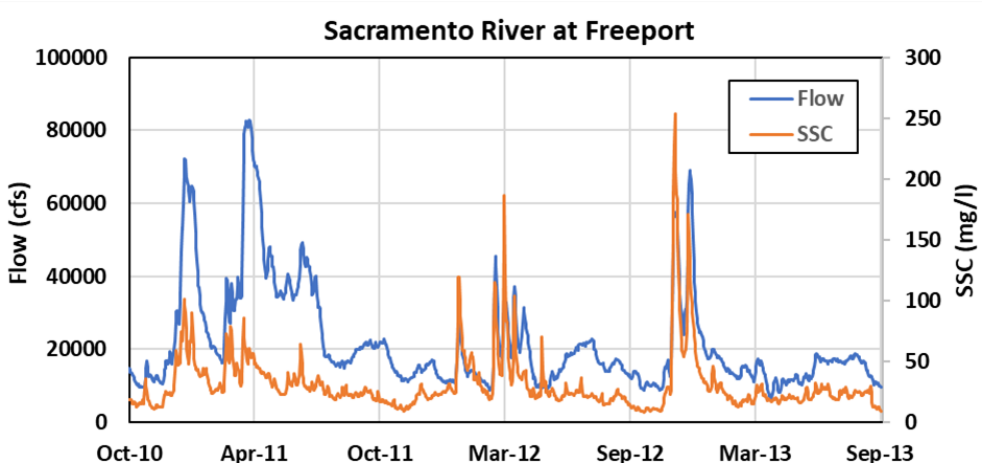

Figure 4-4 Boundary Flow and Suspended Sediment Concentration at Vernalis

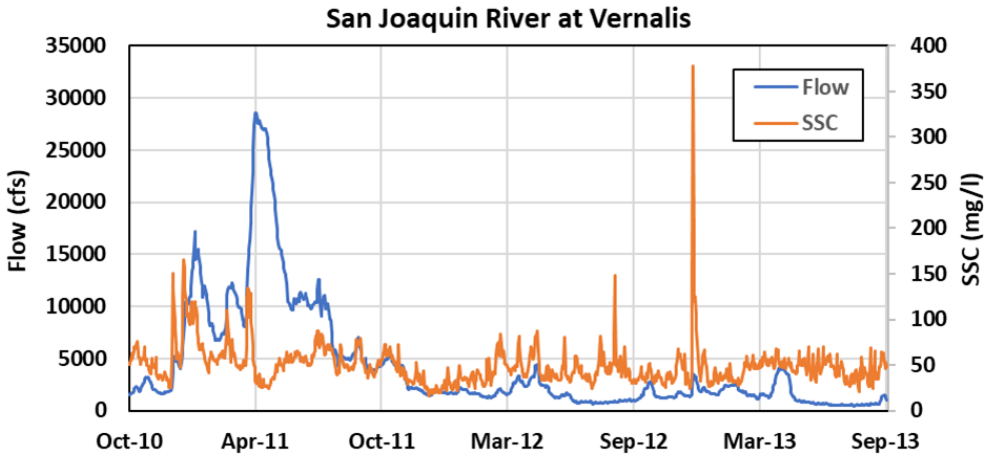

The most downstream suspended sediment concentration (SSC) data available is from Mallard Island, though the DSM2 seaside boundary, Martinez/Benicia Bridge, is about 12 miles downstream. There are some spare SSC data from the USGS sediment portal at Suisun Bay at Benicia Bridge and continuous 15-minutes turbidity data from the USGS at the same location. A simple regression fitting is used to derive the relationship between SSC and turbidity. The 15-minutes SSC data at Martinez is thus derived from the 15-minutes turbidity data and the regression equation. The derived time series is shown in Figure 4-5 with observed SSC data at Mallard Island as reference, and the plot indicates the calculated time series at Martinez as having similar pattern and slightly higher amplitude as at Mallard Island.

Figure 4-5 Comparison of Regressed Suspended Sediment Concentrations at Martinez and Observed SSC at Mallard Island

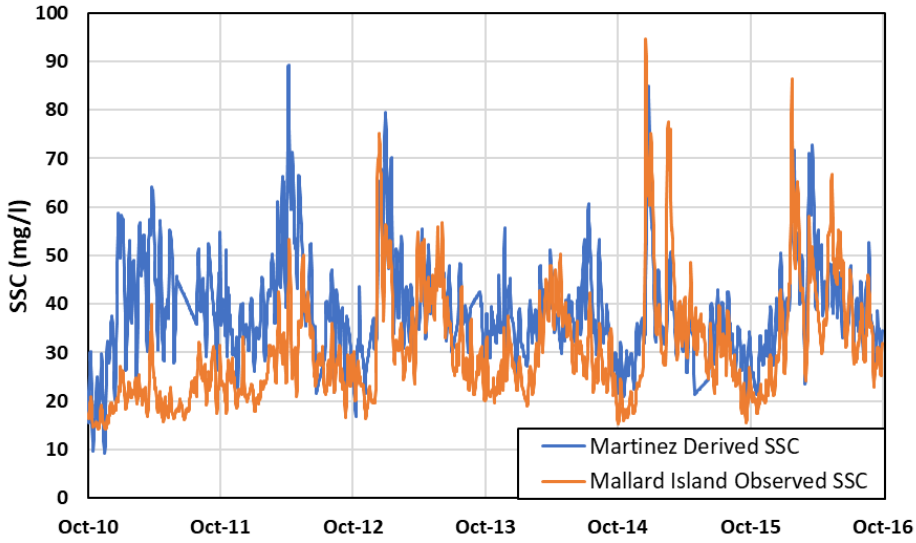

(2) Partition the sediment by particle size and percentage at boundary

The given suspended sediment concentration is a lumpsum of mixed particle types. The preliminary approach is dividing the concentration into sand and fines and then evaluating the ability to achieve the calibration based on this assumption. The grain size for sand (> 0.0625 millimeters [mm]) and the grain size for silt and clay (< 0.0625 mm) will be treated as parameters that needed to be calibrated.

The available measurements at boundaries are SSC. The other variable is the percentage of sand and fines, taken from SSC data. The USGS Sediment Portal website has metadata that provides static percentages for sand, silt, and clay for each site. Even though the sediment particle distribution should vary with time, with limited data, a fixed value is a good guess. It has been observed that locations at boundaries contain more sand than locations inside of the Delta. Vernalis has 47.9 percent of sand in its sediment and Freeport has 36.2 percent of sand in its sediment. The SSC data can be partitioned into coarse (sand) and fines (silt and clay) by using the constant percentage of sand, silt, and clay provided at the USGS Sediment Portal website (Table 4-2). Nevertheless, the flexibility to vary those percentages

as part of the calibration practice and evaluate those percentages as the calibration parameter is being kept.

Table 4-2 Percentage of Sand and Fines at Boundaries from Metadata

Boundary Location	Sand (%)	Fines (%)
Freeport	36.2	63.8
Vernalis	47.9	52.1
Eastside	41.5	58.5
Yolo	27.2	72.8
Martinez	10.0	90.0

4.2.3 Hydrodynamics information

The hydrodynamics information is obtained from DSM2-HYDRO simulations. The standard historical modeling setup is used but with some modifications to address the fine resolution of sediment data. There are two changes. One is using 15-minute Godin-filtered boundary flow data instead of using daily averaged data. This makes the flow data synchronize with the sediment data at the dominant sediment source. The other is using the beta version of Delta Channel Depletion (DCD) (Liang and Suits 2018) agricultural drainage flows instead of Delta Island Consumptive Use (DICU) monthly data in hope of describing the rainfall events more precisely.

The river discharge boundaries are Sacramento River at Freeport, San Joaquin River at Vernalis, Yolo Bypass, Mokelumne River, and Calaveras River, and there is a stage boundary at Martinez.

There have been continuous efforts in calibrating Delta electroconductivity (EC) for DSM2-HYDRO and DSM2-QUAL. Since those results are well established, this study adopts Manning's n and dispersion coefficients that were calibrated for salinity simulation, and these parameters are assumed adequate for suspended sediment.

4.3 Model Description

The sediment transport model is the extension module that is built on top of DSM2-GTM. It utilizes the advection and dispersion terms for the pollutant transport and implements the reaction term for sedimentation process. The

details on the general transport equation and the empirical equations used for this module development are discussed in this section.

4.3.1 Role of erosion and deposition in general transport model

In a collaborative project with University of California, Davis, Ateljevich et al. (2011) developed a second-order upwind one-dimensional Eulerian model of advection, dispersion, and reactions or sources. This numerical scheme has been implemented and applied to the Sacramento-San Joaquin Delta water quality simulation (Hsu et al. 2016). The advective-diffusive part of the model describes basic conservative transport, and the generalized reaction term can be tailored to non-conservative water quality kinetics, including sediment transport.

In conservative form, this is the equation.

$$\frac{\partial(\boldsymbol{A}(\boldsymbol{x},\boldsymbol{t})\boldsymbol{C}(\boldsymbol{x},\boldsymbol{t}))}{\partial \boldsymbol{t}}+\frac{\partial(\boldsymbol{Q}(\boldsymbol{x},\boldsymbol{t})\boldsymbol{C}(\boldsymbol{x},\boldsymbol{t}))}{\partial \boldsymbol{x}}=\frac{\partial}{\partial \boldsymbol{x}}\left(\boldsymbol{A}(\boldsymbol{x},\boldsymbol{t})\boldsymbol{K}(\boldsymbol{x},\boldsymbol{t})\frac{\partial \boldsymbol{C}(\boldsymbol{x},\boldsymbol{t})}{\partial \boldsymbol{x}}\right)+\boldsymbol{A}(\boldsymbol{x},\boldsymbol{t})\boldsymbol{S}\left(\boldsymbol{x},\boldsymbol{t},\boldsymbol{C}(\boldsymbol{x},\boldsymbol{t})\right) \quad (\mathbf{1})$$

↑ ↑ ↑ ↑

Time evolution Advection Dispersion Source/Reaction

where

$\boldsymbol{x}$ is distance along the channel,

$\boldsymbol{t}$ is time,

$\boldsymbol{A}$ is the cross-sectional area,

$\boldsymbol{C}$ is the scalar concentration,

$\boldsymbol{Q}$ is the flow,

$\boldsymbol{K}$ is the longitudinal dispersion coefficient modeled using the diffusion analogy,

$\boldsymbol{S}$ is the source or reaction term (deposition, erosion, lateral inflow, and other forms of sources and sinks) per unit area of a cross-section.

Equation (Eq.) (1) describes the mass conservation of a pollutant in a dissolved phase or suspended sediment away from the streambed. The erosion and deposition processes are implemented as source and sink term in the transport equation. *Erosion* is the flux of particles from a sediment bed into the overlying water column, and *deposition* is the flux of particles back to the sediment bed. The movement of sediment particles in a water column is a result of advection, dispersion, and settling. The vertical fluxes term determines the mass exchange between the water column and the sediment bed, and they are calculated by empirical equations that are the function of hydrodynamic bed shear-stress and sediment properties.

4.3.2 General sediment properties and equations

Sediment entrainment and deposition are complex physical processes that are usually approximated by empirical equations. Erosion of cohesive sediment occurs whenever the flow velocity or the flow-induced shear stress over the bed exceeds a certain critical value. The erosion rate of cohesive sediment is calculated according to the formula of Krone-Partheniades (1962), while the deposition flux is expressed by a classical Krone (1962) formula. The net vertical sedimentation fluxes are treated as source and sink terms in DSM2-GTM's general transport equation. The key problem for sediment transport research under non-equilibrium conditions is to determine the near-bed sediment flux and to add it as a source and a sink to feed in the transport equation.

Most of sediment equations are in Système international (d'unités) (SI) units, and so all the equations in this report are in SI units unless otherwise specified. There are some common properties and variables for both non-cohesive sediment and cohesive sediment calculation. They're also indicators of the initiation of motion or deposition or mode of sediment transport. The constant variables for sediment and water properties are given in Table 4-3.

Table 4-3 Constants for Suspended Sediment Module

Variable	Description	Value
g	Gravitational acceleration	9.80665 m/s^2
ρ_w	Water density	1000 kg/m^3
P_s	Sediment density	2650 kg/m^3
k	Von Karman's constant	0.41
v	Kinematic viscosity of water at 10 °C	1.307x10^{-6} m^2/s
G	Specific gravity = sediment density/water density	2.65

The sedimentation related variables, such as settling velocity, shear velocity, bed shear stress, and Rouse number, are illustrated below.

(1) Settling Velocity, w_s

The settling velocity is also called the fall velocity or terminal velocity. Van Rijn (1993) suggested the following equations for natural sediment particles. D is the D_{50} particle size. For small particles (medium particle size D = D_{50} < 10^{-5} m), it is calculated with Stock's Law (Eq. (2)).

$$w_s = \frac{gD^2(G-1)}{18\nu} \qquad for\ 1 < D \leq 100\ \mu m \tag{2}$$

$$w_s = \frac{10\nu}{D}\left[\left(1 + \frac{0.01(G-1)gD^3}{\nu^2}\right)^{0.5} - 1\right] \qquad for\ 100 < D \leq 1000 \mu m \tag{3}$$

$$w_s = 1.1 \cdot [(G-1)gD]^{0.5} \qquad for\ 1000 \mu m \leq D \tag{4}$$

There are other empirical equations available. Rubey's formula is based on the expression of the drag coefficient for a sand particle in clear water.

$$w_s = \frac{8\upsilon_m}{D}\left[\left(1 + 0.0139{d_*}^3\right)^{0.5} - 1\right] \tag{5}$$

$$d_* = D\left[\frac{(G-1)g}{\upsilon_m^2}\right]^{1/3} \tag{6}$$

where υ_m is the kinematic viscosity of the water-sediment mixture.

Dietrich (1982) suggested the following equation for the fall velocity of natural particles:

$$\log w_s^* = -3.76715 + 1.92944(logD^*) - 0.09815(logD^*)^2$$

$$-0.00575(logD^*)^3 + 0.00056(logD^*)^4 \qquad (7)$$

$$w_s = w_s^* \cdot [(G-1)gD]^{0.5} \qquad for\ \ 10\ \mu m \le D \qquad (8)$$

$$w_s = \frac{gD^2(G-1)}{18\nu} \qquad for\ \ 10\ \mu m > D \qquad (9)$$

The settling velocity calculated by those three empirical equations are shown in Figure 4-6. Both Rubey's and Van Rijn's formulas yield practically the same results.

Figure 4-6 Calculated Settling Velocities from Three Empirical Equations

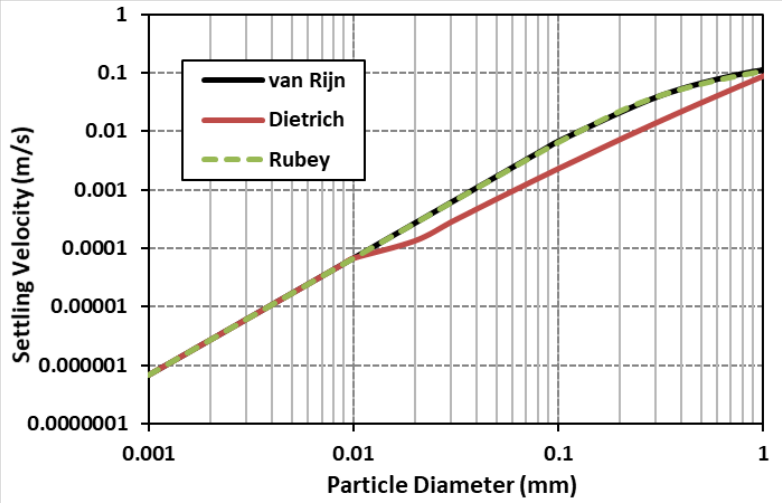

(2) Dimensionless Critical Shear Stress, τ^*_c

Shields (1936) determined experimentally that a minimum or critical Shields number (τ^*_c) required initiating motion of the grains of a particle. The Shields diagram empirically shows that dimensionless critical shear stress is a function of a certain form of the particle Reynolds number.

$$\tau_c^* = f(Re_p) \tag{10}$$

Brownlie (1981) fitted a curve to the experimental line of Shields and obtained the following fit:

$$\tau_c^* = 0.22Re_p^{-0.6} + 0.06 \cdot \exp\left(-17.77Re_p^{-0.6}\right) \tag{11}$$

Where the explicit particle Reynolds number Re_p is:

$$Re_p = \frac{\sqrt{(G-1)gDD}}{\nu} \tag{12}$$

The critical shear stress is obtained by:

$$\tau_{cr} = \rho_w gD(S-1)\tau_c^* \tag{13}$$

The calculated critical shear stress with respect to particle size is shown in Figure 4-7. For fine particles, the value ranges from 0.1N/m^2 to 0.17 N/m^2, and around 0.17 N/m^2 to 0.25 N/m^2 for fine sand.

Figure 4-7 Calculated Critical Shear Stress with Respect to Sediment Particle Sizes

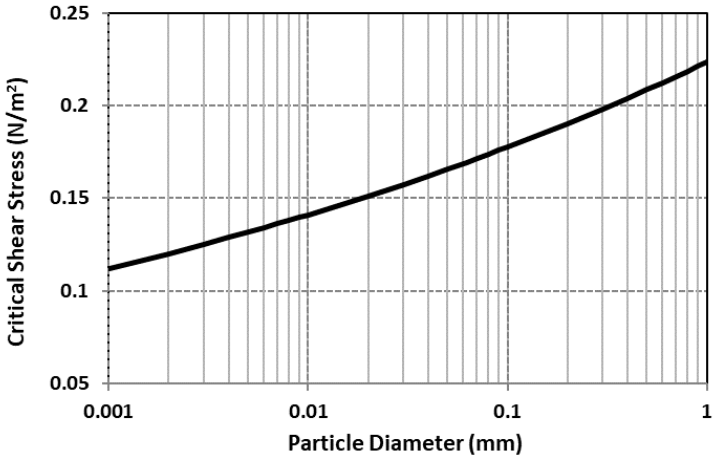

(3) Shear Velocity, u_*

Shear velocity u_* is related to the mean flow velocity, $\bar{u}$, through the generalized Darcy-Weisbach friction factor, C_f, which can be approximated by Manning's n.

$$u_* = \frac{\bar{u} n \sqrt{g}}{\phi R_h^{1/6}} \tag{14}$$

Where ϕ = 1 if SI units, 1.468 if English units, $\bar{u}$ is the cross-sectional averaged velocity, n is Manning's n, and R_h is the hydraulic radius.

(4) Bed Shear Stress, τ_b

$$\tau_b = \rho_w u_*^2 \tag{15}$$

4.3.3 Equations for Cohesive Sediment

The source and sink terms in the general transport equations depend on whether the local hydrodynamic conditions cause the bed to become eroded or allow deposition to occur. Empirical relations are used, and the possible formulations for the evaluation are given below. The Krone-Partheniades equation has been widely used and accepted in estuarine sediment modeling. One example is that the study done by Achete et al (2015) is using Delft3D Flexible Mesh software with a water quality model, Delft-WAQ (DELWAQ). DELWAQ solves sediment source and sink terms by applying the Krone-Partheniades formulation for cohesive sediment transport.

Erosion of cohesive sediment occurs whenever the flow velocity or the flow-induced shear stress over the bed exceeds a certain critical value. Many efforts have been made to relate the critical flow velocity or the critical shear stress to the sediment parameters. The erosion rate of cohesive sediment is calculated according to this formula by Krone-Partheniades (1962):

$$E = M \cdot \left(\frac{\tau_b}{\tau_{cr}} - 1\right) \quad for\ \tau_b \geq \tau_{cr} \tag{16}$$

Where E is the erosion flux (kg/(m^{2}s)) and M is the erosion coefficient (kg/(m^{2}s)). The erosion coefficient depends on the material of bed sediments. Cao and Du suggested that M should be a function of the sediment porosity. Parchure and Mehta (1985) addressed that M does not uniquely correlate with soil mechanical indices, but also relies on physicochemical parameters characterizing the inter-particle bond strength. Because those properties are poorly known, this parameter can simply be considered as a calibrated parameter.

A classical expression for the deposition flux of cohesive suspended matter to the bed is given by this formula by Krone (1962):

$$D = w_s \cdot c_b \cdot \left(1 - \frac{\tau_b}{\tau_{cr}}\right) \quad (17)$$

D is the deposition flux of suspended sediment (kg/(m^{2}s)), w_s is the settling velocity (m/s), c_b is the near-bed sediment concentration (kg/m^3), τ_b is the bed shear stress (Pa), and τ_{cr} is the critical shear stress for deposition (Pa). Equation (17) is usually approximated as:

$$D = w_s \cdot c_b \quad (18)$$

The approximation is made assuming that deposition takes place regardless of the prevailing bed shear stress. Since τ_{cr} is considered much larger than τ_b, the second term in Equation (17) can be disregarded. Several studies on sediment transport applied some sort of decay rate to represent the deposition process. By looking at Equation (18), the decay rate is a constant to approximate the sediment particle settling velocity which might magically do the trick, especially for net depositional areas. Nevertheless, without the thorough consideration of the sediment mechanism, it could not provide the resuspension rate and the decay rate might nibble away at the concentrations.

4.4 Model Calibration and Validation

As most of the sediment equations are empirical equations, they may be only applicable for certain ranges of sediment particles or flow conditions. The parameters also heavily depend on calibration to settle the equations. Therefore, calibration is crucial for this sediment modeling. Two keys for a successful calibration are good quality of observed data and parameter

adjusting. Water Years 2011, 2012, and 2013 are used as the period for initial calibration. These calibration years are classified as wet, below normal, and dry years, respectively. The wide range of hydrology provides a good picture of sedimentation patterns in the Delta and provides confidence in the model performance. The validation period is from October 2013 to September 2016. The validation years are two critical years followed by a below normal year.

The empirical equations that were mentioned herein are solely depending on sediment particle sizes, erosion coefficient, empirical parameter, flow velocity, and water depth. As flow and water depth are determined by DSM2-HYDRO, GTM-SED has no role to alter them. The sediment boundaries are Freeport for the Sacramento River, Vernalis for the San Joaquin River, Cache Slough near Hastings Tract for the Yolo Bypass, and Mokelumne River at Walnut Grove Road. The other east tributaries Cosumnes and Calaveras do not have SSC data and are approximated by using the time series from Mokelumne River.

4.4.1 Calibration parameters

The adjustable parameters GTM-SED are sediment particle sizes for coarse (sand) and fines (silt and clay), erosion coefficients in the empirical equation, and possibly the percentage of sand and fines at boundaries. The suspended sediment concentration is divided into two types, sand and fines, by using the percentage of each sediment type from metadata. Note that the proportion of sand and fines used in the model should add up to 100 percent of the suspended sediment. Initial testing applied these variables globally to observe overall response and sensitivity to adjustments and then evaluated regions in which sediment tended to be overestimated or underestimated. The calibration process is started with the intent of using one set of parameters to observe how the system responds. Throughout the modeling timespan, the computed results from STM-SED reproduce observed peaks and capture trends when the concentration falls. The field measurements are mostly cross-sectional averaged values, so a one-dimensional model to describe the system seems sufficient.

The parameters to fine tune the model are the seasonable pattern of SSC for agricultural return flows and other factors. The initial calibration assumes one set of sediment particle sizes and erosion coefficient for the Delta and lets the transport process dominate the overall settling and resuspending.

Further implementations are developing several SSC seasonable patterns for DCD flows and assigning those patterns to DSM2 nodes grouping by the designated DICU subregions.

The root mean square error (RMSE) metrics are used to quantify errors for the goodness of fit to the observed data among hundreds of calibration runs. The equation is shown as Eq. (19), where $X_{modelled}$ is the modelled output, and $X_{observed}$ is the observed data and n is the number of data points. The RMSE metrics provide an effective approach to narrow down the choices of combinations of the calibrated parameters. The RMSE is zero when the model and data have equal variability. The RMSE is a measure for overall discrepancy between modeling output and observed data. The chosen combinations will be plotted as time series for further assessment.

$$\mathrm{RMSE} = \left(\frac{\sum_{i=1}^{n} (X_{modelled} - X_{observed})^2}{n} \right)^{0.5} \quad (19)$$

(1) Erosion Coefficient

The erosion coefficient is a crucial parameter of the amount to be resuspended. The initial calibration setup uses constant SSC 20 mg/l for DCD flow, and the percentages from metadata are used to divide sediment particle types (sands and fines) at boundaries. The sand particle size is assumed 0.0625 millimeters (mm), 0.1 mm, and 0.5 mm, and the fine particle size is initially assumed 0.001 mm and 0.015 mm. The parameter is compared in the order of ten from 10^{-9} kg/m^2/s to 10^{-7} kg/m^2/s. The comparison is shown in Figure 4-8 for Rio Vista and Jersey Point and Figure 4-9 for Old River at Bacon Island and Mallard Island.

There is no significant difference observed from the modeling outputs of sand with particle sizes of 0.0625, 0.1, and 0.5 mm. The results for fines sized at 0.015 mm are mostly overlapped around the blue line, while fines sized at 0.001 mm are around the orange line. This indicates that particles sized at over 0.0625 mm are mostly deposited as they travel downstream, and the model is not sensitive enough for particle sizes beyond that. Therefore, the sand particle size of 0.0625 mm will be used to present sand particles, but the particle size for fines still needs further calibration. The data points fall within the bounds of erosion coefficient 10^{-7}, 10^{-8}, and 10^{-9} kg/m^2/s and fines sizes of 0.001 mm and 0.015 mm.

Figure 4-8 Comparison of Erosion Coefficients at Rio Vista and Jersey Point

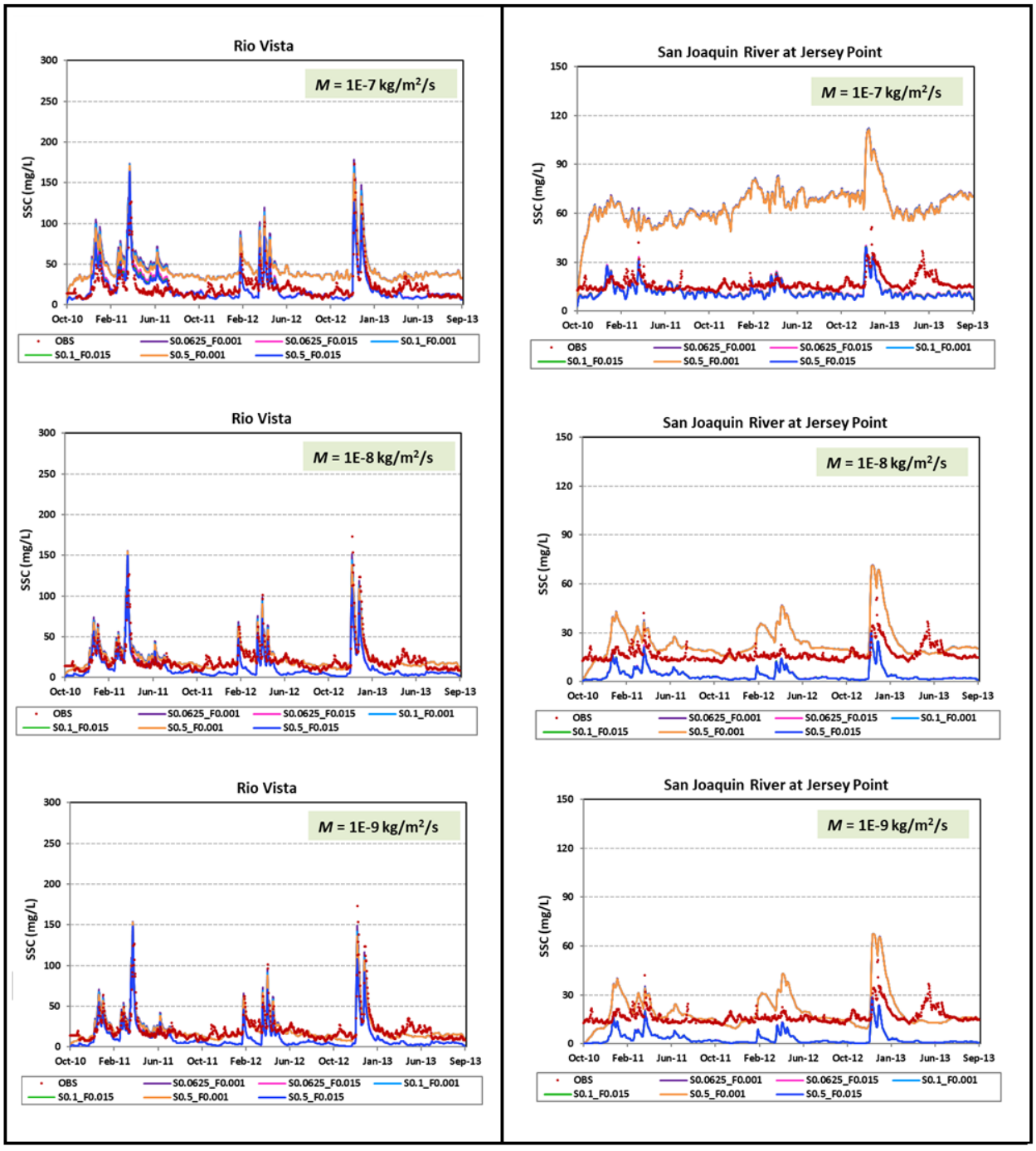

Figure 4-9 Comparison of Erosion Coefficients at Old River at Bacon Island and Mallard Island

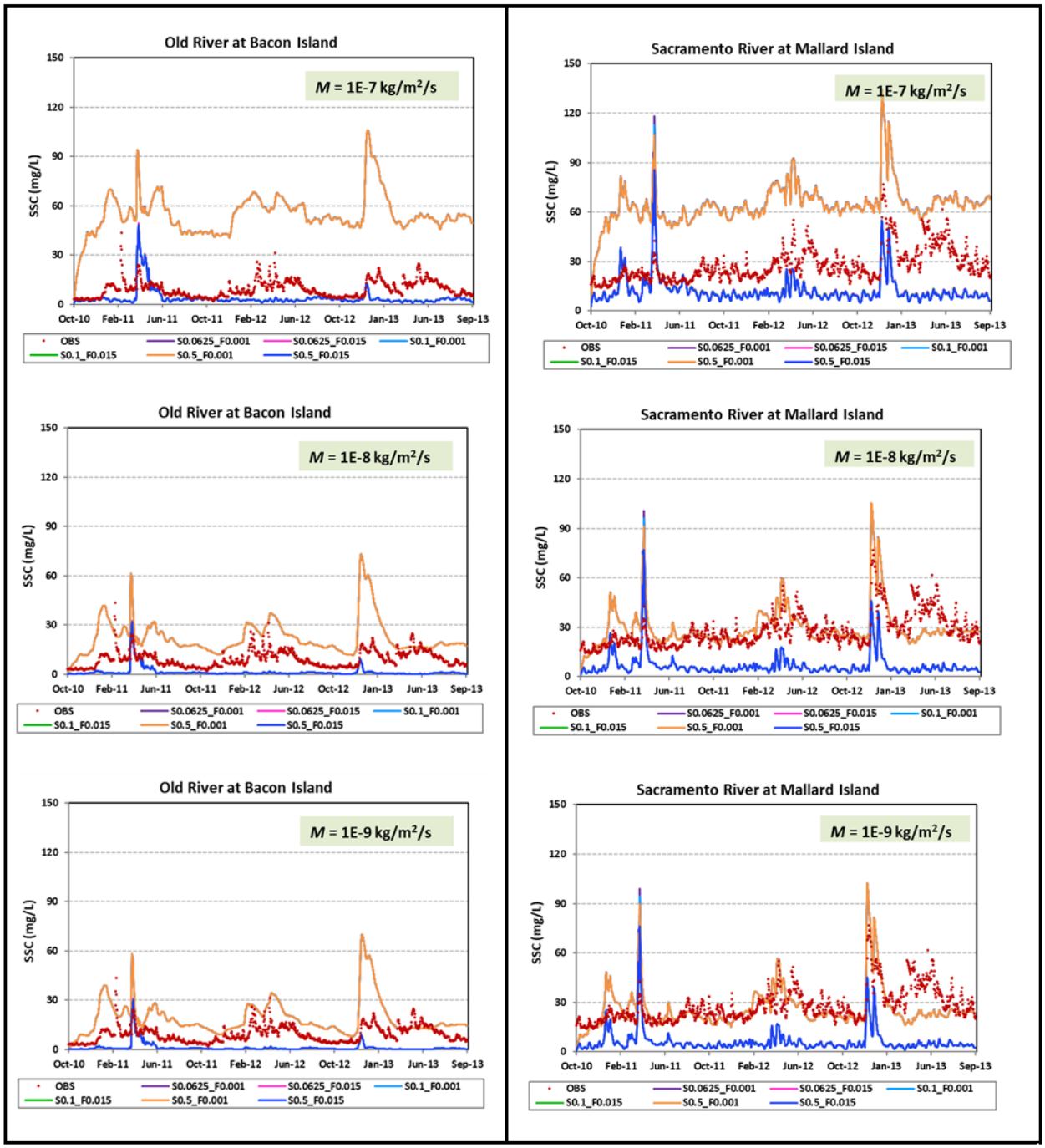

(2) Sediment Particle Sizes

The RMSE values from data and modeled outputs are calculated to quantify the difference among various combinations. The RMSE values for erosion coefficient 10^{-7} kg/m^2/s, 10^{-8} kg/m^2/s, and 10^{-9} kg/m^2/s are shown in Table 4-4, Table 4-5, and Table 4-6, respectively. Green highlighting indicates the lowest RMSE value at each location. Yellow highlighting indicates the best particle size for fines, on average, for that specific erosion coefficient. Consequently, for a sand particle size of 0.0625 mm, the ideal particle sizes for fines for M 10^{-7} kg/m^2/s are 0.01 mm and 0.011 mm, for M 10^{-8} kg/m^2/s are 0.004 mm and 0.005 mm, and for M 10^{-9} kg/m^2/s are 0.004 mm and 0.005 mm.

Table 4-4 Root Mean Square Errors with Erosion Coefficient 10^{-7} kg/m^2/s and Sand 0.0625 mm (mg/l)

Fines	GEO	MIN	RIO	CCH	MOK	OLD	LPS	MID	STK	JPT	MLD
0.006 mm	13.03	15.33	15.85	15.68	14.89	15.51	10.11	13.18	34.94	18.43	12.97
0.007 mm	12.71	14.95	14.74	14.68	13.13	12.18	8.15	10.01	33.49	14.57	11.52
0.008 mm	12.44	14.61	13.78	13.84	11.73	9.85	6.54	7.85	32.42	11.37	11.31
0.009 mm	12.21	14.31	12.99	13.16	10.67	8.41	5.41	6.53	31.68	8.80	11.93
0.01 mm	12.00	14.03	12.36	12.63	9.95	7.69	4.85	5.83	31.22	6.86	12.97
0.011 mm	11.82	13.77	11.89	12.23	9.53	7.47	4.87	5.51	30.97	5.61	14.17
0.012 mm	11.65	13.54	11.57	11.96	9.35	7.54	5.28	5.40	30.90	5.06	15.39
0.013 mm	11.51	13.32	11.38	11.80	9.37	7.74	5.87	5.37	30.95	5.13	16.54
0.014 mm	11.39	13.13	11.31	11.74	9.54	7.98	6.51	5.39	31.10	5.59	17.61
0.015 mm	11.29	12.95	11.34	11.76	9.82	8.22	7.12	5.42	31.30	6.23	18.58

Table 4-5 Root Mean Square Errors with Erosion Coefficient 10^{-8} kg/m²/s and Sand 0.0625 mm (mg/l)

Fines	GEO	MIN	RIO	CCH	MOK	OLD	LPS	MID	STK	JPT	MLD
0.001 mm	6.50	7.43	7.90	10.22	10.55	15.95	11.19	18.16	24.52	11.35	10.80
0.002 mm	6.53	7.15	7.66	9.96	9.94	13.60	10.24	15.24	24.38	9.80	10.65
0.003 mm	6.70	6.98	7.55	9.76	9.45	10.98	9.05	11.91	24.32	8.36	11.04
0.004 mm	6.95	6.92	7.60	9.67	9.19	8.69	7.78	8.85	24.38	7.45	11.98
0.005mm	7.24	6.94	7.79	9.69	9.20	7.11	6.57	6.44	24.57	7.24	13.26
0.006 mm	7.52	7.00	8.08	9.82	9.41	6.38	5.58	4.88	24.88	7.58	14.65
0.007 mm	7.79	7.07	8.46	10.04	9.78	6.36	4.95	4.24	25.27	8.24	16.01
0.008 mm	8.03	7.16	8.89	10.32	10.23	6.73	4.75	4.27	25.71	9.03	17.29
0.009 mm	8.26	7.24	9.35	10.66	10.73	7.24	4.95	4.59	26.18	9.82	18.46
0.010 mm	8.47	7.33	9.84	11.03	11.26	7.74	5.41	4.95	26.65	10.57	19.50

Table 4-6 Root Mean Square Errors with Erosion Coefficient 10^{-9} kg/m²/s and Sand 0.0625 mm (mg/l)

Fines	GEO	MIN	RIO	CCH	MOK	OLD	LPS	MID	STK	JPT	MLD
0.001 mm	6.61	6.73	7.41	9.80	9.64	13.46	10.30	15.74	24.97	9.58	10.95
0.002 mm	6.74	6.56	7.39	9.71	9.33	11.63	9.49	13.30	24.97	8.79	11.31
0.003 mm	7.00	6.50	7.48	9.66	9.14	9.51	8.41	10.40	25.04	8.17	12.09
0.004 mm	7.33	6.54	7.71	9.70	9.16	7.73	7.27	7.73	25.21	8.01	13.22
0.005 mm	7.67	6.65	8.05	9.84	9.39	6.66	6.20	5.69	25.49	8.31	14.53
0.006 mm	7.99	6.78	8.45	10.07	9.76	6.36	5.37	4.52	25.85	8.90	15.86
0.007 mm	8.29	6.92	8.91	10.36	10.23	6.59	4.89	4.19	26.27	9.63	17.13
0.008 mm	8.56	7.06	9.39	10.70	10.75	7.06	4.82	4.39	26.72	10.38	18.31
0.009 mm	8.81	7.20	9.90	11.07	11.29	7.58	5.10	4.77	27.17	11.10	19.38
0.010 mm	9.04	7.33	10.41	11.46	11.83	8.06	5.60	5.14	27.63	11.76	20.33

(3) Percentages of Sand and Fines

To investigate the sensitivity of the proportions used to divide the suspended sediment into sand and fines at boundaries, the Freeport and Vernalis percentage is changed from 10 percent to 90 percent at increments of 10 percent. Other locations still use values from metadata. Table 4-7 shows the list of combinations with smaller RMSE. M is the erosion coefficient in kg/m²/s, the Fines column is fines particle size in mm, and SAC x%_SJR y% means Sacramento River boundary has x proportion of sand and San Joaquin River boundary carries y proportion of sand. Table 4-8 shows the comparison of proportions from metadata and calibration. The results show that the calibrated fraction yields a slightly better fit to the observed data than metadata, and that is expected. The improvement of modeling observed in time series plots are not obvious at most locations. The noticeable locations are Old River at Bacon Island and Middle River at Middle River as shown in Figure 4-10. This indicates that for high flow periods the sand content is higher than the metadata suggested at Vernalis. For the preliminary calibration, the calibrate percentages for Sacramento River and San Joaquin River will be used to present the results.

Table 4-7 List of Combinations with Smaller RMSE Values

M	Fines	Fraction	GEO	MIN	RIO	CCH	MOK	LPS	OLD	MID	STK	JPT	MLD
10^{-7}	**0.01**	Metadata	12.00	14.03	12.36	12.63	9.95	4.85	7.69	5.83	31.22	6.86	12.97
10^{-7}	**0.01**	SAC 70%_ SJR 90%	10.94	12.33	10.07	10.64	11.20	4.73	6.21	3.96	30.35	4.24	13.36
10^{-7}	**0.011**	Metadata	11.82	13.77	11.89	12.23	9.53	4.87	7.47	5.51	30.97	5.61	14.17
10^{-7}	**0.011**	SAC 70%_ SJR 90%	10.90	12.23	10.17	10.72	11.33	5.45	6.51	4.16	30.52	4.06	14.81
10^{-8}	**0.004**	Metadata	6.95	6.92	7.60	9.67	9.19	7.78	8.69	8.85	24.38	7.45	11.98
10^{-8}	**0.004**	SAC 40%_ SJR 70%	7.12	6.83	7.58	9.59	9.35	7.05	7.19	5.84	25.89	6.94	11.97
10^{-8}	**0.005**	Metadata	7.24	6.94	7.79	9.69	9.20	6.57	7.11	6.44	24.57	7.24	13.26
10^{-8}	**0.005**	SAC 40%_ SJR 70%	7.41	6.88	7.87	9.69	9.50	5.97	6.05	3.96	26.24	7.07	13.36
10^{-9}	**0.004**	Metadata	7.33	6.54	7.71	9.70	9.16	7.27	7.73	7.73	25.21	8.01	13.22
10^{-9}	**0.004**	SAC 40%_ SJR 70%	7.56	6.53	7.89	9.75	9.51	6.57	6.55	4.96	27.35	7.91	13.34
10^{-9}	**0.005**	Metadata	7.67	6.65	8.05	9.84	9.39	6.20	6.66	5.69	25.49	8.31	14.53
10^{-9}	**0.005**	SAC 40%_ SJR 70%	7.90	6.66	8.29	9.95	9.84	5.64	5.96	3.59	27.67	8.43	14.71

Table 4-8 Calibrated Sand and Fines Fraction Versus Metadata

Calibrated/Metadata	Percentage Sand	Percentage Fines
Sacramento River Metadata	36.2	63.8
Sacramento River Calibrated	40	60
San Joaquin River Metadata	47.9	52.1
San Joaquin River Calibrated	70	30

Figure 4-10 Comparison of Percentages from Metadata and Calibrated Fraction (M 10^{-8} kg/m^2/s)

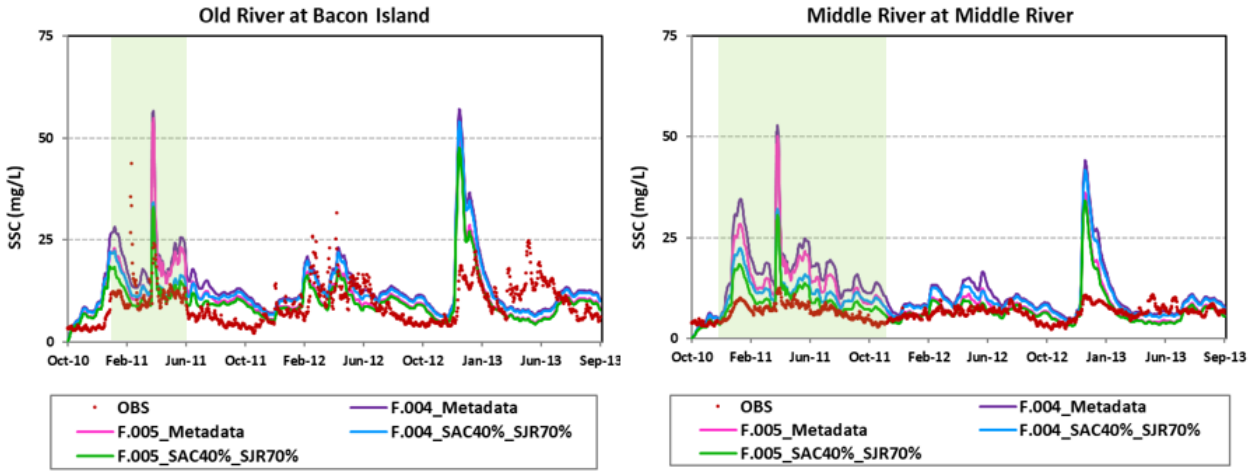

The RMSE analysis has narrowed down the combinations that yield good calibration results. Further investigation is carried out by visual inspection of the time series plot as the RMSE metrics are too close to provide further detail information. The combinations are erosion coefficient (M) 10^{-7} kg/m^2/s with fines particle size 0.01 mm and 0.011 mm, M 10^{-8} kg/m^2/s with fines 0.004 mm and 0.005 mm, and M 10^{-9} kg/m^2/s with fines 0.004 mm and 0.005 mm. The comparison plots are shown in Figure 4-11. The green highlighting indicates periods during which the erosion coefficient of 10^{-7} kg/m^2/s overestimates SSC, and those are usually high-flow periods. In general, the results from erosion coefficient 10^{-8} and 10^{-9} with fines of 0.004 mm and 0.005 mm are fairly close. The orange highlighting indicates that M 10^{-7} and 10^{-8} kg/m^2/s overestimate high flows in 2013 at Old River and Middle River locations. When moving to Jersey Point and Mallard Island, M 10^{-9} kg/m^2/significantly underestimates sediment concentration. Erosion coefficient 10^{-8} kg/m^2/s with fine size 0.004 mm works well at Jersey Point and Mallard Island when compared with others. Therefore, the final combination used to present the results is erosion coefficient 10^{-8} kg/m^2/s, particle size of sand 0.0625 mm, particle size of fines 0.004 mm, percentage of sand at Sacramento River boundary 40 percent, and proportion of sand at San Joaquin River boundary 70 percent.

Figure 4-11 Time Series Plots for Selected Combinations of Erosion Coefficients and Fine Particle Size

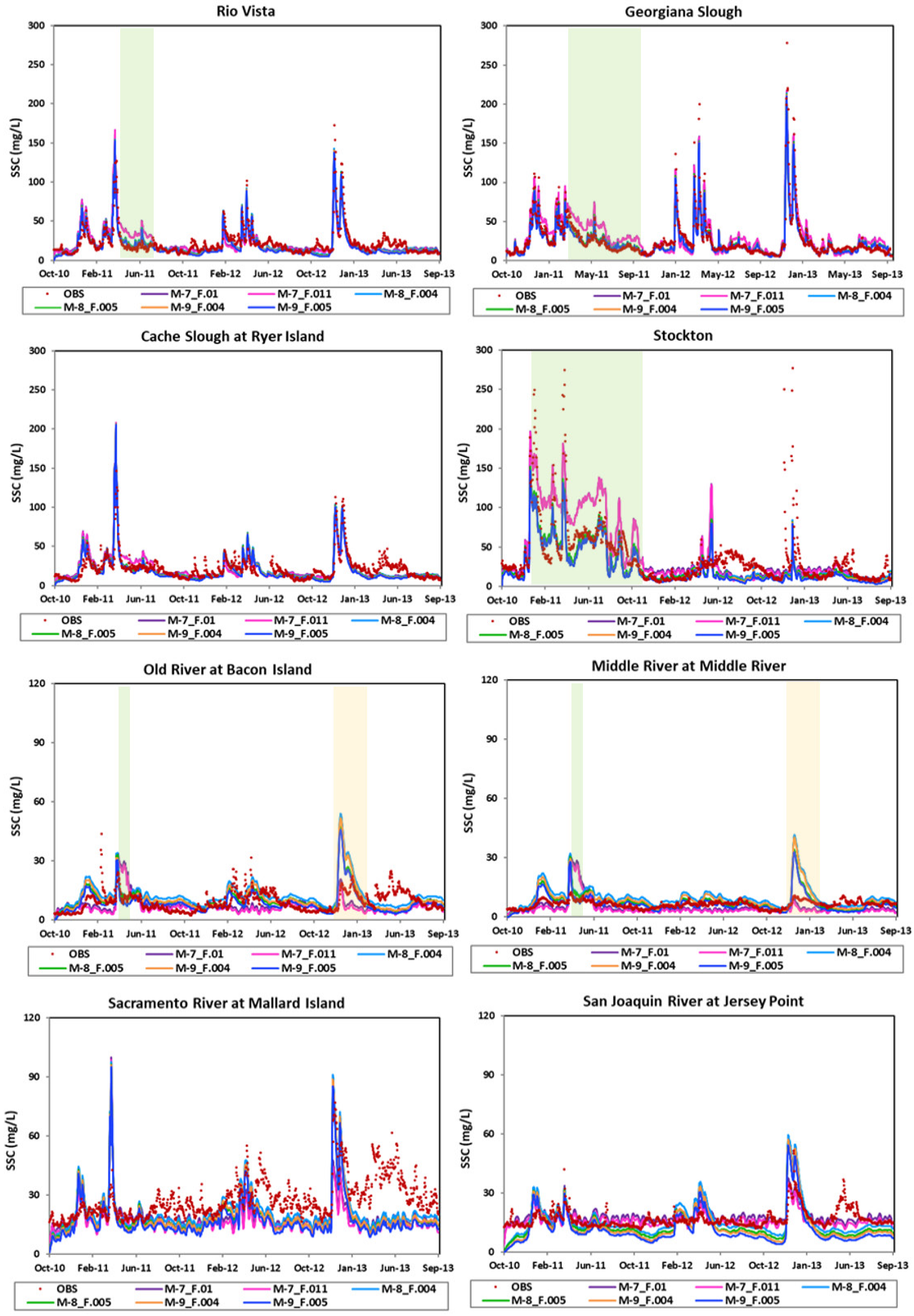

4.4.2 Results from Suspended Sediment Calibration and Validation

Based on the evaluation and comparison among the calibrated parameters and factors, the preliminary calibration results for GTM-SED are shown in Table 4-9, Preliminary Calibrated Parameters for GTM-SED. Other boundaries are using percentages from metadata. The calibration period is from October 2010 to September 2013 (wet, below normal, and dry years) and the results are summarized in Figure 4-12. The validation period is from October 2013 to September 2016 (critical, critical, and below normal years), and the results are summarized in Figure 4-13. Overall, GTM-SED matches the field data closely in capturing the pattern, extreme events, and trends.

Table 4-9 Preliminary Calibrated Parameters for GTM-SED

Parameter	Parameter Value
Erosion Coefficient	10^{-8} kg/(m^2s)
Particle size for sand	0.0625 mm
Particle size for fines	0.004 mm
Sacramento River boundary	40% sand, 60% fines
San Joaquin River boundary	70% sand, 30% fines

4.4.3 Suspended sediment concentration for delta channel depletion drainages

Aside from flows from upstream boundaries, the drainages or return flows are another flow source contributing to the river system. The drainage flow data are obtained from the study of Delta Channel Depletion (DCD) (Liang and Suits 2018). Ideally, Delta island runoff with heavier sediment loads can be introduced to the river system by utilizing DCD. More work is required to investigate ways to incorporate those considerations into the sediment model, either by input data or possible model adjustment. In the preliminary calibration, a constant sediment concentration is assumed for the drainage flows. GTM-SED has the functionality to handle time-varying inputs for each flow source. Further study is needed to assign seasonal concentration patterns for the return flows and to fine-tune the calibration.

Figure 4-12 Results of Suspended Sediment Calibration

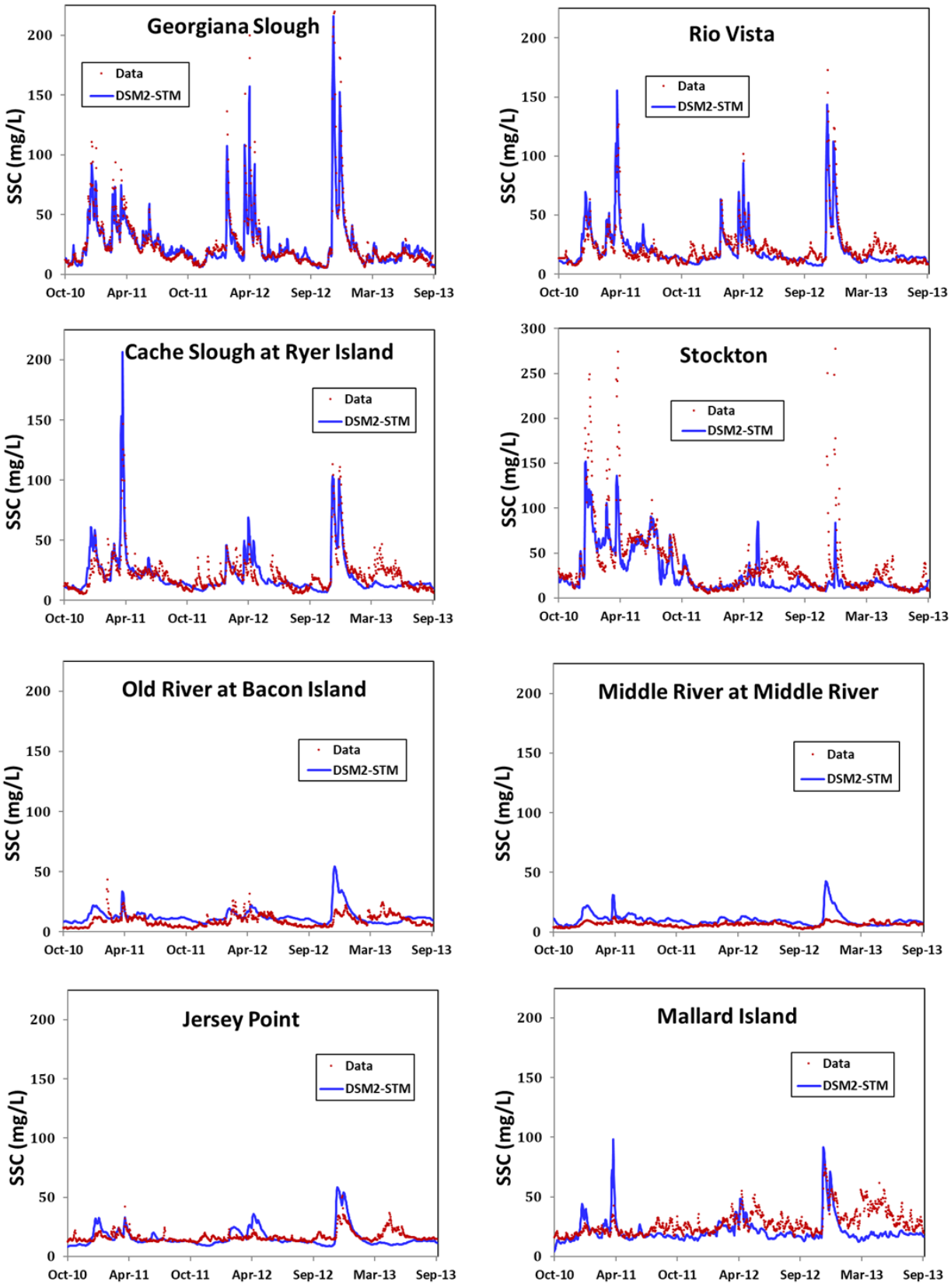

Figure 4-13 Results of Suspended Sediment Validation

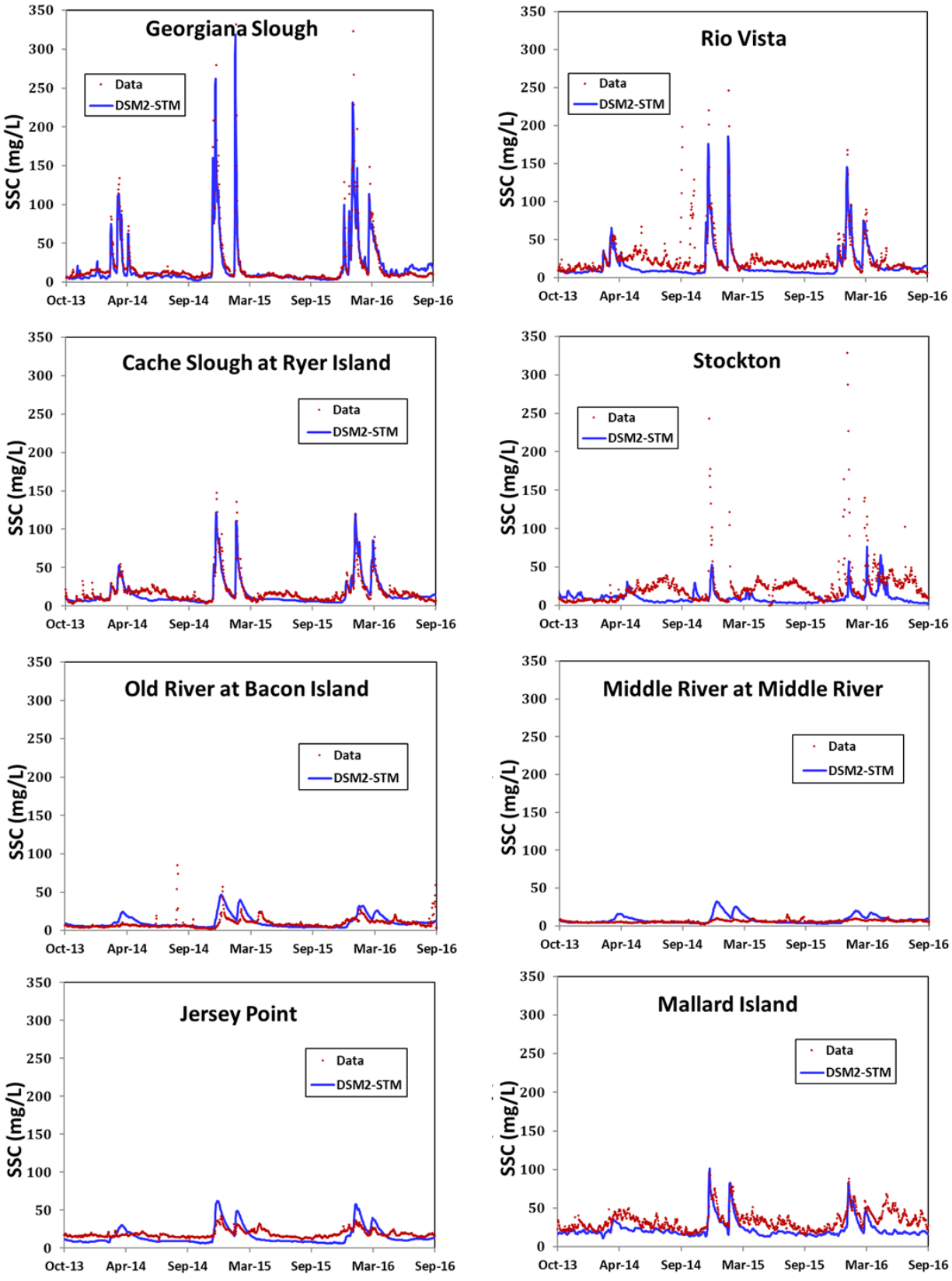

4.4.4 Investigation of Simulation as Conservative Constituent

This section compares the results from simulating suspended sediment as a conservative constituent. The purpose is to investigate the difference with and without introducing erosion and deposition mechanisms into the system. The gray lines in Figure 4-14 are the results of simulating SSC as a conservative constituent, which only incorporates advection and dispersion processes. It may describe the data sufficiently at upstream locations, such as Rio Vista. Nevertheless, when traveling downstream in a net depositional system, the model without sedimentation processes yields numbers that overestimate what the actual observed data suggested. The conclusion drawn from either observed data or GTM-SED is that the sediment contents in central and south Delta are fairly low despite high sediment from boundaries. Most of the sediment gets deposited before it reaches those areas. A model without the sedimentation mechanism cannot capture the picture of clear water in the central and south Delta.

Figure 4-14 Comparison of Results by Simulating Sediment as Conservative Constituent

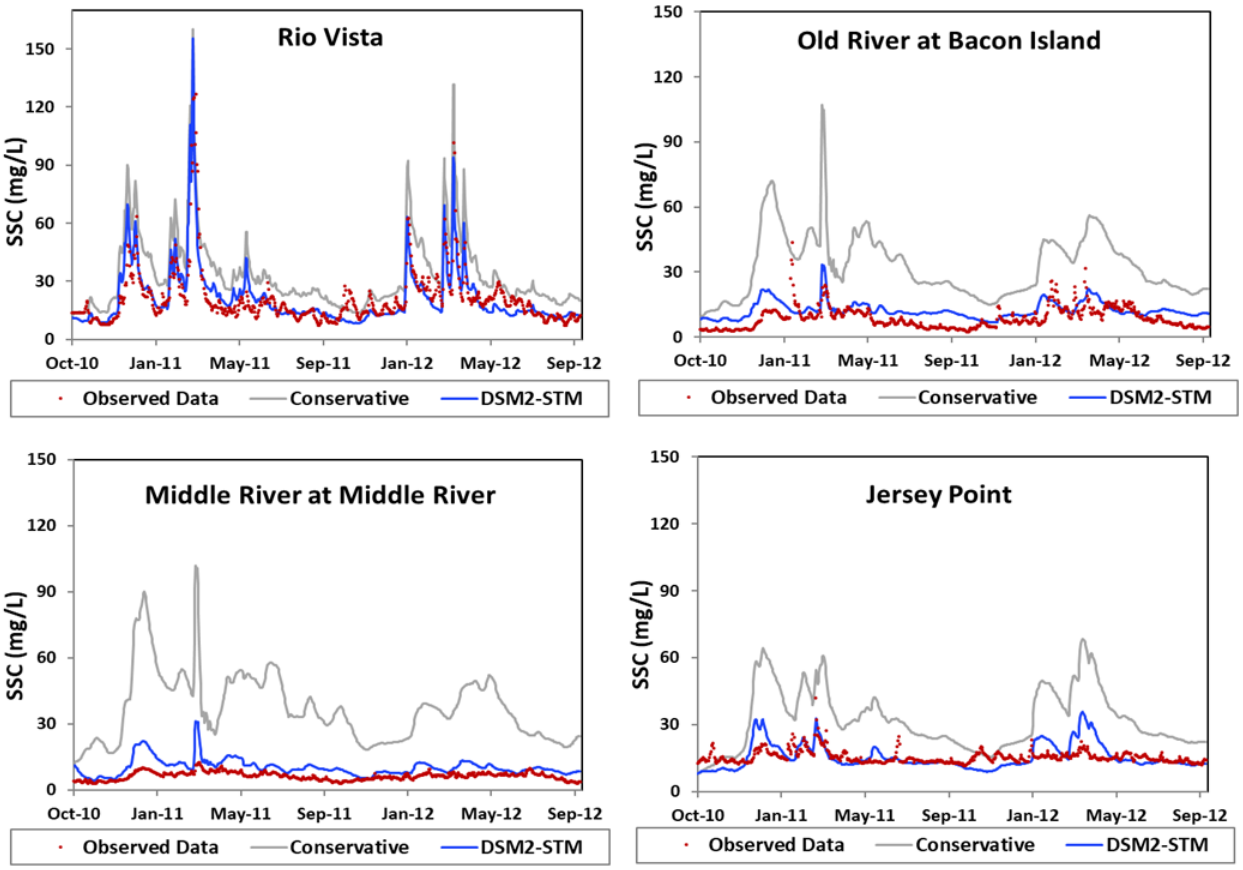

4.4.5 Evaluation of the effects from wind and rainfall

The National Oceanic and Atmospheric Administration (NOAA) has collected hourly meteorological data nationwide. The available parameters include dry-bulb temperature, wet-bulb temperature, wind speed, wind direction, pressure, relative humidity, precipitation, etc. Several studies have investigated the effects of those local climatological events on suspended sediment concentration. The goal of evaluating the time series and correlation here is to explore the possibility of improving some periods which may be affected by those local events.

At most locations in the Delta, the computed results from GTM-SED follow the trends of the observed data and are in reasonable agreement with the magnitude of the sediment concentration. At some locations, especially in the central and south Delta, short term differences between simulated and observed values appear to be related to small tributary inflows or strong winds. An example from Little Potato Slough is shown in Figure 4-15. The orange highlighted period indicates that the sediment spikes seen in the field data cannot be related to boundary inputs and so are likely a result of localized weather events.

These events make fine-tuning the model challenging. High wind speed does increase sediment concentration, but without direct association with hydrology for a one-dimensional model, rainfall seems a more intuitive option than wind to implement the model. In addition, wind speed data tends to be highly variable in magnitude and direction, while storm events are usually well defined. The use of Delta island runoff serves as the intent to capture the effect from the rainfall events. These are topics for future investigation.

Figure 4-15 The Effect of Local Storm and High Wind Events on High Suspended Sediment Concentrations

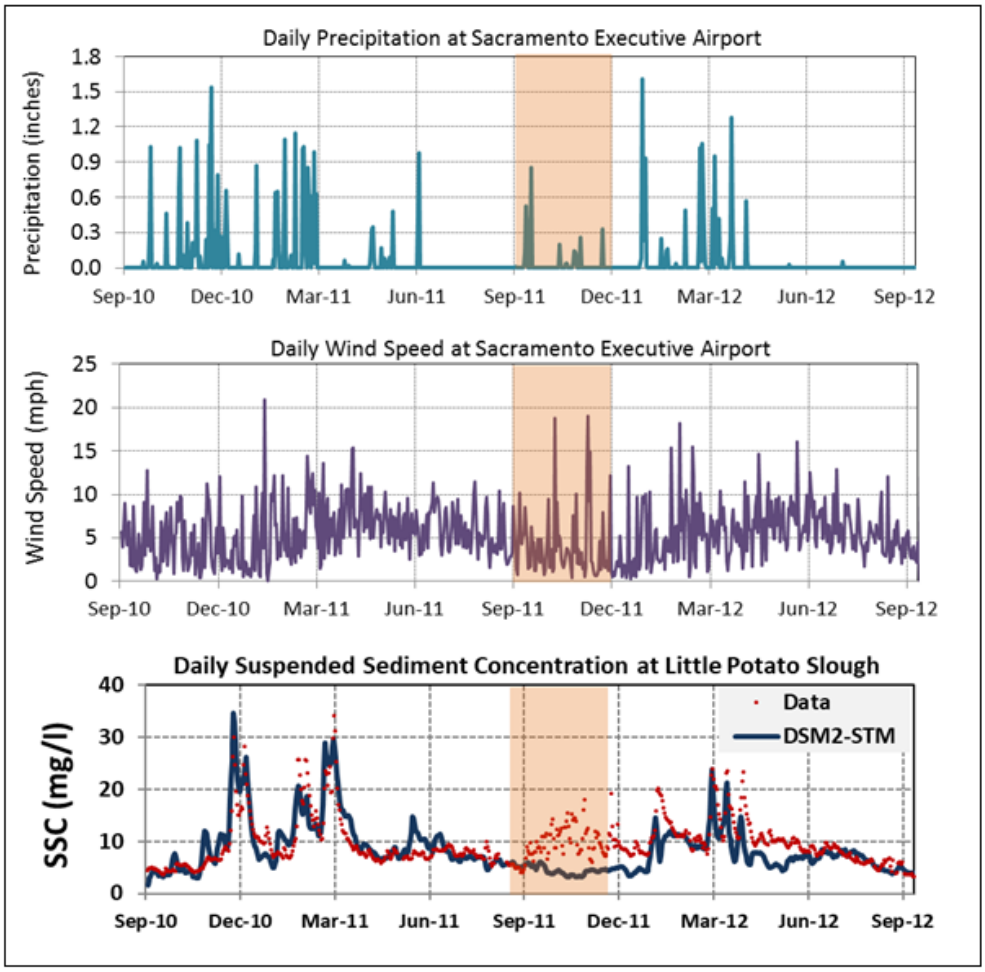

4.5 Sediment Budget Analysis

Several studies were used to determine sediment pathways as a first step toward sediment budget estimates in the Delta area (Schoellhamer et al. 2012). Those studies were based on data analysis and conceptual hindcast models. The sediment budget analysis will provide managers with general information regarding the effects of sediment or turbidity on fish migration and salvage in terms of quantity and pathway of the sediment loads. The sediment budget is calculated from models to evaluate the approximation from the model outputs; however, since the gauges have continuous data collection, the sediment budget calculated from data should be the number that goes to affect analyses and decision-making.

4.5.1 Annual Sediment Budget

Sediment flux is a useful tool for a quantitative analysis of the sediment budget from a certain region and over a length of time. Most studies and analyses are interested in the annual sediment budget. This is defined by the product of water velocity (V) times cross sectional area (A) times SSC (C) as Eq. (20).

$$\text{Sediment Flux } F_{sed} = V \cdot A \cdot C \tag{20}$$

The annual sediment flux is calculated at the sampling location to compare the estimates between modeling outputs and observed data. The comparisons for Water Year 2011, 2012, 2013, 2014, 2015, and 2016 are shown in Figure 4-16. DSM2 allows users to output concentration at any location of interest as long as it is within the channel network system. This practice demonstrates GTM-SED and provides reasonable sediment budget estimates that are close to those calculated from data. Further, this application can be used to track the sedimentation between two cross sections. This may provide quantified results to evaluate a channel being net erosive or net depositional.

4.5.2 Sediment Pathway Analysis

A Delta sediment budget is usually analyzed by a pathway model which calculates sediment loads entering and exiting the north, central, and south Delta regions. The influxes to the north Delta are the ends of the Freeport, Yolo, and Mokelumne rivers, and the exiting fluxes are Rio Vista (RIO), Mokelumne River at Andrus Island (MOK), and Little Potato Slough (LPS). The influxes to the central Delta are Rio Vista (RIO), Mokelumne River at Andrus Island (MOK), Little Potato Slough (LPS), Jersey Point (JPT), Middle River at Middle River (MID), and Old River at Bacon Island (OLD). The exiting point of the central Delta is Mallard Island (MAL). The influx to the south Delta is Vernalis (VNS) and the exiting sediment fluxes are calculated from Stockton (STK), Old River at Bacon Island (OLD), and Middle River at Middle River (MID). The modeled and observed annual sediment budget for the primary pathways in the Delta are shown in Figure 4-17. Although the pathway budgets are mostly around the same range, some years or areas show noticeable discrepancies. As mentioned earlier, the numbers calculated from models are only for testing. As long as data are available, the measurements should be the numbers used for decision making and impact analyses.

Figure 4-16 Comparison of Annual Sediment Budget at Sampling Locations

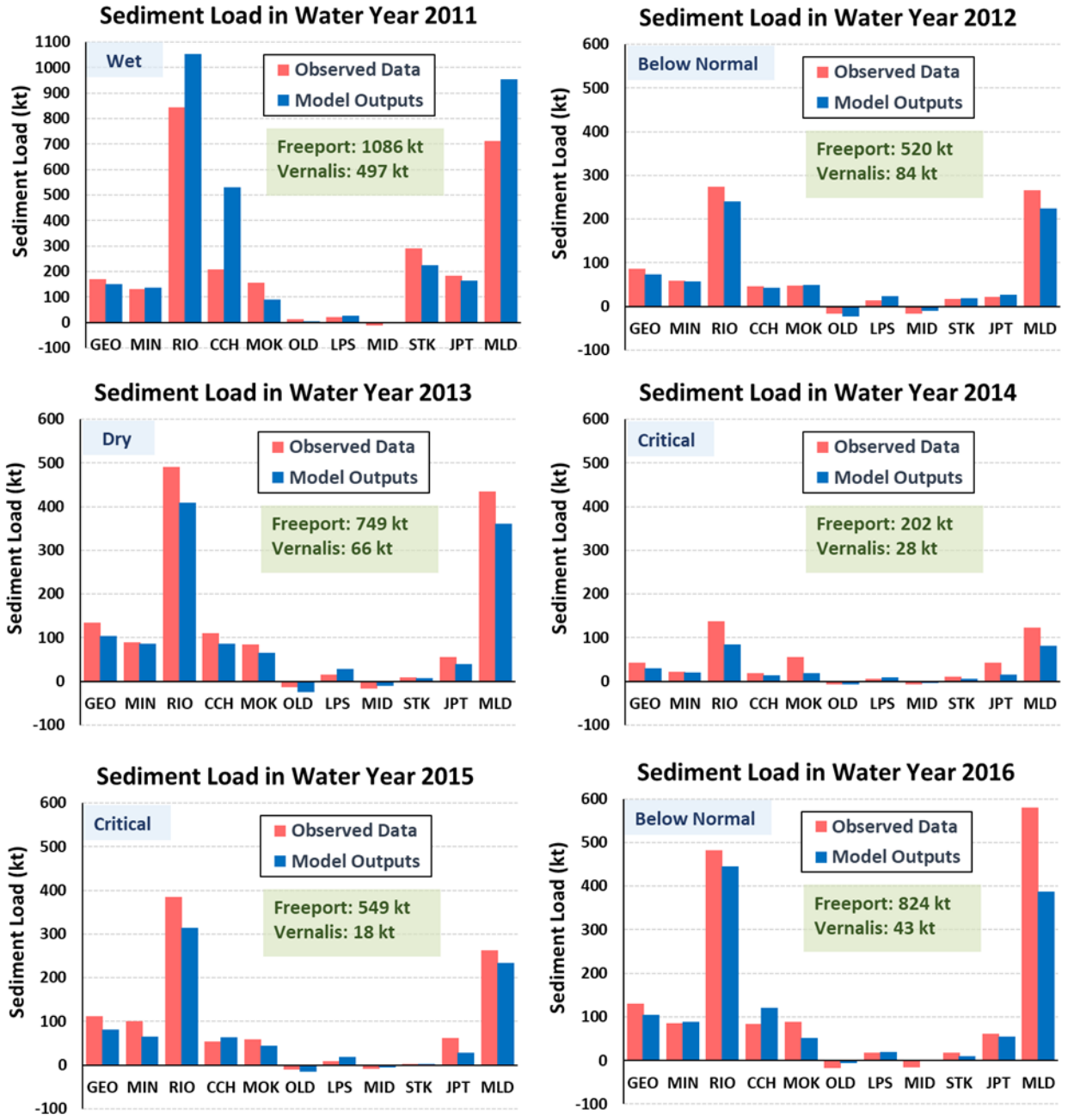

Figure 4-17 Results for Sediment Pathway Analysis

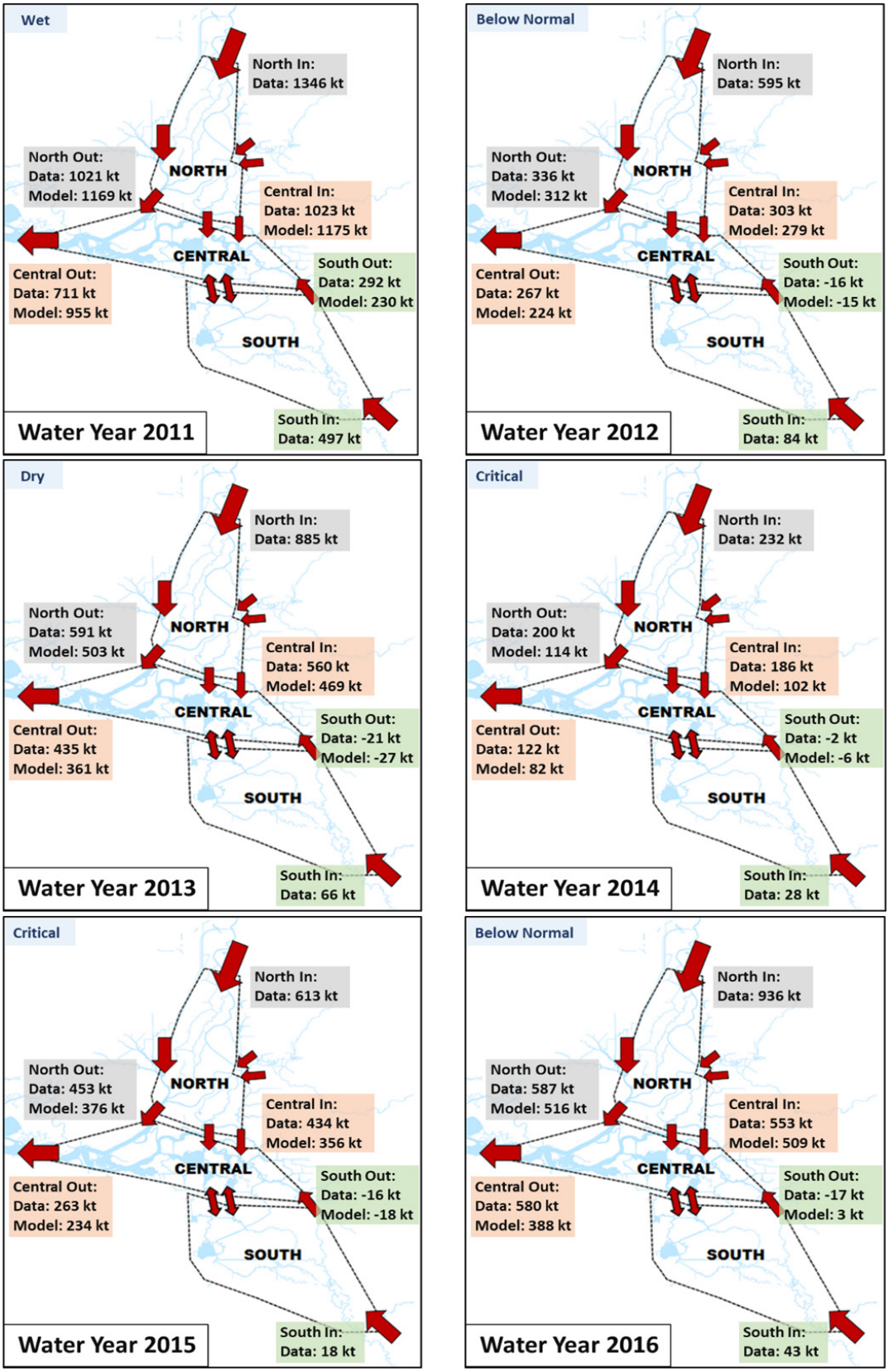

4.6 Turbidity Analysis

4.6.1 Conversions between SSC and Turbidity

Simulated suspended sediment is being investigated as a bridge to estimating water turbidity. First, a correlation between turbidity and suspended sediment data is found. The suspended sediment concentration can be calculated with the site-specific regression equation.

$$\log_{10}(SSC) = a \cdot \log_{10}(Turbidity) + b \quad (21)$$

Using 15-minutes turbidity and sediment data from USGS's website, the best-fit parameters a and b are estimated to complete the equation. The results for Rio Vista, Middle River, and Jersey Point are shown in Figure 4-18. These equations work well at those locations, indicating that suspended sediment concentration and turbidity are highly correlated, and that the conversion is linear and straightforward.

Figure 4-18 Regression Equations for Suspended Sediment Concentration and Turbidity

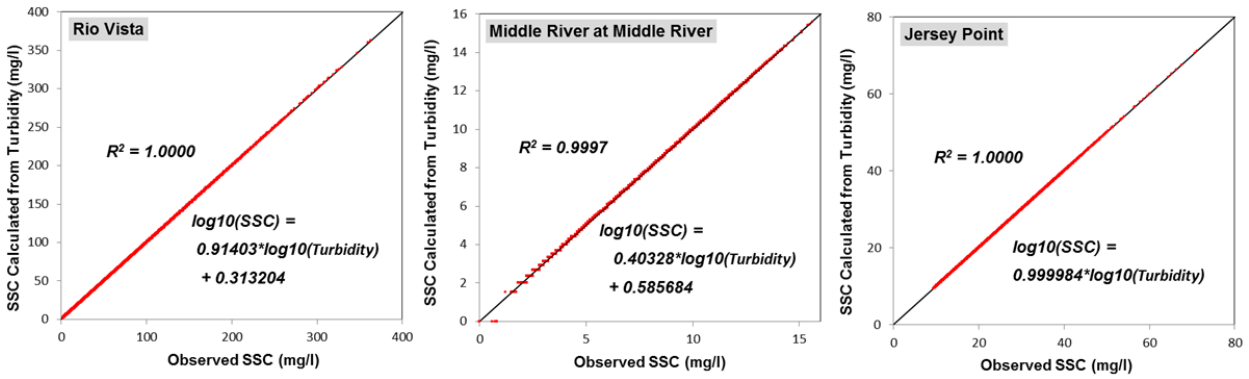

4.6.2 Previous Turbidity Model

Previous DSM2-based Delta turbidity studies by Resource Management Associates (RMA) (2008), Chilmakuri (2010), and Liu (2011) adopted the carbonaceous biochemical oxygen demand (BOD) function to simulate turbidity with the deoxygenation rate coefficient set to zero and the settling rate calibrated to simulate the loss related to settling. This approach was called the Delta Turbidity Model. RMA calibrated this model using the 2008 wet season from December 2007 to March 2008, while Liu (2011) calibrated based on the 2010 wet season from December 2009 to April 2010. These studies found that a model without both a resuspension mechanism and a

consideration of flow velocity cannot capture system turbidity well under different hydrological conditions.

Figure 4-19 Schematic for Simulated Turbidity Comparison

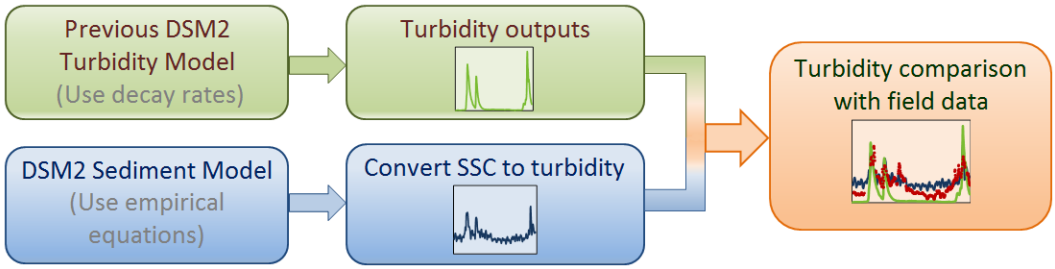

GTM-SED takes flow velocity into account and calculates resuspension based on the changes in flows. GTM-SED simulates suspended sediment concentration, which can then be converted to turbidity by derived regression equations. To compare GTM-SED with the previous turbidity model, it can mimic that model by including simple decay rates in calculating turbidity (Figure 4-19). The results at Rio Vista and Jersey Point (Figure 4-20) suggest that the sediment model better agrees with the observed data than does the turbidity model, which tends to overestimate the peaks and underestimate during the dry season.

Figure 4-20 Turbidity Results Comparison Among GTM-SED, Previous DSM2 Turbidity Model, and Observed Data at Rio Vista and Jersey Point

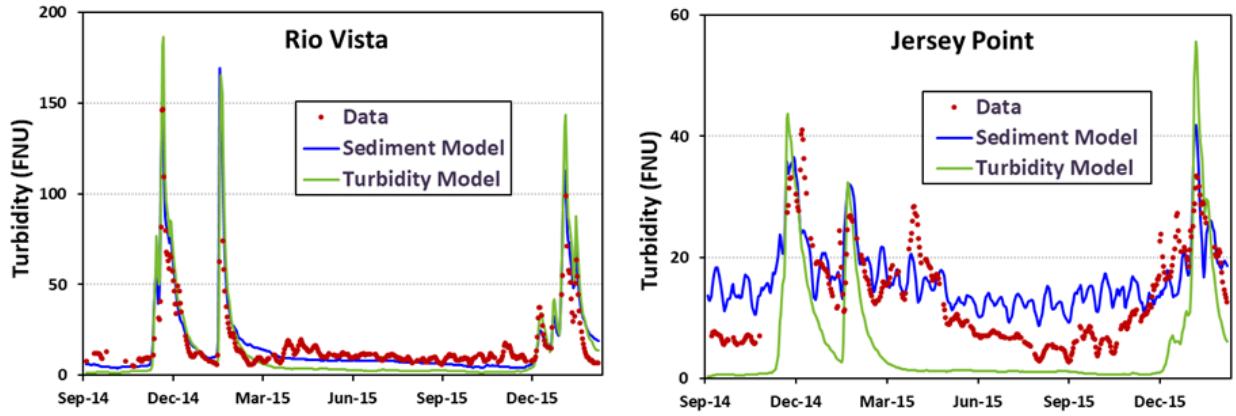

The processed suspended sediment concentrations are estimated by a regression equation derived from the turbidity data taken from unfiltered water. Therefore, it is expected that suspended sediment concentration and turbidity are highly correlated. Successful derivation of these regression equations would make it easy to work on the conversion between two variables. These regression equations are site-specific and subject to change when more data are available.

4.7 Visualization of Sediment Movement

One advantage from modeling is to have model grids filled with simulated values, and this provides continuous information both spatially and temporally. A visualization tool called *DSM2 Animator* (Sandhu 2016) was made available. This tool provides a web interface for users to specify the binary file generated from DSM2-GTM. It visualizes the result on the map for different time frames, enabling users to create animation or screenshots to observe the sediment movement. The DSM2 Animator also helps modelers or developers detect any abnormal outputs from any channels in the network. Animation video is a dynamic way to observe the sediment transport process and enables seeing that the sediment content in central and south Delta area remains low even when high-sediment flows come from the boundaries. Most of the sediment gets deposited before it gets to the central and south Delta region generally referred to as the *Delta donut hole area* (blue circle). Several screenshots in Figure 4-21 are used to demonstrate the visualization of the modeling results from GTM-SED.

Figure 4-21 Screenshots from DSM2 Animator for GTM-SED Output HDF5 File

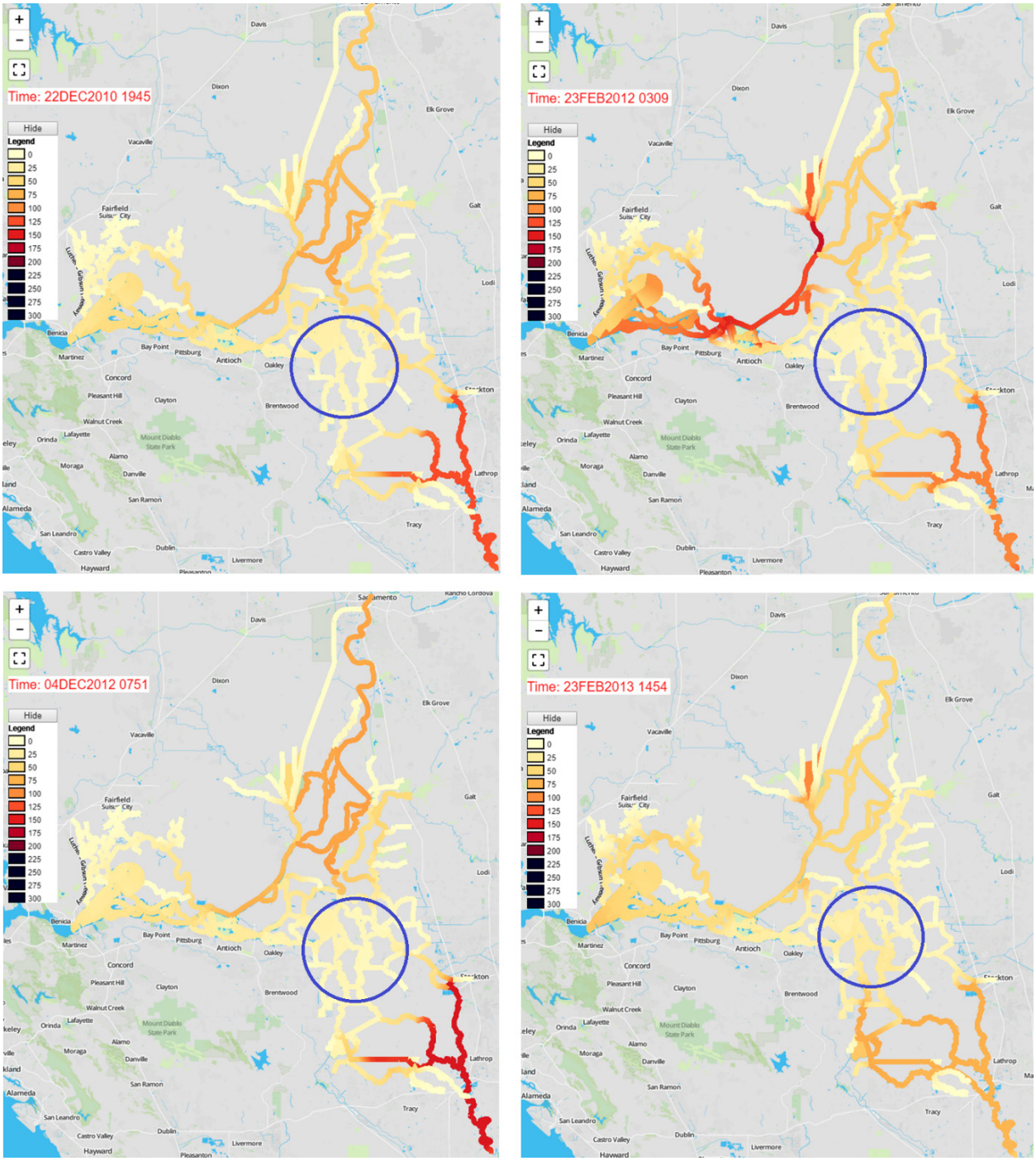

4.8 Summary

- The DSM2 Sediment Model, a time-efficient tool used to estimate suspended sediment concentrations in the Sacramento-San Joaquin Delta, reasonably agrees with the observed data. The model provides a systematic way to describe suspended sediment concentrations, while good quality continuous field data enhances the robustness of the model. Once the development, calibration, and analyses are finalized, documented, and released, further integrations with other applications and studies are expected (see Chapter 5 for integration of bed sediment).
- DSM2 Sediment Transport Model (GTM-SED) accomplishments so far include integrating a sediment module into DSM2-GTM, successfully simulating suspended sediment for the full Delta using a full cycle of DSM2-HYDRO, and calibrating and validating the model with field data. Users can easily use the input system to modify sediment-related variables, including erosion coefficient, number of sediment particle types (sands, fines, etc.), particle size for each type, percentages for each type at model boundaries, and sediment concentration for boundaries and interior drainage flows.
- The preliminary calibration is accomplished by adjusting erosion coefficients, sediment particle sizes, and fractions of sand and fines from the boundaries. The intent is to observe the sensitivity of those variables globally and detect the locations that would be overestimated and underestimated. This one set of calibrated parameters is, in an average-sense, used to describe the entire Delta. Further improvements could include spatial or temporally dependent variables and fine-tuning the model with better estimates of sediment concentration in the channel return flows. Also, more field measurements will help us understand the system and make model improvements.
- GTM-SED uses a Eulerian grid with modular code design, which facilitates experienced code developers when adding extensions and working on further code integrations. Currently, a parallel effort is ongoing for developing sediment bed (see Chapter 5) and mercury modules. These two modules serve as extensions to DSM2-GTM. David Hutchinson from Reed Harris Environmental Ltd. is responsible for sediment bed and mercury code development, and the Modeling

Support Branch from DWR is providing technical support for the integration effort.

- Currently, GTM-SED does not compute morphological changes or bed-load transport. It uses hydrodynamics information from DSM2-HYDRO. Effects from wind and waves are not considered either, which may affect model accuracy for certain areas for certain periods.

GTM-SED now provides a preliminarily calibrated and validated suspended sediment transport model of the Delta. This suspended sediment model can be run as a standalone application of the Delta Simulation Model 2 (DSM2) and it will also be a critical piece of the mercury cycling model that is under development.

4.9 Acknowledgements

This development was initiated by Eli Ateljevich from DWR and Fabian Bombardelli and Kaveh Zamani from University of California, Davis. We want to acknowledge Tara Morgan-King and David Schoellhamer from USGS for providing the field data and reports. We thank Carol DiGiorgio, David Hutchinson, and Reed Harris from the mercury cycling model development team for providing discussions and feedback during the model development. We also thank the Chief of the Modeling Support Branch, Tara Smith, for supporting this project.

4.10 References

Achete FM, Wegen M, van der Roelvink D, and Jaffe B. 2015. "A 2-D process-based model for suspended sediment dynamics: a first step towards ecological modeling." Hydrology and Earth System Sciences, 19, 2837-3857.

Chilmakuri Chandra. 2010. "Turbidity Simulation in the Delta using DSM2." DSM2UG Newsletter.

Delta Mercury Control Program. 2011. "Amendments to the Water Quality Control Plan for the Sacramento River and San Joaquin River Basins for the Control of Methylmercury and Total Mercury in the Sacramento-San Joaquin River Delta Estuary." Attachment 1 to Resolution No. R5-2010-0043.

Liu Lianwu. 2011. "Turbidity Modeling with DSM2." Methodology for Flow and Salinity Estimates in the Sacramento-San Joaquin Delta and Suisun Marsh. 32nd Annual Progress Report from the California Department of Water Resources to the State Water Resources Control Board.

Liang Lan, and Suits Bob. 2018. "Calibrating and Validating Delta Channel Depletion Estimates." Methodology for Flow and Salinity Estimates in the Sacramento-San Joaquin Delta and Suisun Marsh. 39nd Annual Progress Report from the California Department of Water Resources to the State Water Resources Control Board.

Hsu E, Ateljevich E, Sandhu P. 2014. "DSM2-GTM." Methodology for Flow and Salinity Estimates in the Sacramento-San Joaquin Delta and Suisun Marsh. 35nd Annual Progress Report from the California Department of Water Resources to the State Water Resources Control Board, Chapter 4.

Hsu E, Ateljevich E, Sandhu P. 2016. "Delta Salinity Simulation with DSM2-GTM." Methodology for Flow and Salinity Estimates in the Sacramento-San Joaquin Delta and Suisun Marsh. 35nd Annual Progress Report from the California Department of Water Resources to the State Water Resources Control Board, Chapter 4.

Morgan-King Tara L, and Wright Scott A. 2013. *Computation of Suspended-Sediment Concentration Data, Sacramento-San Joaquin River Delta, California, Water Years 2011–2013: U.S. Geological Survey Data Series Report.*

Parchure T, Mehta A. 1985. "Erosion of Soft Cohesive Sediment Deposits." Journal of Hydraulic Engineering 111(10).

Partheniades E. 1962. *A Study of Erosion and Deposition of Cohesive Soils in Salt Water*. PhD thesis, University of California, Berkeley, 182 p.

Resource Management Associates, Inc. 2008. "Sacramento-San Joaquin Delta Turbidity Modeling." Appendix A Technical Memorandum, Fairfield, California: Prepared for the Metropolitan Water District of Southern California.

Sandhu P. 2016. "OMG! Yet Another Animator." DSM2 Users Group Meeting, December 2016.

Schoellhamer D, Manning A, Work P. 2017. "Erosion characteristics and horizontal variability for small erosion depths in the Sacramento-San Joaquin River Delta, California, USA." Ocean Dynamics, DOI 10.1007/s10236-017-1047-2.

Wright S and Schoellhamer D. 2005. "Estimating Sediment Budgets at the Interface between Rivers and Estuaries with Application to the Sacramento-San Joaquin River Delta." In: Water Resources Research, Vol. 41.

Methodology for Flow and Salinity Estimates in the Sacramento-San Joaquin Delta and Suisun Marsh

40th Annual Progress Report
June 2019

Chapter 5
GTM-SED Sediment Bed Integration

Authors: Ali Abrishamchi, Kijin Nam
Delta Modeling Section
Bay-Delta Office
California Department of Water Resources


DEPARTMENT OF WATER RESOURCES
STATE OF CALIFORNIA

Contents

Figures

Tables

5 GTM-SED Sediment Bed Integration

5.1 Introduction

The California Department of Water Resources' (DWR's) Delta Modeling Section has been developing a new General Transport Model (GTM) as a part of the Delta Simulation Model 2 (DSM2) modeling suite (California Department of Water Resources 2014), and it is now being used to simulate the salinity of the Sacramento-San Joaquin River Delta (Delta) (California Department of Water Resources 2016). GTM was specifically designed so that other water quality modules could be added to it. In fact, a suspended sediment module, GTM-SED, is being developed as this report is being written and has been preliminarily calibrated for the Delta (California Department of Water Resources 2019). In parallel, a group of mercury experts has been developing GTM modules for mercury and bed sediments, since sediment in the river bed is closely tied to the fate of mercury. This chapter describes the recent integration of this sediment bed module into GTM-SED to better represent the interaction of bed sediments with the suspended sediment in the water column. The revised GTM-SED module was then preliminarily recalibrated to reflect the effect of the updates. This chapter describes the integration of bed sediment into GTM-SED, related code updates, and re-calibration results.

Figure 5-1 Delta Simulation Model 2 (DSM2) With Newly Integrated Sediment Bed Module Highlighted

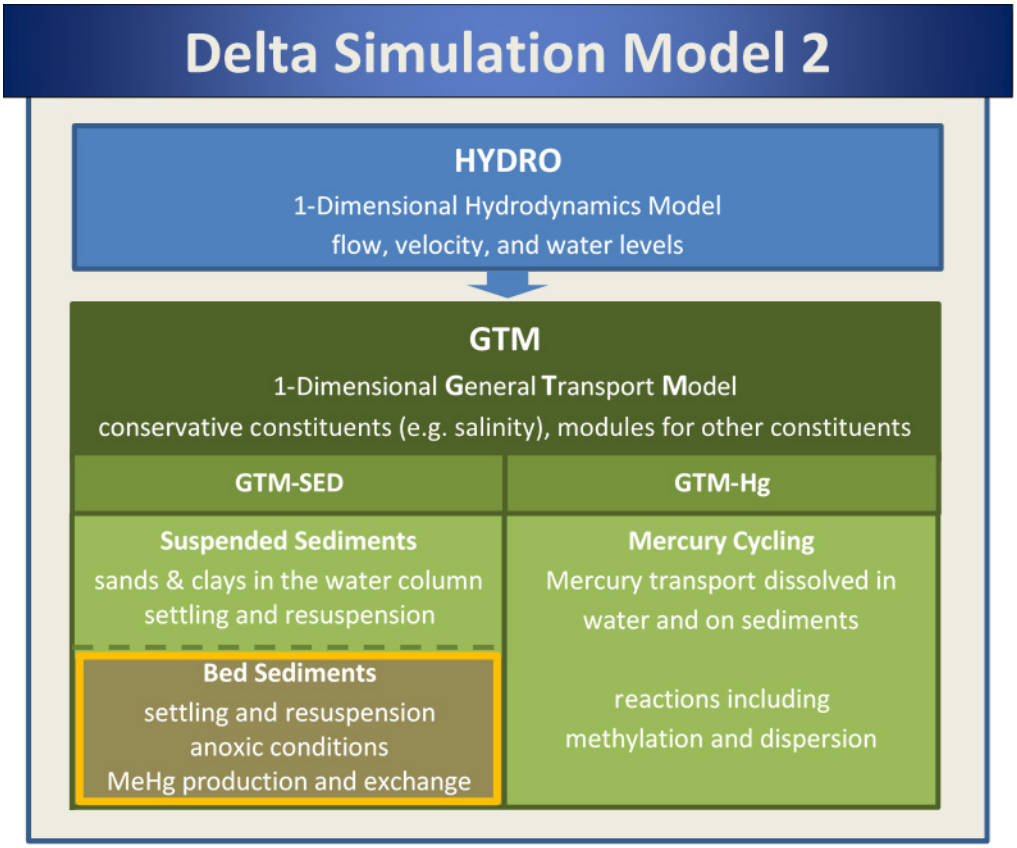

5.2 Sediment bed in GTM-SED

This chapter covers the integration of the sediment bed representation developed to support mercury modeling into GTM-SED to create a standalone module that represents suspended and bed sediments. The fate of mercury in water is closely related to bed sediments because mercury settles in the sediment bed and can be converted into highly toxic Methylmercury by microorganisms. This tendency means that modeling sediment in the water column and bed is an important step for mercury cycle modeling. The mercury and sediment bed module in GTM are being developed by consultants. While the mercury module development is ongoing, the bed sediment work reached a point where it could be integrated in to the GTM-SED module. This section will introduce the key concepts in the sediment bed implementation that are relevant to the updating GTM-SED to create a standalone sediment transport module.

The sediment bed model has two layers and three zones, as shown in Figure 5-2. The zones are divided based on average water level by pre-processing DSM2 HYDRO outputs to represent the three zones (mostly wet, inter-tidal, and mostly dry) as Zones 1, 2, and 3, respectively. The zones are used to simulate mercury reaction depending on the water level. The sediment bed has two layers in the module to simulate mercury reaction properly, and suspended sediment in the water column interacts only with the first sediment bed layer (Bed Layer 1). The thickness of the first bed layer is maintained constant by burial from Bed Layer 1 to Bed Layer 2 and by erosion from Bed Layer 2 to Bed Layer 1.

Figure 5-2 The Conceptual Bed Layers and Zones in GTM-SED Sediment Bed Module

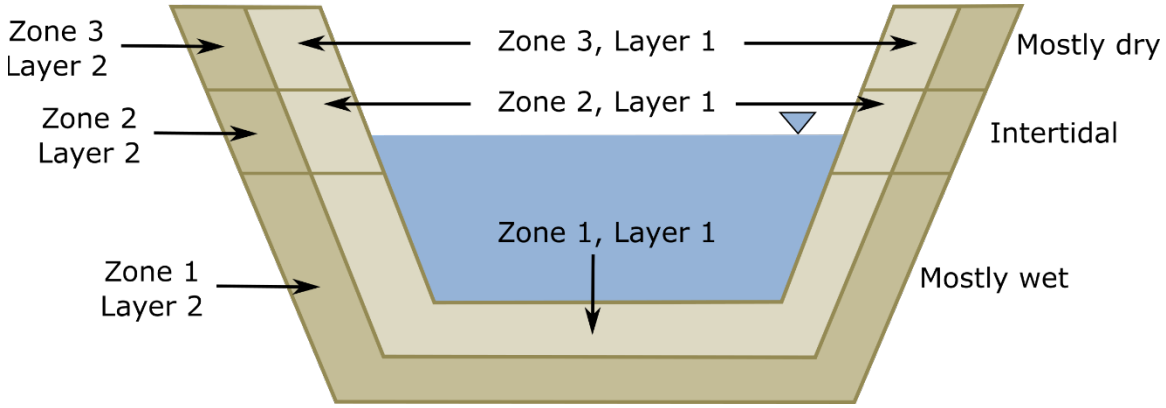

The sediment bed module also introduced organic sediment, which when decomposing can play a role in mercury reactions. As a result, there are three sediment types represented in the model: sands, fine inorganics, and fine organics. The percentage of each sediment type is referred to as the *sediment ratio*.

5.3 Changes in GTM-SED

To integrate the sediment bed module with the suspended sediment module, parts of the GTM-SED sediment codes have been updated. In this process, other parts of GTM that are not directly related to sediment were updated and improved as well.

5.3.1 Changes in the erosion and deposition implementation

Calculation of erosion from the first bed layer to the water column was updated with the sediment composition of Zone 1 of Bed Layer 1 from the sediment bed module. The equation for the updated erosion estimate is (Ariathurai and Arulanandan 1978):

$$E_q = M(1-p)f_q\left(\frac{\tau_{b,q}}{\tau_{cr,q}} - 1\right) \quad \text{for } \tau_{b,q} \geq \tau_{cr,q}$$

where E_q is the erosion flux of a sediment class q, M is the erosion coefficient, p is the sediment porosity of the sediment bed, f_q is the volumetric fraction of sediment class q, $\tau_{b,q}$ is the bed shear stress for sediment class q, and $\tau_{cr,q}$ is the critical shear stress for class q. The difference from the previous erosion implementation is that this version includes the sediment component in the sediment bed and sediment porosity. In this implementation, the bed porosity is assumed to be constant everywhere, so it is not multiplied explicitly but is included in the erosion coefficient as a calibration parameter.

This erosion estimate is distributed proportionally to the wet area of each zone at each time step. Next, the sediment bed module calculates burial and decomposition in all of the zones and layers and then updates the amount of sediment in the bed. Erosion rates are limited based on the sediment availability in the bed, and the adjusted erosion amount is fed back into the suspended sediment calculation. In previous versions of the suspended sediment module that did not have this sediment bed representation (California Department of Water Resources 2019), the erosion calculation did

not account for sediment bed compositions directly but rather implicitly in the calibration.

It should be noted that the sediment deposition calculation did not change with the implementation of the sediment bed; however, sediment deposition is distributed to each zone based on the wet area of the zones in the first layer.

5.3.2 Sediment ratios for return flows from Delta islands

The previous suspended sediment implementation assumed the equal ratio of sediments (sands and fines) in the return flows from the Delta islands. This implementation is updated so that users need to enter the sediment compositions of every Delta island return flow into the model's input file. Since organic sediments have also been added to the model, the user will specify the percentage of sands, fine inorganics, and fine organics in the input file.

5.3.3 Updates of compilers and libraries

As part of the update effort, the compiler environment of the DSM2 GTM model has been migrated to a more recent Intel compiler suite (Microsoft Visual Studio 2015) derived from an old Intel compiler suite (Microsoft Visual Studio 2008). Two libraries that the DSM2 suite depends on, Boost and HDF5, have been updated to more recent versions as well. All these updates are available publicly at GitHub, dsm2-gtm branch at https://github.com/CADWRDeltaModeling/dsm2/tree/dsm2_gtm at the time of writing this chapter.

5.4 GTM-SED calibration

The Delta GTM-SED module is recalibrated after the integration and updates of the codes and inputs. Calibration settings for this exercise followed the direction of previous calibrations as described by Hsu, et al. (California Department of Water Resources 2019), which occurred before the integration. The period of the calibration study was from October 2010 to September 2013, and the validation period includes the following three years, 2014, 2015, and 2016. The DSM2 HYDRO model was first run for the study period, using historical conditions, and its hydrodynamics output was used throughout the calibration as input to the DSM2 GTM simulations.

One major difference in this study from the previous calibrations is that the fine sediment class is split into two classes, inorganic and organic, with identical particle sizes. The two fine classes behave exactly same way except that the organic fine sediment can be decomposed in the sediment bed unlike the inorganic portion. The initial ratio between the organic and inorganic fines in the sediment bed is based on the labile content from analysis of sediment field samples (Marineau and Wright 2017).

The initial conditions of the suspended sediment and sediment bed for the calibration are from one of the calibration runs itself. This approach is chosen because the model spins up easily with a warm initial condition and because interpolation of the sparse sediment bed data for the initial condition in the complex network of Delta channels is not a simple problem. A cold start with zero suspended sediment and a uniform sediment bed composition was tried, and it was found that the model spun up in a month and was not sensitive to the initial condition of the sediment bed.

The calibration parameters were the erosion coefficient and the sizes of sediment particle classes. Since the continuous field data of suspended sediment concentration (SSC) are available in the total SSC without size distribution, model results in individual sediment classes are aggregated into total SSC and then compared with the field data available at stations, as shown in Table 5-1 and Figure 5-3. Multiple combinations of the calibration parameters were selected and run using scripts that manage inputs and post-process outputs. The root mean square error (RMSE) was used to measure the performance of calibration scenarios, which are then used for subsequent calibration. For the sake of brevity, only selected key runs are reported in this chapter.

5.4.1 Calibration of the erosion coefficient

The SSC is calibrated by adjusting the erosion coefficient first. A wide range of erosion coefficients, from 10^{-3} to 10^{-10} kilograms per square meter per second ($kg/m^2/s$), were tested to assess the sensitivity of the model results to different values of the erosion coefficient, although some of these erosion coefficients may be physically unrealistic. The same sediment sizes from the previous calibration effort are used: As shown in Table 5-2, the inorganic and organic fine particle size was set to 0.004 mm, which is the low limit of the silt class, and the sand particle size was assigned to be 0.0625 mm.

Table 5-1 Description of U.S. Geological Survey Sediment Monitoring Stations

Station	USGS Station	Description
CCH	11455350	CACHE SLOUGH A RYER ISLAND
DWS	11455335	SACRAMENTO R DEEP WATER SHIP CHANNEL NR RIO VISTA
GEO	11447903	GEORGIANA SLOUGH NR SACRAMENTO R
JPT	11337190	SAN JOAQUIN R A JERSEY POINT CA
LIB	11455315	CACHE SLOUGH A S LIBERTY ISLAND NR RIO VISTA CA
LPS	11336790	LITTLE POTATO SLOUGH A TERMINOUS CA
MID	11312676	MIDDLE R AT MIDDLE RIVER CA
MIN	11455165	MINER SLOUGH A HWY 84 BRIDGE
MLD	11185185	SUISUN BAY A MALLARD IS CA
MOK	11336930	MOKELUMNE R A ANDRUS ISLAND NR TERMINOUS CA
NFM	11336685	N MOKELUMNE NR WALNUT GROVE CA
OLD	11313405	OLD R A BACON ISLAND CA
RIO	11455420	SACRAMENTO R A RIO VISTA CA
SFM	11336680	S MOKELUMNE R A NEW HOPE BR NR WALNUT GROVE CA
STK	11304810	SAN JOAQUIN R BL GARWOOD BRIDGE A STOCKTON CA
UCS	11455280	CACHE SLOUGH NR HASTINGS TRACT NR RIO VISTA CA

Figure 5-3 U.S. Geological Survey Suspended Sediment Stations Across the Delta

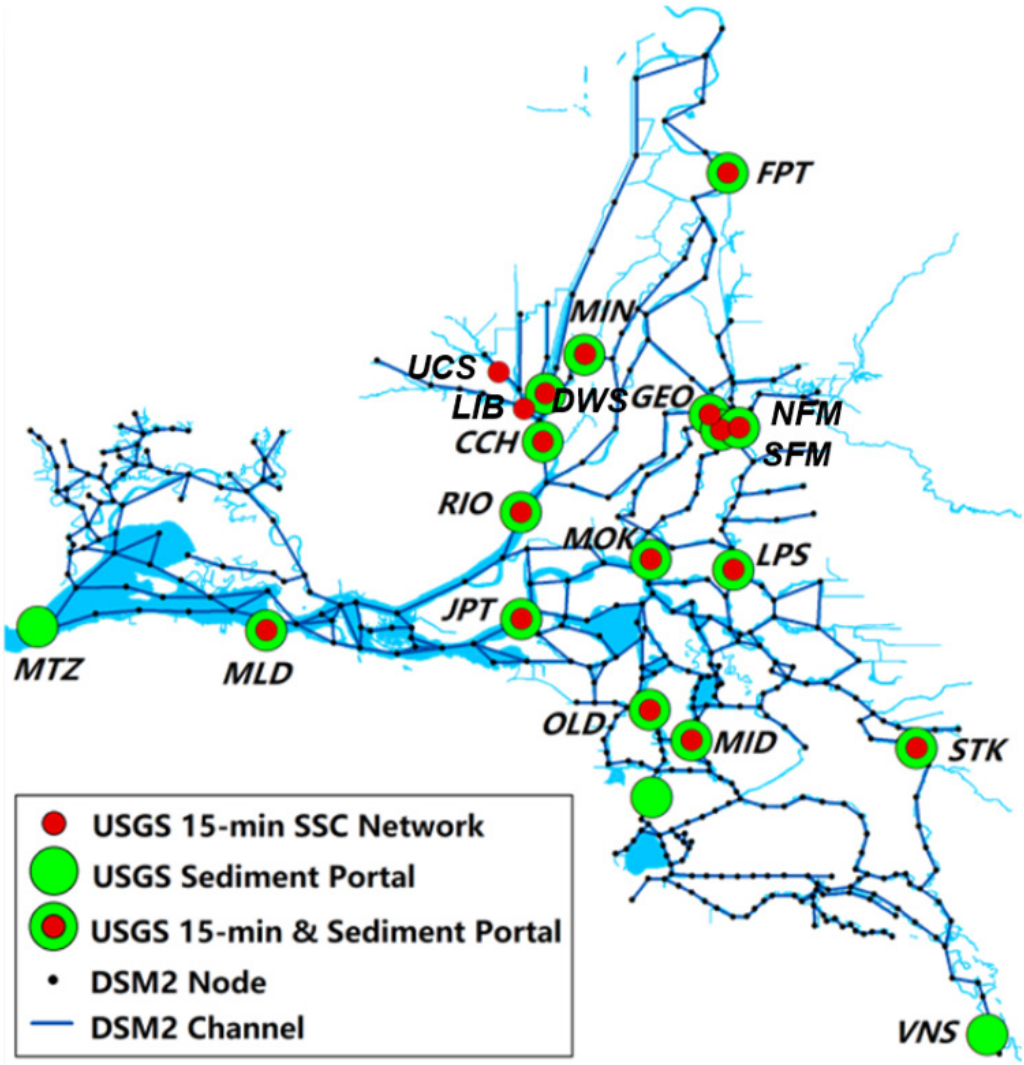

Table 5-2 Erosion Coefficient Sensitivity Analysis for GTM Scenarios

Parameters	Scn1	Scn2	Scn3	Scn4	Scn5	Scn6	Scn7	Scn8
Erosion Coefficient ($kg/m^2/s$)	10^{-3}	10^{-4}	10^{-5}	10^{-6}	10^{-7}	10^{-8}	10^{-9}	10^{-10}
Sand (mm)	0.0625	0.0625	0.0625	0.0625	0.0625	0.0625	0.0625	0.0625
Fines[1] (mm)	0.004	0.004	0.004	0.004	0.004	0.004	0.004	0.004

[1] Inorganic and organic fines.

The RMSE between the 15-minute simulated SSC and 15-minute interpolated observed data is shown in Table 5-3. The scenarios with the lowest RMSEs per station are highlighted in the tables throughout this chapter. RMSE varies for different scenarios and stations, but Scenarios 5, 6, 7, and 8 have lower RMSEs. Scenario 6, with an erosion coefficient of 10^{-8} kg/m^2/s, showed a good overall performance with the lowest RMSE for JPT, RIO, GEO, and other stations. This erosion coefficient is similar to the previously calibrated one even though the sediment bed is integrated, and the erosion implementation is updated.

As shown in Figure 5-4, the higher the erosion coefficient is, the higher the SSC is. The SSC became high quickly when the erosion coefficient was bigger than 10^{-7}, but the model is not sensitive to the erosion coefficients less than 10^{-8}.

Table 5-3 Root Mean Square Errors for Scenarios with Different Erosion Coefficients

Station	Scn1	Scn2	Scn3	Scn4	Scn5	Scn6	Scn7	Scn8
CCH	722.6	342.9	137.0	35.4	12.9	11.8	11.8	11.8
DWS	809.7	420.7	135.0	19.8	13.9	17.3	17.7	17.8
GEO	851.2	291.3	104.2	34.0	8.8	8.3	8.5	8.5
JPT	1240.5	836.1	309.3	79.0	11.0	7.6	8.1	8.2
LIB	655.1	331.9	131.8	35.4	18.7	19.1	19.2	19.2
LPS	627.8	243.2	74.7	21.9	9.2	6.9	6.8	6.7
MID	716.2	414.0	142.5	45.9	10.6	5.5	5.2	5.1
MIN	836.8	258.9	98.2	34.6	10.8	8.1	8.0	8.0
MLD	1011.2	605.7	229.9	60.6	11.6	14.3	14.8	14.9
MOK	823.6	472.2	162.8	44.7	12.3	10.9	11.0	11.0
NFM	863.1	289.2	92.1	20.2	8.0	6.7	6.7	6.7
OLD	848.3	594.4	208.3	58.3	12.1	7.1	6.9	6.9
RIO	915.7	460.9	163.3	40.1	10.4	8.9	9.0	9.0
SFM	859.5	285.7	67.8	16.8	15.0	15.7	15.8	15.8
STK	2079.2	740.9	257.9	77.7	28.7	30.6	31.2	31.2
UCS	41.1	47.1	47.1	47.4	47.6	47.9	47.9	47.9

Figure 5-4 Suspended Sediment Concentrations Using Different Erosion Coefficients

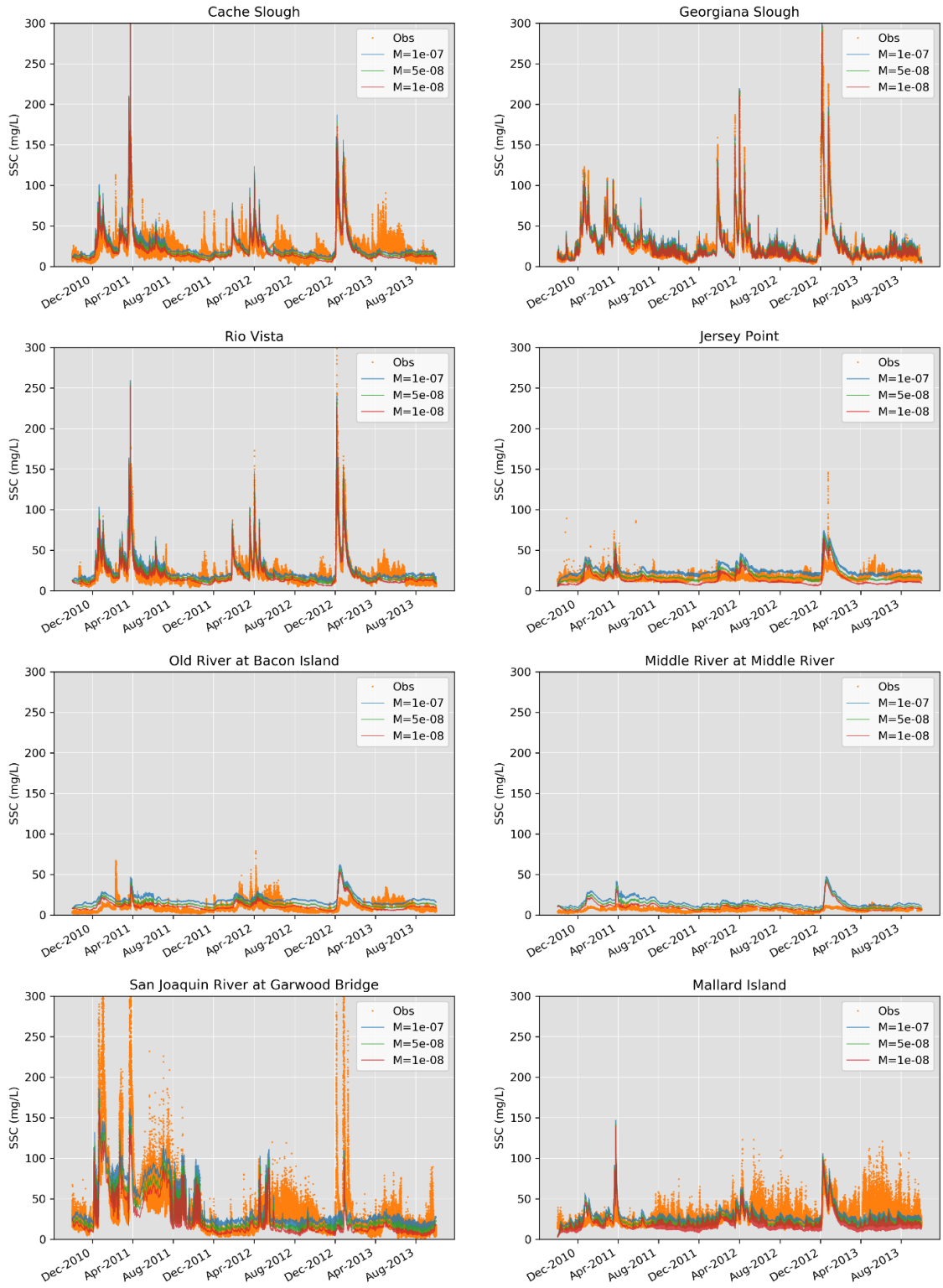

Note: d_{sand} = 0.0625 mm, d_{fine} = 0.004 mm.

5.4.2 Particle size sensitivity analysis

According to the Wentworth grade scale (Wentworth 1922), gravel-sized particles have a nominal diameter of 2 millimeters (mm), sand-sized particles have nominal diameters from less than 2 mm to greater than 0.0625 mm (< 2 mm to > 0.0625 mm), silt-sized particles have nominal diameters from less than 0.0625 mm to greater than 0.004 mm (< 0.0625 mm to > 0.004 mm), and clay is less than 0.004 mm. The following sections will analyze the sensitivity of the SSC to different sand and fine particle sizes.

5.4.2.1 Fine particle size sensitivity analysis

Based on the United States Geological Survey (USGS) fractions definition, silt-sized particle diameters range from 0.004 mm to 0.0625 mm. For GTM sensitivity analysis on fine particles, a group of simulations was set up with the following characteristics: the minimum and maximum of the 0.004 mm to 0.0625 mm range were selected to represent the fine particle sizes, and a single particle size value of 0.5 mm was assigned to represent sand, as shown in Table 5-4. These simulations were performed for erosion coefficients ranging from 10^{-7} to 10^{-10} kg/m^2/s. RMSE values of the calibration scenarios are reported in Table 5-5, and three scenarios are compared with the field data in Figure 5-5.

Table 5-4 Fine Particle Size Sensitivity Analysis GTM Scenarios

Parameters	Scn1	Scn2	Scn3	Scn4	Scn5	Scn6	Scn7	Scn8
Erosion Coefficient	10^{-7}	10^{-8}	10^{-9}	10^{-10}	10^{-7}	10^{-8}	10^{-9}	10^{-10}
Sand (mm)	0.5	0.5	0.5	0.5	0.5	0.5	0.5	0.5
Fines[1] (mm)	0.004	0.004	0.004	0.004	0.0625	0.0625	0.0625	0.0625

[1] Inorganic and organic fines.

As shown in Table 5-5, all of the scenarios with a fine particle size of 0.004 mm (Scenarios 1 to 4) had a smaller RMSE compared with their counterparts with fine particle size of 0.0625 mm (Scenarios 5 and 6). Therefore, the lowest value of the fine particle size range seems to be a better representative for the inorganic and organic fines.

SSC is quite sensitive to the fine particle size, unlike the sand particle size in the next section, where a small fine sediment size resulted in high SSC

resulting from slow settling and easy resuspension. It is shown in Figure 5-5 that the two simulations with the fine class size of 0.0625 mm consistently stayed too low compared to the field data and the other simulations.

Table 5-5 Root Mean Square Errors for Scenarios with Different Fine Particle Sizes

Station	Scn1	Scn2	Scn3	Scn4	Scn5	Scn6	Scn7	Scn8
CCH	11.6	11.4	11.5	11.5	20.7	21.3	21.4	21.4
DWS	14.0	17.4	17.8	17.8	29.8	29.9	29.9	29.9
GEO	8.1	8.6	8.8	8.8	14.0	15.7	15.9	15.9
JPT	10.7	7.6	8.1	8.1	16.9	17.3	17.3	17.3
LIB	17.8	18.8	19.0	19.0	28.1	28.6	28.6	28.6
LPS	9.2	6.9	6.8	6.7	11.1	11.1	11.1	11.1
MID	10.5	5.5	5.2	5.1	6.6	6.7	6.7	6.7
MIN	9.7	7.9	7.8	7.8	12.5	13.2	13.4	13.4
MLD	11.4	14.2	14.7	14.8	29.5	29.7	29.7	29.7
MOK	12.6	11.5	11.6	11.6	22.4	23.0	23.0	23.0
NFM	6.6	6.3	6.4	6.4	11.6	11.9	11.9	11.9
OLD	12.1	7.1	6.9	6.9	10.7	10.7	10.7	10.7
RIO	9.3	9.0	9.2	9.2	21.5	22.2	22.3	22.3
SFM	15.2	16.0	16.1	16.1	19.8	20.3	20.3	20.3
STK	28.1	30.8	31.5	31.5	36.1	37.2	37.4	37.5
UCS	47.6	47.9	47.9	47.9	48.6	48.6	48.6	48.6

Figure 5-5 Suspended Sediment Concentrations Using Different Fine Particle Sizes

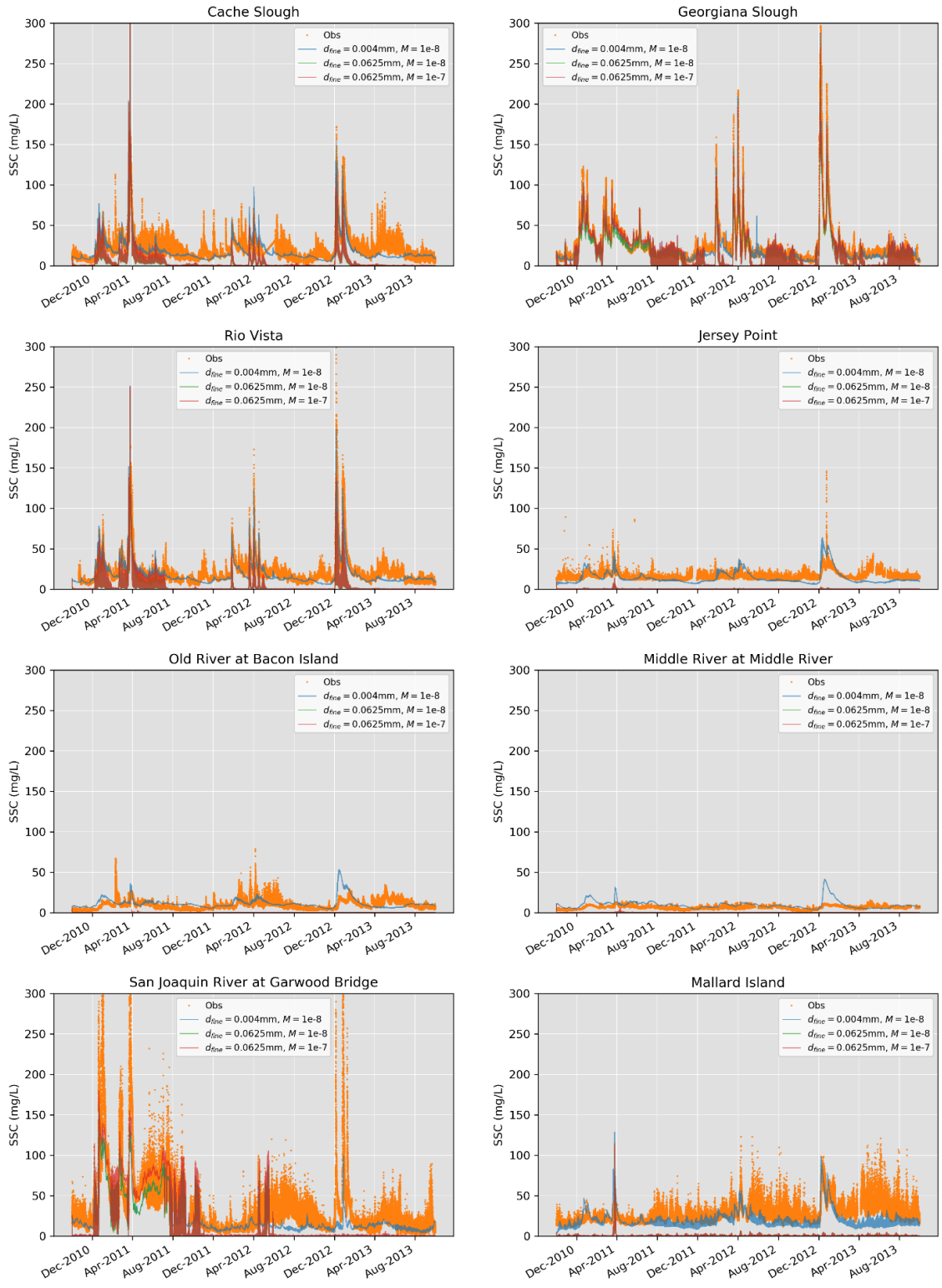

Note: d_{sand} = 0.5 mm.

5.4.2.2 Sand particle size sensitivity analysis

Sand-sized particles have nominal diameters from 0.0625 mm to 2 mm (Wentworth 1922), and so three different particle sizes within this range were assigned to sand to assess the sensitivity of the SSC to these particle sizes. This group of GTM runs were set for a single particle size of 0.004 mm for inorganic and organic fines, while the erosion coefficient changes from 10^{-7} to 10^{-10} kg/m^2/s, as shown in Table 5-6.

Table 5-6 Sand Particle Size Sensitivity Analysis GTM Scenarios

Parameters	Scn1	Scn2	Scn3	Scn4
Erosion Coefficient (kg/m^2/s)	10^{-7}	10^{-8}	10^{-9}	10^{-10}
Sand (mm)	2	2	2	2
Fines[1] (mm)	0.004	0.004	0.004	0.004

Parameters	Scn5	Scn6	Scn7	Scn8
Erosion Coefficient (kg/m^2/s)	10^{-7}	10^{-8}	10^{-9}	10^{-10}
Sand (mm)	0.5	0.5	0.5	0.5
Fines[1] (mm)	0.004	0.004	0.004	0.004

Parameters	Scn9	Scn10	Scn11	Scn12
Erosion Coefficient (kg/m^2/s)	10^{-7}	10^{-8}	10^{-9}	10^{-10}
Sand (mm)	0.0625	0.0625	0.0625	0.0625
Fines[1] (mm)	0.004	0.004	0.004	0.004

[1] Inorganic and organic fines.

Based on the calculated RMSE in Table 5-7, the model performs slightly better for sand particle sizes in the mid and high ranges (0.5 mm and 2 mm, respectively), but SSC is not sensitive to sand particle size in general, as shown in the RMSEs and Figure 5-6. All the calibration cases yielded results close to one another. Combination of sand particle sizes of 0.5 mm and 2 mm with erosion coefficient of 10^{-8} kg/m^2/s and fine particle size of 0.004 mm resulted in a slightly better model results, as seen in Scenarios 2 and 6.

Table 5-7 Root Mean Square Errors for Scenarios with Different Sand Particle Sizes

Station	Scn1	Scn2	Scn3	Scn4	Scn5	Scn6	Scn7	Scn8	Scn9	Scn10	Scn11	Scn12
CCH	11.5	11.4	11.5	11.5	11.6	11.4	11.5	11.5	12.9	11.8	11.8	11.8
DWS	14.0	17.4	17.8	17.8	14.0	17.4	17.8	17.8	13.9	17.3	17.7	17.8
GEO	7.9	8.6	8.9	8.9	8.1	8.6	8.8	8.8	8.8	8.3	8.5	8.5
JPT	10.7	7.6	8.1	8.1	10.7	7.6	8.1	8.1	11.0	7.6	8.1	8.2
LIB	17.7	18.8	19.0	19.0	17.8	18.8	19.0	19.0	18.7	19.1	19.2	19.2
LPS	9.2	6.9	6.8	6.7	9.2	6.9	6.8	6.7	9.2	6.9	6.8	6.7
MID	10.5	5.5	5.2	5.1	10.5	5.5	5.2	5.1	10.6	5.5	5.2	5.1
MIN	9.3	7.8	7.8	7.8	9.7	7.9	7.8	7.8	10.8	8.1	8.0	8.0
MLD	11.4	14.2	14.7	14.8	11.4	14.2	14.7	14.8	11.6	14.3	14.8	14.9
MOK	12.7	11.6	11.7	11.7	12.6	11.5	11.6	11.6	12.3	10.9	11.0	11.0
NFM	6.3	6.3	6.3	6.4	6.6	6.4	6.4	6.4	8.0	6.7	6.7	6.7
OLD	12.1	7.1	6.9	6.9	12.1	7.1	6.9	6.9	12.1	7.1	6.9	6.9
RIO	9.3	9.0	9.3	9.3	9.3	9.0	9.2	9.3	10.4	8.9	9.0	9.1
SFM	15.2	16.1	16.2	16.2	15.2	16.0	16.1	16.1	15.0	15.7	15.8	15.8
STK	27.9	30.9	31.5	31.6	28.1	30.8	31.5	31.5	28.7	30.6	31.2	31.2
UCS	47.7	47.9	47.9	47.9	47.7	47.9	47.9	47.9	47.7	47.9	47.9	47.9

Figure 5-6 Suspended Sediment Concentrations from Using Different Sand Particle Sizes

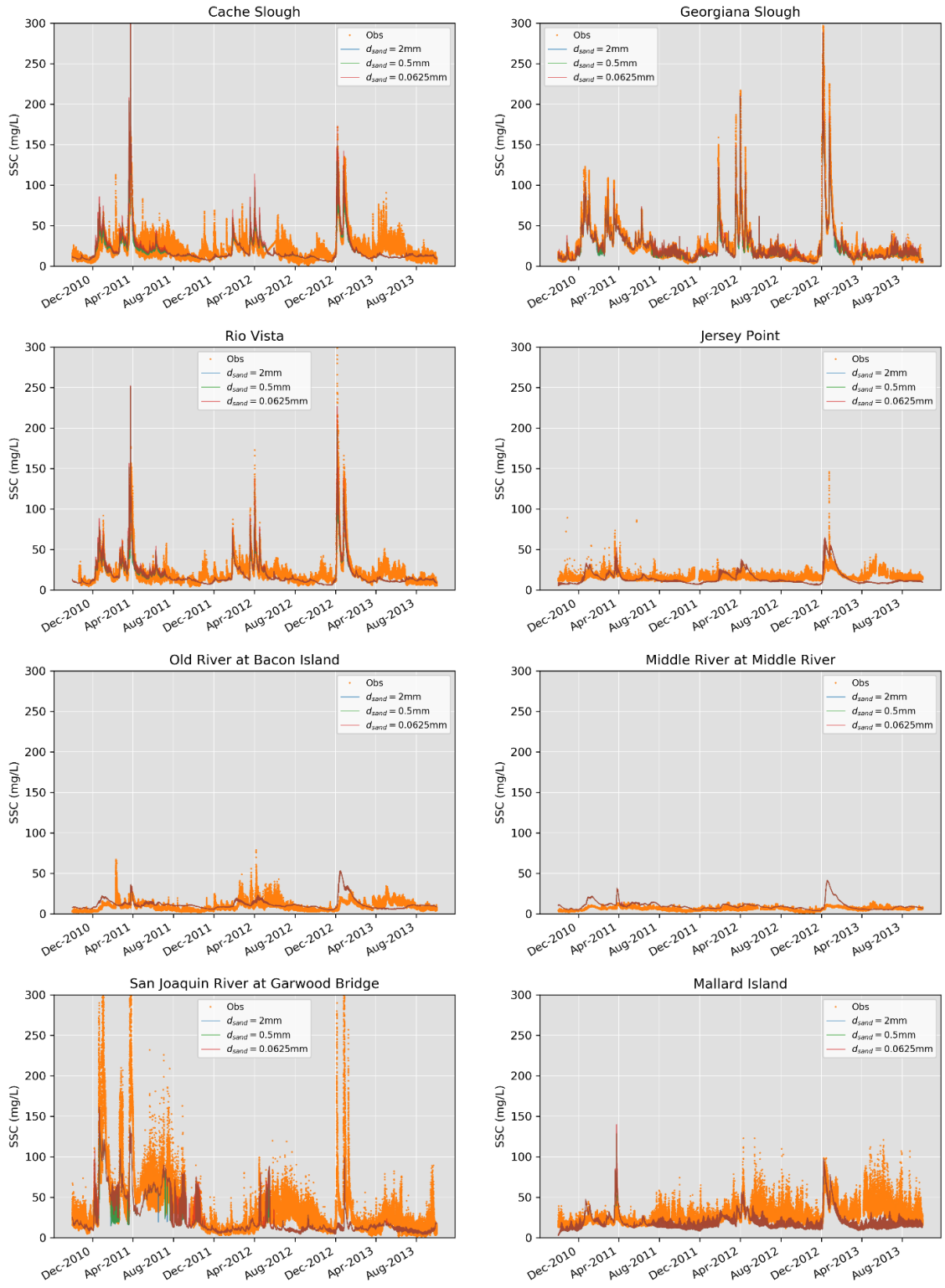

Note: d_{fine} = 0.004 mm, M = 1e-8 kg/m^2/s.

5.4.3 Observed suspended sediment ratios at the river boundaries

In the calibration sets reported in Chapter 4 (California Department of Water Resources 2019), the sediment bed ratios came from a metadata file containing the measured sand, clay, and silt contents in the bed. Consequently, it was assumed that the known sediment ratios from the bed were a reasonable initial estimate for the suspended sediment proportions (percentage of sand and percentage of fines) in the upstream boundary flows. Those parameters were used as the initial values for suspended sediment ratios in the first set of calibrations, and these values were then modified through further calibration (Table 5-8). For every simulation presented in this chapter, the specified ratio of sands and fines is used throughout the simulation and does not vary seasonally.

Table 5-8 Bed Material and Calibrated Suspended Sediment Ratios at River Boundaries

Station	USGS Site Number	USGS measured bed sand content (%), initial value used for suspended sediment in the 1st round of calibration[1]	Calibrated suspended sediment value (%) after 1st round of calibration[1]	USGS measured bed fines content (%), initial value used for suspended sediment in the 1st round of calibration[1]	Calibrated suspended sediment value (%) after 1st round of calibration[1]
Sacramento River at Freeport	11447650	36	40	64	60
San Joaquin River near Vernalis	11303500	48	70	52	30
Cache creek at Yolo	11452500	27	27	73	73
Mokelumne River at New Hope Bridge	11336680	42	42	58	58
Calaveras near San Andreas	11308000	33	42	67	58
Cosumnes River at Michigan Bar	11335000	38	42	62	58
Suisun Bay at Benicia Bridge (Martinez)	11455780	10	10	90	90

[1]California Department of Water Resources 2019.

In this section, the previous calibration is extended by examining the model results for two representations of the suspended sediment ratios at the river boundaries: (1) the previously calibrated suspended sediment ratios and (2) measured suspended sediment ratios based on the averaged USGS measured suspended sediment at or close to the GTM boundaries as shown in Table 5-9. The SSC field data suggest that, on average, more fine particles and less sand need to be in the boundary flows. Eight different scenarios to assess the accuracy of the simulation results in comparison with the previously calibrated suspended sediment ratios at the river boundaries are introduced in Table 5-10. Note that in the new simulations, the percentage of fines includes both organic and inorganic fines, since organic fines were added to the model with the new sediment bed representation.

Table 5-9 Observed vs. Calibrated Suspended Sediment Ratios at River Boundaries

Station	USGS Site Number	Calibrated suspended sand ratio (%) after 1st round of calibration[1]	USGS measured suspended sand ratio (%)	Calibrated suspended fines ratio (%) after 1st round of calibration[1]	USGS measured suspended fines ratio (%)
Sacramento River at Freeport	11447650	40	14[2]	60	86[2]
San Joaquin River near Vernalis	11303500	70	21[3]	30	79[3]
Yolo bypass near Woodland	11453000	27	10[4]	73	90[4]
Mokelumne River near Walnut Grove	11336680	41	12[5]	59	88[5]
Calaveras River near San Andreas	11308000	41	8[6]	59	92[6]
Cosumnes River at Michigan Bar	11335000	41	29[7]	59	71[7]
Suisun Bay at Benicia Bridge (Martinez)	11455780	10	10[8]	90	90[8]

[1]California Department of Water Resources 2019.

[2] Long-term average of available data from 5/23/1973 till 1/17/2017.

[3] Long-term average of available data from 10/5/1965 till 1/24/2017.

[4] Long-term average of available data from 2/4/1957 till 7/7/2016.

[5] Long-term average of available data from 7/25/2012 till 2/16/2017.

[6] Long-term average of available data from 11/12/1973 till 3/28/1979.

[7] Long-term average of available data from 11/19/1965 till 7/10/2015.

[8] Long-term average of available data from 11/8/2005 till 2/8/2017.

Table 5-10 GTM Scenarios with Observed Suspended Sediment Ratios at River Boundaries

Parameters	Scn1	Scn2	Scn3	Scn4	Scn5	Scn6	Scn7	Scn8
Erosion Coefficient ($kg/m^2/s$)	10^{-7}	10^{-8}	10^{-9}	10^{-10}	10^{-7}	10^{-8}	10^{-9}	10^{-10}
Sand (mm)	0.5	0.5	0.5	0.5	0.0625	0.0625	0.0625	0.0625
Fines[1] (mm)	0.004	0.004	0.004	0.004	0.004	0.004	0.004	0.004

[1] Inorganic and organic fines.

In general, the RMSE values reported in Table 5-11 are bigger than those of their counterpart scenarios (Scenarios 5 to 12) in Table 5-5 for the first round of the calibration. SSCs with low erosion coefficients matched better to the observed values, but it does not seem enough to compensate for a high amount of fine sediment from the boundary flows. Figure 5-7 shows a comparison of Scenario 2 to a corresponding scenario from Section 5.4.2.1. The higher fine ratios at the boundary flows resulted in higher SSC all the time, everywhere, but there are some seasonal variations in the amount of the error. It is known that the ratios of sand and fine sediment in the river flow depend on the amount of flow and seasons, and this error may be reduced by using seasonally varying sediment ratios at the boundaries.

The RMSE values in Table 5-11 indicate that the scenario group with a bigger sand particle size of 0.5 mm (Scenarios 1 to 4) produced better simulation results compared with those with sand particle size from the lower end of the range (Scenarios 5 to 8). This finding agrees with the finding from Section 5.4.2.1.

Table 5-11 Root Mean Square Errors for Scenarios with Observed Suspended Sediment Ratios at River Boundaries

Station	Scn1	Scn2	Scn3	Scn4	Scn5	Scn6	Scn7	Scn8
CCH	15.7	13.0	12.8	12.8	16.8	13.4	13.2	13.2
DWS	12.1	14.3	14.6	14.6	12.2	14.3	14.6	14.6
GEO	9.4	7.9	7.9	7.9	10.4	8.0	8.0	8.0
JPT	17.4	11.3	11.1	11.1	17.7	11.3	11.1	11.1
LIB	19.8	18.9	18.9	18.9	20.7	19.2	19.2	19.2
LPS	15.1	12.5	12.2	12.2	15.1	12.5	12.2	12.2
MID	19.4	14.1	13.6	13.5	19.5	14.1	13.6	13.5
MIN	12.1	9.0	8.8	8.7	13.1	9.3	9.0	9.0
MLD	16.1	15.5	15.7	15.8	16.3	15.6	15.8	15.8
MOK	15.5	11.5	11.2	11.2	15.7	11.4	11.1	11.1
NFM	8.5	7.1	7.0	7.0	9.5	7.4	7.2	7.2
OLD	19.0	13.0	12.5	12.5	19.1	13.0	12.5	12.5
RIO	14.1	10.3	10.1	10.1	15.2	10.7	10.4	10.4
SFM	14.8	15.2	15.3	15.3	14.8	15.1	15.2	15.2
STK	31.9	29.1	29.2	29.2	32.7	29.3	29.3	29.4
UCS	47.4	47.6	47.6	47.6	47.4	47.6	47.6	47.6

Figure 5-7 Suspended Sediment Concentrations with USGS SSC Ratios at the Boundaries

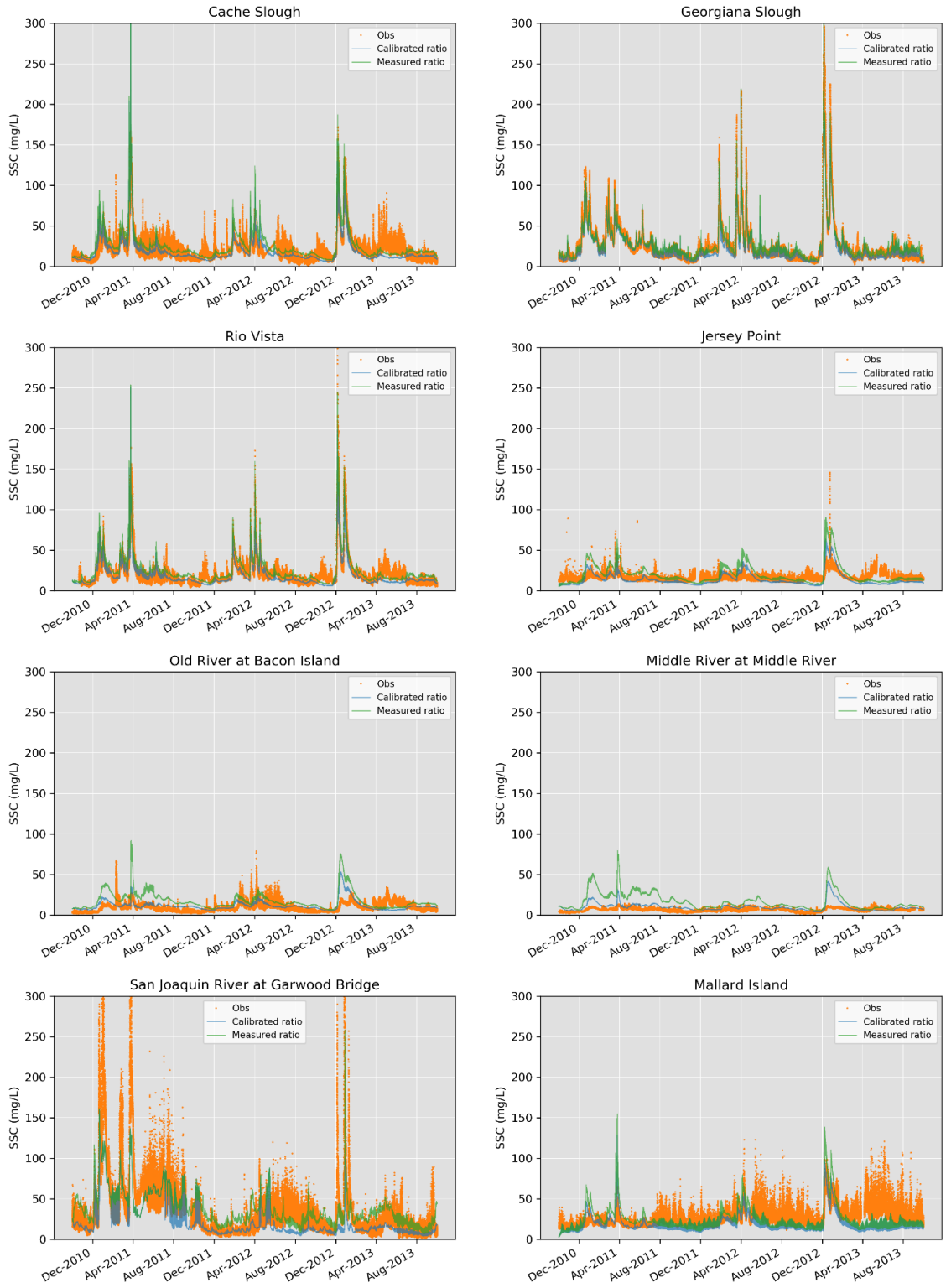

Note: d_{sand} = 0.5 mm, d_{fine} = 0.004 mm, M = 1e-8 kg/m^2/s.

5.4.4 Sensitivity analysis for the ratio of sand at the river boundaries

To assess the model's sensitivity to the assigned suspended sediment ratios for the river boundaries, a 50 percent reduction in boundary sand suspended sediment ratio was incorporated, as shown in Table 5-12. The specification of these scenarios is described in Table 5-13. The scenarios in this section have conditions similar to the conditions of the scenarios in the previous section, notably the boundary SSC values using USGS data.

Table 5-12 Base vs. Reduced Sand Ratios at River Boundaries

Station (GTM node)	Base GTM Study	Reduced Boundary Suspended Sand GTM Study
Sacramento (330)	40% sand, 60% fines	20% sand, 80% fines
Vernalis (17)	70% sand, 30% fines	35% sand, 65% fines
Yolo (316)	27.2% sand, 72.8% fines	13.6% sand, 86.4% fines
Mokelumne (447)	41.5% sand, 58.5% fines	20.75% sand, 79.25% fines
Calaveras (21)	41.5% sand, 58.5% fines	20.75% sand, 79.25% fines
Cosumnes (446)	41.5% sand, 58.5% fines	20.75% sand, 79.25% fines
Martinez (361)	10% sand, 90% fines	5% sand, 95% fines

Table 5-13 GTM Scenarios for Reduced Sand Ratios at the River Boundaries

Parameters	Scn1	Scn2	Scn3	Scn4	Scn5	Scn6	Scn7	Scn8
Erosion Coefficient	10^{-7}	10^{-8}	10^{-9}	10^{-10}	10^{-7}	10^{-8}	10^{-9}	10^{-10}
Sand (mm)	0.5	0.5	0.5	0.5	0.0625	0.0625	0.0625	0.0625
Fines[1] (mm)	0.004	0.004	0.004	0.004	0.004	0.004	0.004	0.004

[1] Inorganic and organic fines.

Comparison of the RMSE values in Table 5-14 with their counterpart values from Scenarios 5 to 12 in Section 5.4.2.1 show that the RMSE values of the simulated SSCs increased in Table 5-14 as the sand suspended sediment ratio reduced at the boundaries.

Table 5-14 Root Mean Square Errors for Scenarios with Reduced Sand Ratio at the River Boundaries

Station	Scn1	Scn2	Scn3	Scn4	Scn5	Scn6	Scn7	Scn8
CCH	14.5	12.2	12.1	12.1	15.8	12.8	12.6	12.6
DWS	12.3	14.9	15.2	15.2	12.3	14.9	15.2	15.2
GEO	8.9	7.7	7.8	7.8	9.9	7.9	7.9	7.9
JPT	15.8	10.1	10.0	10.0	16.1	10.1	10.0	10.0
LIB	19.0	18.6	18.6	18.6	20.1	19.0	19.0	19.0
LPS	13.8	11.2	11.0	11.0	13.8	11.2	11.0	11.0
MID	16.9	11.6	11.1	11.0	17.0	11.6	11.1	11.0
MIN	11.4	8.5	8.3	8.3	12.5	8.8	8.6	8.6
MLD	14.8	14.7	15.0	15.0	15.0	14.7	15.0	15.1
MOK	14.5	11.0	10.8	10.8	14.6	10.8	10.6	10.6
NFM	7.9	6.6	6.5	6.5	9.0	7.0	6.9	6.8
OLD	17.2	11.2	10.8	10.7	17.2	11.2	10.8	10.7
RIO	12.7	9.4	9.3	9.3	13.9	9.9	9.7	9.6
SFM	14.6	15.1	15.2	15.2	14.7	15.0	15.1	15.1
STK	29.7	28.5	28.7	28.8	30.6	28.6	28.8	28.9
UCS	47.4	47.7	47.7	47.7	47.4	47.7	47.7	47.7

Figure 5-8 Suspended Sediment Concentrations with Reduced Sand at the Boundaries

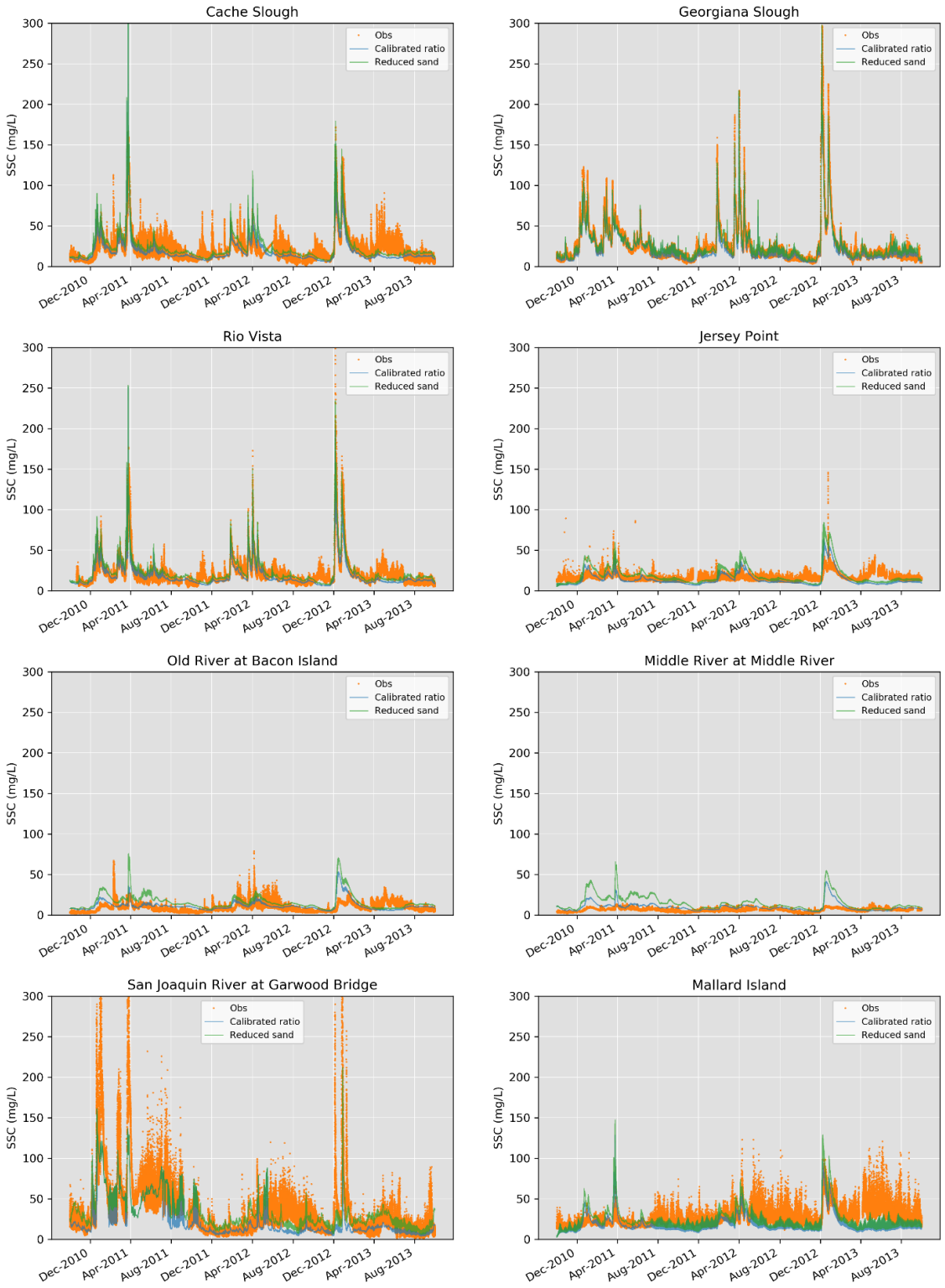

Note: d_{sand} = 0.5 mm, d_{fine} = 0.004 mm, M = 1e-8 kg/m^2/s.

5.4.5 Sensitivity analysis for sediment bed initial conditions

A non-uniform initial condition for the model domain's bed composition in these GTM simulations was adapted from the bed composition from the end time of an earlier GTM simulation. The intention of this section is to analyze the effect of the initial condition of the bed composition on the simulated SSCs. To do so, a uniform bed composition was assumed for the whole model domain. Organic ratio of the sediments was determined to be 4 percent of the bed material. This ratio is calculated from the loss on ignition (LOI) of the bed samples reported as the summary of bed material characteristics during the fall of 2010 from the Sacramento-San Joaquin Delta (Marineau and Wright 2017). In addition, the inorganic fines and sand were assigned 19 percent and 77 percent of the bed material, respectively.

Table 5-15 Sand Particle Size Sensitivity Analysis GTM Scenarios

A. Uniform sediment bed composition initial condition

Parameters	Scn1	Scn2	Scn3	Scn4
Erosion Coefficient	10^{-8}	$5x10^{-8}$	10^{-8}	$5x10^{-8}$
Sand (mm)	0.5	0.5	0.0625	0.0625
Fines[1] (mm)	0.004	0.004	0.004	0.004

B. Non-uniform sediment bed composition initial condition

Parameters	Scn5	Scn6	Scn7	Scn8
Erosion Coefficient	10^{-8}	$5x10^{-8}$	10^{-8}	$5x10^{-8}$
Sand (mm)	0.5	0.5	0.0625	0.0625
Fines[1] (mm)	0.004	0.004	0.004	0.004

[1] Inorganic and organic fines.

Incorporating a uniform sand and fines composition for the bed initial condition did not make significant changes in simulated SSCs when compared with the observed data, such as comparing the RMSEs of Scenarios 1 to 4 with the ones for Scenarios 5 to 6 in Table 5-18. This suggests that sediment bed condition does not affect the simulated SSCs strongly.

Table 5-16 Root Mean Square Errors for Scenarios with and Without Uniform Sediment Bed Composition Initial Conditions

A. Uniform sediment bed composition initial condition

Station	Scn1	Scn2	Scn3	Scn4
CCH	11.5	11.2	11.8	11.8
DWS	17.6	16.6	17.5	16.5
GEO	8.6	8.0	8.3	7.9
JPT	7.8	7.0	7.8	7.1
LIB	18.9	18.5	19.1	18.9
LPS	6.8	7.3	6.9	7.4
MID	5.3	6.4	5.4	6.4
MIN	7.8	8.2	8.1	8.8
MLD	14.4	13.1	14.5	13.2
MOK	11.6	11.4	10.9	10.8
NFM	6.4	6.3	6.8	7.1
OLD	7.0	7.8	7.0	7.8
RIO	9.1	8.7	9.0	8.9
SFM	16.0	15.7	15.7	15.4
STK	31.0	29.4	30.7	29.3
UCS	47.9	47.8	47.9	47.8

B. Non-uniform sediment bed composition initial condition

Station	Scn5	Scn6	Scn7	Scn8
CCH	11.4	11.1	11.8	11.9
DWS	17.4	15.8	17.3	15.7
GEO	8.6	7.9	8.3	7.9
JPT	7.6	7.3	7.6	7.4
LIB	18.8	18.2	19.1	18.6
LPS	6.9	7.9	6.9	7.9
MID	5.5	7.5	5.5	7.6
MIN	7.9	8.3	8.1	9.0
MLD	14.2	12.2	14.3	12.3
MOK	11.5	11.6	10.9	11.0
NFM	6.3	6.3	6.7	7.1
OLD	7.1	8.8	7.1	8.8
RIO	9.0	8.6	8.9	8.9
SFM	16.0	15.6	15.7	15.3
STK	30.8	28.8	30.6	28.7
UCS	47.9	47.8	47.9	47.8

5.4.6 Central Delta suspended sediment concentration

Figure 5-9 and Figure 5-10 show the simulated SSC throughout the Delta for two selected dates and times. These DSM2 Animator snapshots are from Scenario 2 in Section 5.4.1. The erosion coefficient, sand, and fine particle sizes in this scenario were set to 10^{-8} kg/m^2/s, 0.5 mm, and 0.004 mm, respectively. These figures show inflows with high suspended sediment concentrations from the Sacramento and San Joaquin rivers into the model, while the SSC decays in the central Delta indicating that the sediment in the upstream rivers settles quickly closer to the central Delta. The previous calibration showed the same low SSC in the central Delta, which is referred as the "donut hole."

Figure 5-9 Simulated Delta Suspended Sediment Concentration on 25 March 2011 at 3:39 p.m.

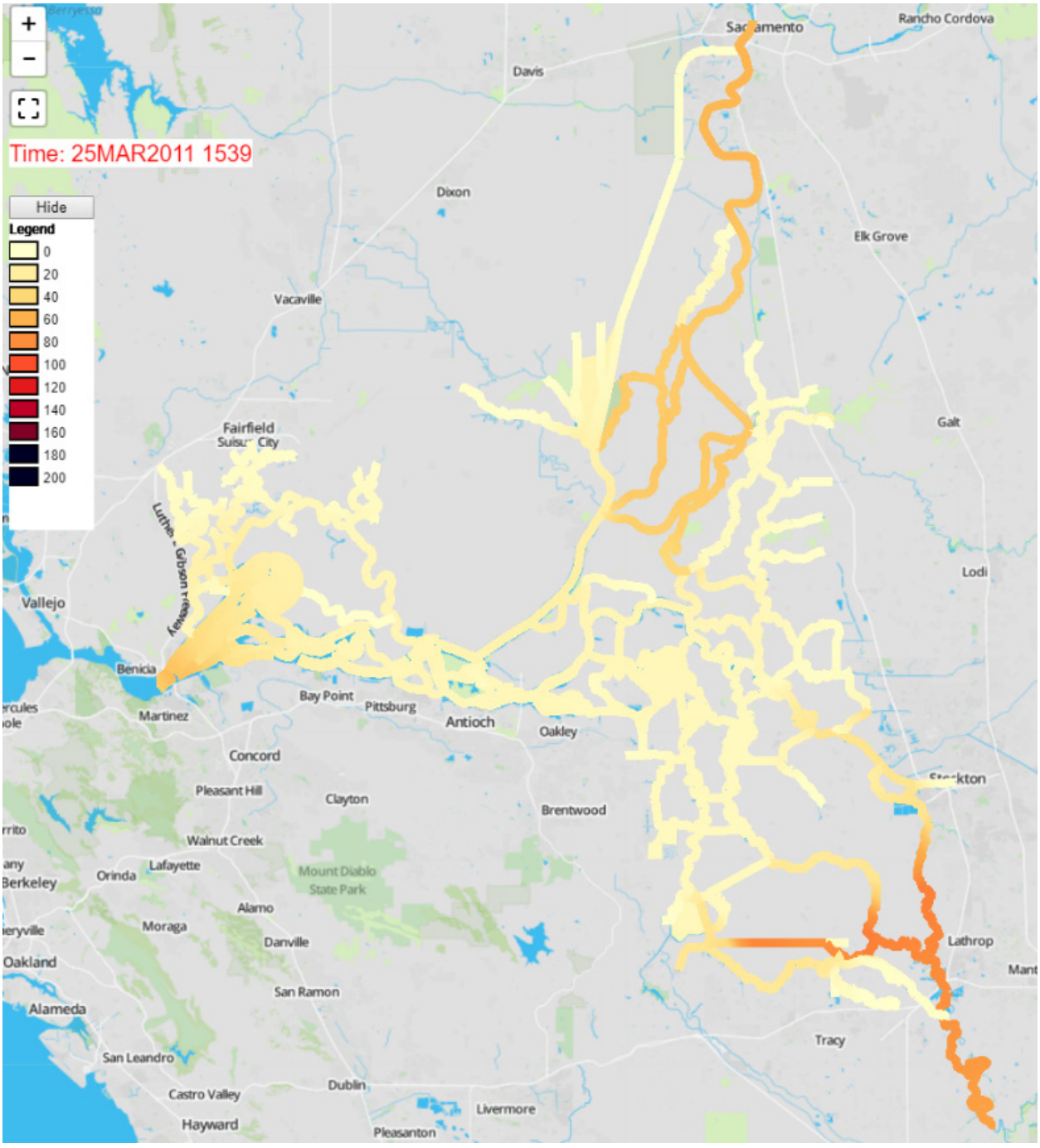

Figure 5-10 Simulated Delta Suspended Sediment Concentration on 10 December 2012 at 1:54 p.m.

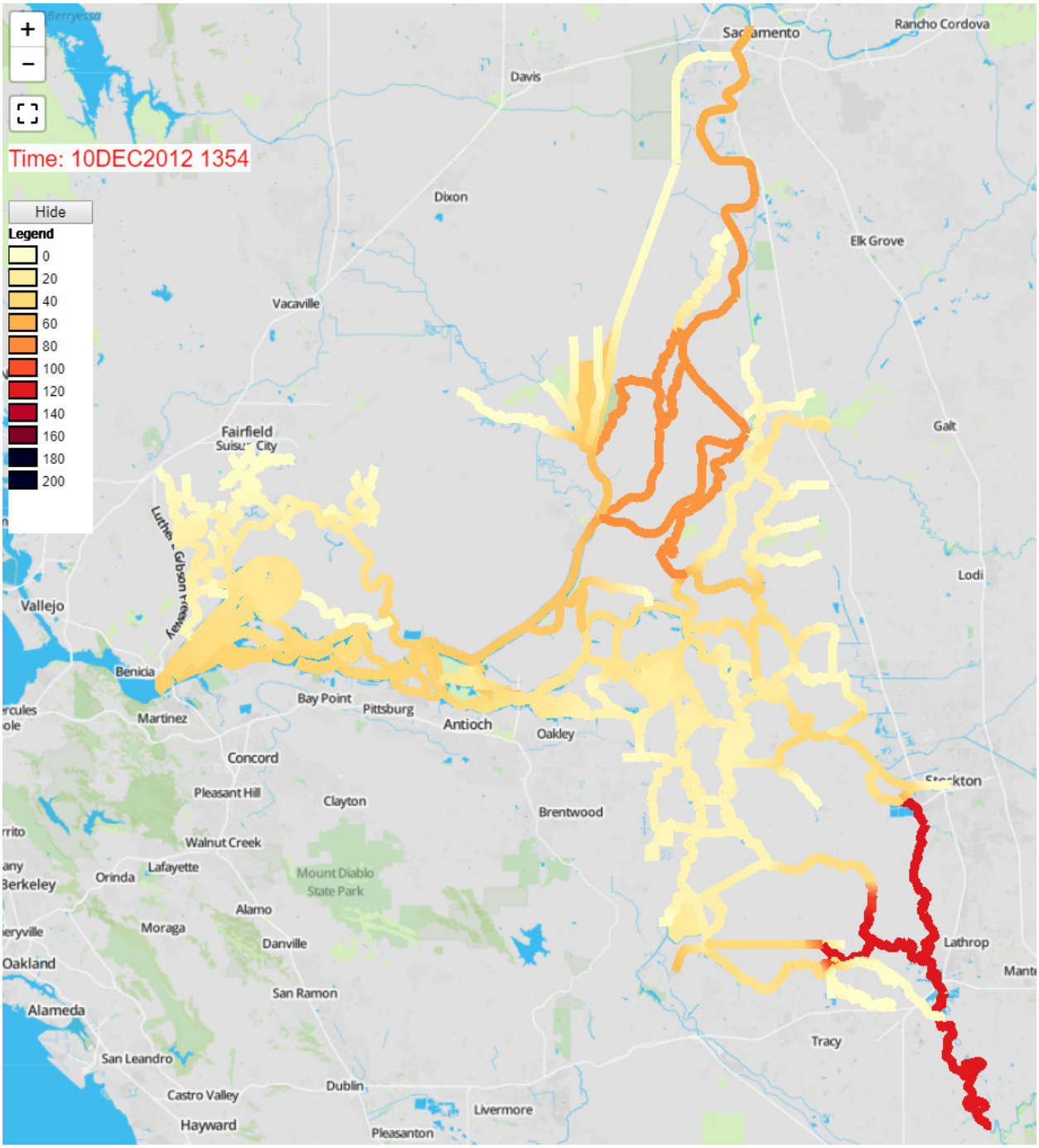

5.5 GTM-SED validation

The three years of calibration in the previous sections included Water Years 2011, 2012, and 2013, which are categorized as wet, below normal, and dry years, respectively. The validation period is also three years, from October 2013 until September 2016. Water Years 2013 and 2014 are categorized as critical years, and Water Year 2015 is a below normal year. Four different validation scenarios are simulated, as shown in Table 5-17. Simulated SSCs for the validation period had relatively lower RMSE values for stations at Cache Slough at Ryer Island (CCH), Middle River (MID), South Fork of the Mokelumne River (SFM), and Cache Slough near Rio Vista (UCS), and the rest of the stations resulted in higher RMSEs when compared with the calibration period (Table 5-18). The RMSE of the Mokelumne station (MOK) is evaluated as very high for the validation period. This is a result from some unreasonably high field SSC measurements at the MOK station during the 2013–2016 period.

Figure 5-11 shows SSCs of the four validation scenarios. Two sets of scenarios, Scn1 and Scn3, and Scn2 and Scn4, with identical fine particle sizes but different sand sizes, resulted in almost identical SSCs, and they almost overlapped one another in the figure. As shown in the calibration period, the model is insensitive to the sand size.

Table 5-17 GTM-SED Validation Scenarios

Parameters	Scn1	Scn2	Scn3	Scn4
Erosion Coefficient	10^{-8}	$5x10^{-8}$	10^{-8}	$5x10^{-8}$
Sand (mm)	0.5	0.5	0.0625	0.0625
Fines[1] (mm)	0.004	0.004	0.004	0.004

[1] Inorganic and organic fines.

Table 5-18 Root Mean Square Errors, Validation vs. Calibration Scenarios

A. Validation (WY2014–WY2016)

Station	Scn1	Scn2	Scn3	Scn4
CCH	9.4	8.6	9.4	8.8
GEO	13.7	13.1	13.3	12.8
JPT	10.2	8.0	10.2	8.0
LPS	10.5	11.1	10.5	11.1
MID	5.2	6.2	5.2	6.2
MIN	19.2	18.9	19.0	18.8
MLD	16.5	13.5	16.4	13.4
MOK	122.4	122.2	122.3	122.1
NFM	11.7	11.6	11.8	11.8
OLD	8.4	9.3	8.4	9.3
RIO	19.8	18.0	19.5	17.8
SFM	13.0	12.6	12.9	12.5
STK	37.2	35.5	37.2	35.5
UCS	26.8	26.7	26.8	26.7

B. Calibration (WY2011–WY2013)

Station	Scn1	Scn2	Scn3	Scn4
CCH	11.4	11.1	11.8	11.9
GEO	8.6	7.9	8.3	7.9
JPT	7.6	7.3	7.6	7.4
LPS	6.9	7.9	6.9	7.9
MID	5.5	7.5	5.5	7.6
MIN	7.9	8.3	8.1	9.0
MLD	14.2	12.2	14.3	12.3
MOK	11.5	11.6	10.9	11.0
NFM	6.3	6.3	6.7	7.1
OLD	7.1	8.8	7.1	8.8
RIO	9.0	8.6	8.9	8.9
SFM	16.0	15.6	15.7	15.3
STK	30.8	28.8	30.6	28.7
UCS	47.9	47.8	47.9	47.8

Figure 5-11 Suspended Sediment Concentrations From the Validation Period

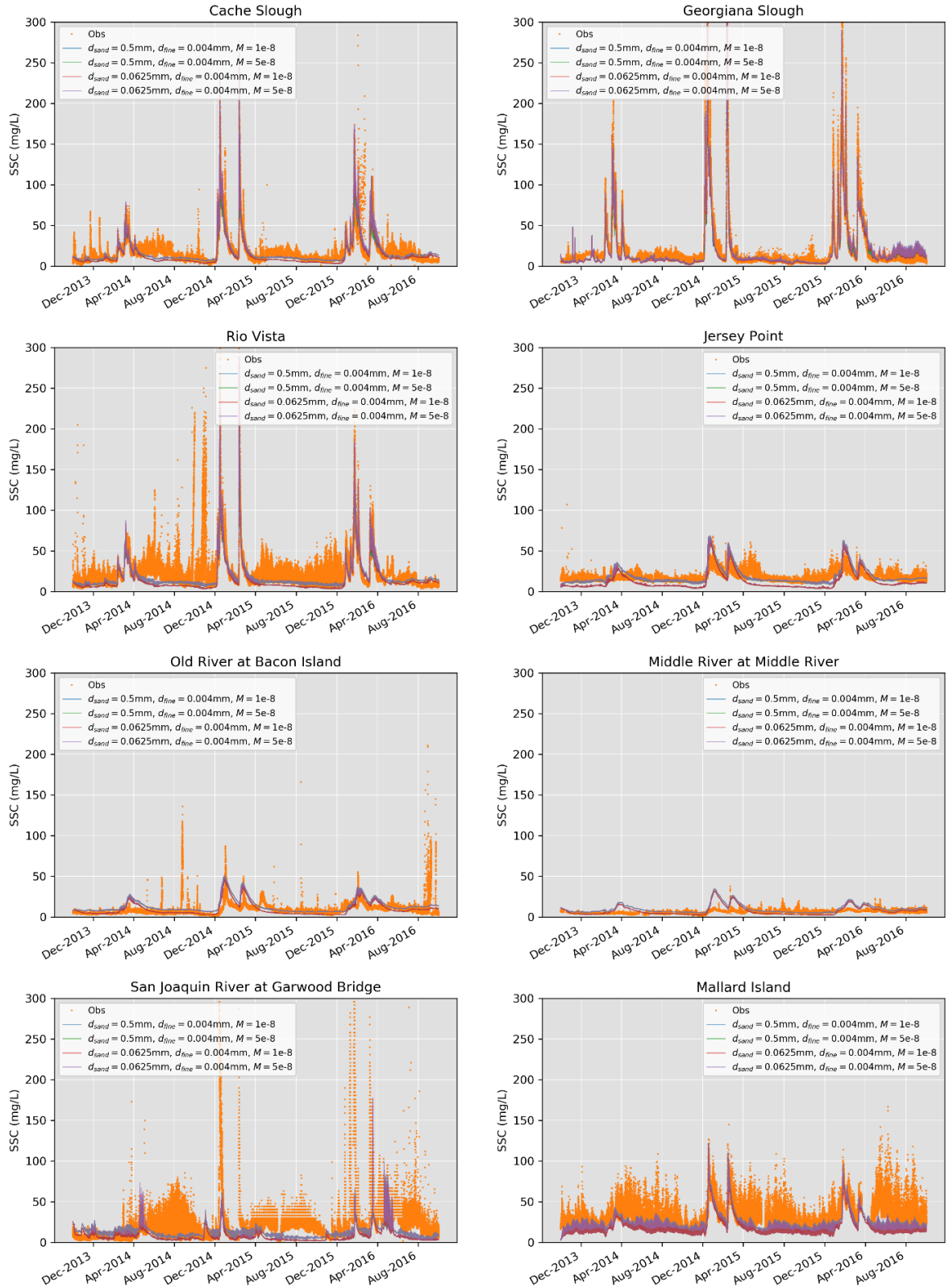

5.6 Conclusions

A sediment bed representation has been integrated into the GTM sediment module (GTM-SED). The sediment bed representation was developed to support the mercury module for DSM2 GTM. The newly integrated sediment bed module updates the previous erosion implementation of GTM-SED by including the sediment bed composition.

The updated suspended sediment model is calibrated by changing the erosion coefficient, particle sizes, and boundary suspended sediment concentration (SSC) compositions. Other minor updates, such as SSC ratios in the return flows from Delta islands, are included throughout the calibrations. The sediment bed is not calibrated in this calibration effort because the sediment bed module is still under development.

The following was observed from this study:

- The SSC in the Delta was calibrated by adjusting the erosion coefficients ranging from 10^{-3} to 10^{-10} kg/m^2/s while keeping the particle sizes as they were reported in the previous calibration in Chapter 4 of this report. The best performing erosion coefficient is between 10^{-8} and 10^{-7} kg/m^2/s, which is about the same from the previous calibration. This indicates that the sediment bed composition, sediment bed interaction with the suspended sediment, and reaction in the sediment bed do not affect the SSC strongly.
- The model is not sensitive to the particle size of the sand class as much as it is sensitive to the size of the fine/clay class, in which a small fine sediment size resulted in higher SSCs because of slow settling and easy resuspension.
- Particle diameters ranging from 0.004 mm to 0.0625 mm were assessed to represent the fine class. The diameter of 0.004 mm, which is the lowest value of the fine particle size range, was found to perform well.
- Simulations were performed for sand particles with diameters ranging from 0.0625 mm to 2 mm, and sand particle sizes of 0.5 mm and 2 mm resulted in more accurate simulation results.
- The study tried SSC compositions based on USGS measurements at the river boundaries, but it did not perform better than the calibrated boundary SSC composition from the previous calibration. The model

appears to need a somewhat heavy loading of suspended sands at the boundaries compared with the field SSC data. It is probably and partly because the model used a set of constant SSC ratios over time at the boundary inflows.

- The sensitivity of the model to the initial condition of the sediment bed was investigated by incorporating a uniform bed based on the USGS field data across the model domain. The simulation results showed that a uniform sediment composition for the whole domain at the beginning of the run did not significantly change the simulated SSCs when compared with a similar simulation that has a bed composition adapted from a spun-up GTM-SED simulation.
- Simulation results showed that the SSC in the central Delta is much lower than that at the upstream Sacramento River and San Joaquin River domain boundaries because of quick settlement of the sediments in the upstream area. This is what created the SSC "donut hole" at the central Delta.
- Details were not reported in this chapter, but it was found that the sediment composition in the return flows from the Delta islands does not affect the SSC in the Delta much. Nevertheless, better data about the sediments in the return flows would help the model to simulate more accurate results, but no data has been found on the Delta island return flow SSCs.

Overall, the updated model performed similarly to the previous implementation and calibration without having to make major changes in any of the parameters. It should be noted that this study has several simplified assumptions that can be improved in the future:

- The compositions of the suspended sediment particles in the boundary flows do not vary over time in this model. This limits calibration of the model over time, and it may not reflect seasonal variations of the suspended sediment boundary conditions, especially during high flow periods that may bring in disparate types of sediment when compared with the other periods. The plan is to update the model so that it can use seasonally varying suspended sediment boundary conditions.
- The model is one-dimensional and it does not account for the wind and wave effect. This may be important in shallow areas when the wind speed is high enough to cause the resuspension of bed particles.

- The model used only two classes of sediment. More sediment classes could improve the SSC simulation in the model, in addition, more sediment data would be necessary to reasonably calibrate multiple classes of sediment.
- The sediment bed initial condition is simplified by adapting bed sediment composition from the last time step of a previous GTM simulation. Incorporating a more realistic sediment bed composition for the initial condition could improve the model performance, but the sediment bed needs to be calibrated properly together with the SSC.

The sediment and mercury modules of DSM2 GTM are still actively being developed, and this study reflects an initial effort of DSM2 GTM-SED modeling. The sediment bed module of the DSM2 GTM model needs to be reviewed further and calibrated to improve the suspended sediment modeling in DSM2 GTM. Some future improvements in the model are expected by using better sediment data. A more systematic and automatic calibration using PEST will be adopted and calibration will be improved as well.

5.7 Acknowledgements

This effort is a continuation of the GTM-SED module improvement, mainly developed by En-Ching Hsu of DWR, who is thanked for her support. The sediment bed part in GTM-SED is being developed by David Hutchinson from a mercury developing team as a part of the GTM Mercury module, he is thanked for his help in the process of the sediment bed integration to GTM-SED. Thank you to Tara Morgan-King and David Schoellhamer of USGS for their valuable information and insight about the sediment data.

5.8 References

Ariathurai R, Arulanandan K. 1978. "Erosion rates of cohesive soils." ASCE Journal of Hydraulic Division 104 (2), 279–283.

California Department of Water Resources. 2014. *Methodology for Flow and Salinity Estimates in the Sacramento-San Joaquin Delta and Suisun Marsh, 35th Annual Progress Report to the State Water Resources Control Board*. "Chapter 4. DSM2-GTM." by Hsu E, Ateljevich E, and Sandhu P. Sacramento (CA). California Department of Water Resources. Bay-Delta Office.

California Department of Water Resources. 2016. *Methodology for Flow and Salinity Estimates in the Sacramento-San Joaquin Delta and Suisun Marsh, 37th Annual Progress Report to the State Water Resources Control Board*. "Chapter 4. Delta Salinity Simulation with DSM2-GTM." Hsu E, Ateljevich E, and Sandhu P. Sacramento (CA). California Department of Water Resources. Bay-Delta Office.

California Department of Water Resources. 2019. *Methodology for Flow and Salinity Estimates in the Sacramento-San Joaquin Delta and Suisun Marsh, 40th Annual Progress Report to the State Water Resources Control Board*. "Chapter 4. DSM2 GTM-SED, Sediment Transport Model." Hsu E and Sandhu P. Sacramento (CA). California Department of Water Resources. Bay-Delta Office.

Marineau MD, Wright SA. 2017. *Bed-Material Characteristics of the Sacramento-San Joaquin Delta, California, 2010-13* (Data Series 1026). U.S. Geological Survey.

Wentworth CK. 1922. "A scale of grade and class terms for clastic sediments." Journal of Geology, v. 30, p. 377-392.